Department of
Industry and Resources

EXPLANATORY NOTES

GEOLOGY OF THE NABBERU AND GRANITE PEAK 1:100 000 SHEETS

by F. Pirajno, J. A. Jones, and R. M. Hocking

1:100 000 GEOLOGICAL SERIES

Geological Survey of Western Australia

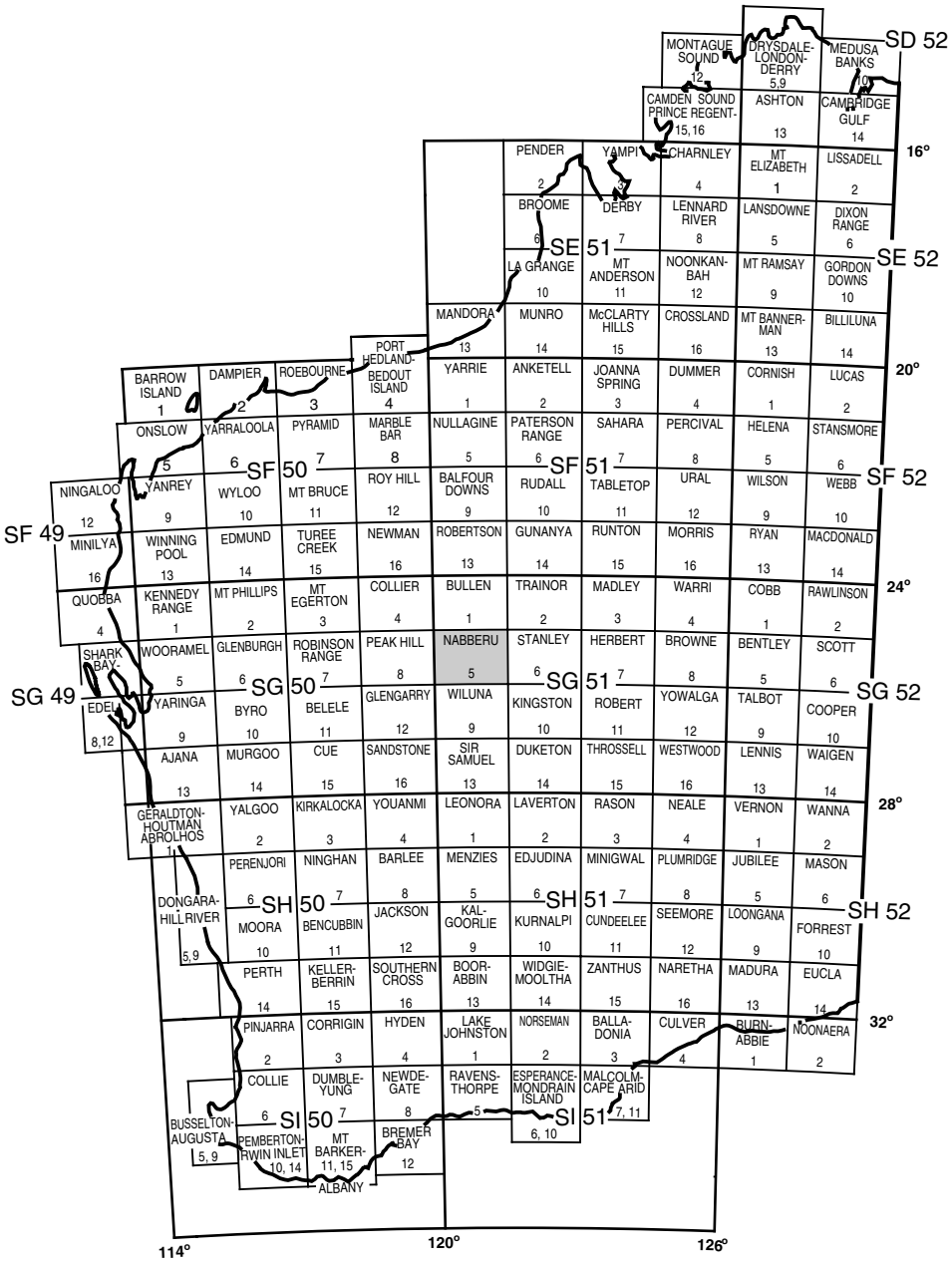

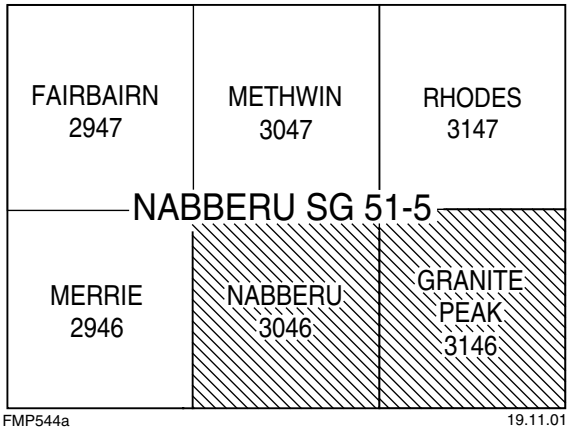

FMP544a 19.11.01

GEOLOGICAL SURVEY OF WESTERN AUSTRALIA

GEOLOGY OF THE NABBERU AND GRANITE PEAK 1:100 000 SHEETS

by
F. Pirajno, J. A. Jones, and R. M. Hocking

Perth 2004

MINISTER FOR STATE DEVELOPMENT
Hon. Clive Brown MLA

DIRECTOR GENERAL, DEPARTMENT OF INDUSTRY AND RESOURCES
Jim Limerick

DIRECTOR, GEOLOGICAL SURVEY OF WESTERN AUSTRALIA
Tim Griffin

REFERENCE
The recommended reference for this publication is:
PIRAJNO, F., JONES, J. A., and HOCKING R. M., 2004, Geology of the Nabberu and Granite Peak 1:100 000 sheets: Western Australia Geological Survey, 1:100 000 Geological Series Explanatory Notes, 48p.

National Library of Australia Card Number and ISBN 0 7307 8930 6

ISSN 1321–229X

Grid references in this publication refer to the Geocentric Datum of Australia 1994 (GDA94). Locations mentioned in the text are referenced using Map Grid Australia (MGA) coordinates, Zone 50. All locations are quoted to at least the nearest 100 m.

Copy editor: M. J. Donaldson
Cartography: S. Dowsett
Desktop Publishing: K. S. Noonan

Published 2004 by Geological Survey of Western Australia

Copies available from:
Information Centre
Department of Industry and Resources
100 Plain Street
EAST PERTH, WESTERN AUSTRALIA 6004
Telephone: (08) 9222 3459 Facsimile: (08) 9222 3444
This and other publications of the Geological Survey of Western Australia may be viewed online at www.doir.wa.gov.au/gswa or purchased through the Department's bookshop at www.doir.wa.gov.au.

Cover photograph:
Breakaway in Wandiwarra Member quartz sandstone and siltstone at the northern margin of NABBERU.

Contents

Appendix

Figures

Table

Geology of the Nabberu and Granite Peak 1:100 000 sheets

by

F. Pirajno, J. A. Jones, and R. M. Hocking

Abstract

The NABBERU and GRANITE PEAK 1:100 000 sheets cover the Palaeoproterozoic Earaheedy Group of the Earaheedy Basin, and the northern part of the Archaean Yandal greenstone belt and granitoid rocks of the Yilgarn Craton. Archaean greenstone and granitoid rocks are exposed in the southwest corner of NABBERU. The greenstone belt consists dominantly of metamorphosed mafic–ultramafic and felsic volcanic rocks, and near the Lockeridge Fault is host to orogenic-style gold mineralization. Granitoids are represented by monzogranite, hornblende-bearing quartz monzonite, and K-feldspar granite. The Teague Granite comprises syenitic rocks that occupy the core of the Shoemaker impact structure. NABBERU – GRANITE PEAK is dominantly covered by the Yelma, Frere, Windidda, and Chiall Formations of the Earaheedy Group. The basal Yelma Formation comprises shale, siltstone, sandstone, and an uppermost stromatolitic carbonate, which is host to Pb–Zn mineralization (Sweetwaters Well Member). The overlying Frere Formation consists of granular iron-formation interbedded with shale and siltstone. The Windidda Formation is composed of stromatolitic carbonate, shale, siltstone, and peloidal jasper, and is laterally equivalent to the upper part of the Frere Formation in the north. The Chiall Formation comprises shale, siltstone, and sandstone, and is subdivided into the Karri Karri (lower), Wandiwarra, and Princess Ranges (upper) Members. The northeast corner of GRANITE PEAK is part of the northwest-trending zone of deformation termed the Stanley Fold Belt. The age of the Earaheedy Group is around 1.8 Ga.

The Shoemaker impact structure, which is 28 km in diameter, is a prominent feature of NABBERU – GRANITE PEAK and is characterized by two annular collars of Earaheedy Group rocks with the Teague Granite in the core. The age of this impact is uncertain, but based on K–Ar and Ar–Ar dating, it could be 568 Ma.

Mineralization hosted by the Earaheedy Group on NABBERU – GRANITE PEAK includes sulfides in stromatolitic dolomite rocks of the Yelma Formation, and minor uranium in calcrete. Potential exists for iron deposits in the granular iron-formation, and for gold in east-trending fractures in the Chiall Formation.

KEYWORDS: Archaean, Proterozoic, Earaheedy Group, iron-formation, base metal deposits, Shoemaker impact structure.

Introduction

The NABBERU* and GRANITE PEAK 1:100 000 map sheets (SG 51-5, 3046 and 3146; Pirajno, 1999; Jones, 2000; henceforth referred to as NABBERU – GRANITE PEAK) are bounded by latitudes 25°30' and 26°00' south and longitudes 120°30' and 121°30' east, and are located in the southern part of NABBERU (1:250 000; Fig. 1). The Cunyu and Granite Peak pastoral leases occupy most of NABBERU – GRANITE PEAK, and the southern parts cover part of the Millrose pastoral lease. Access is provided by the Wiluna–Carnegie Road, which runs through the eastern part of GRANITE PEAK, and station tracks from the west, through Cunyu Station and the Canning Stock Route. The nearest town is Wiluna, about 100 km to the southwest.

The area covered by NABBERU – GRANITE PEAK has an arid climate with average temperatures† ranging between 24 and 39°C in summer, with a recorded maximum of 47°C, and 6 to 20°C in winter, with a recorded minimum of –4°C. Rainfall is sporadic and averages 232 mm a year. Evaporation rates are up to 2500 mm a year.

Tectonic units on NABBERU – GRANITE PEAK include Archaean granites and greenstones of the Yilgarn Craton (Eastern Goldfields Granite–Greenstone Terrane; Tyler and Hocking, 2001) and Palaeoproterozoic sedimentary

* Capitalized names refer to standard 1:100 000 map sheets, unless otherwise indicated.

† Climate data from the Bureau of Meteorology — averaged from data from the following areas: Wiluna, Three Rivers, Meekatharra (Peak Hill), and Earaheedy.

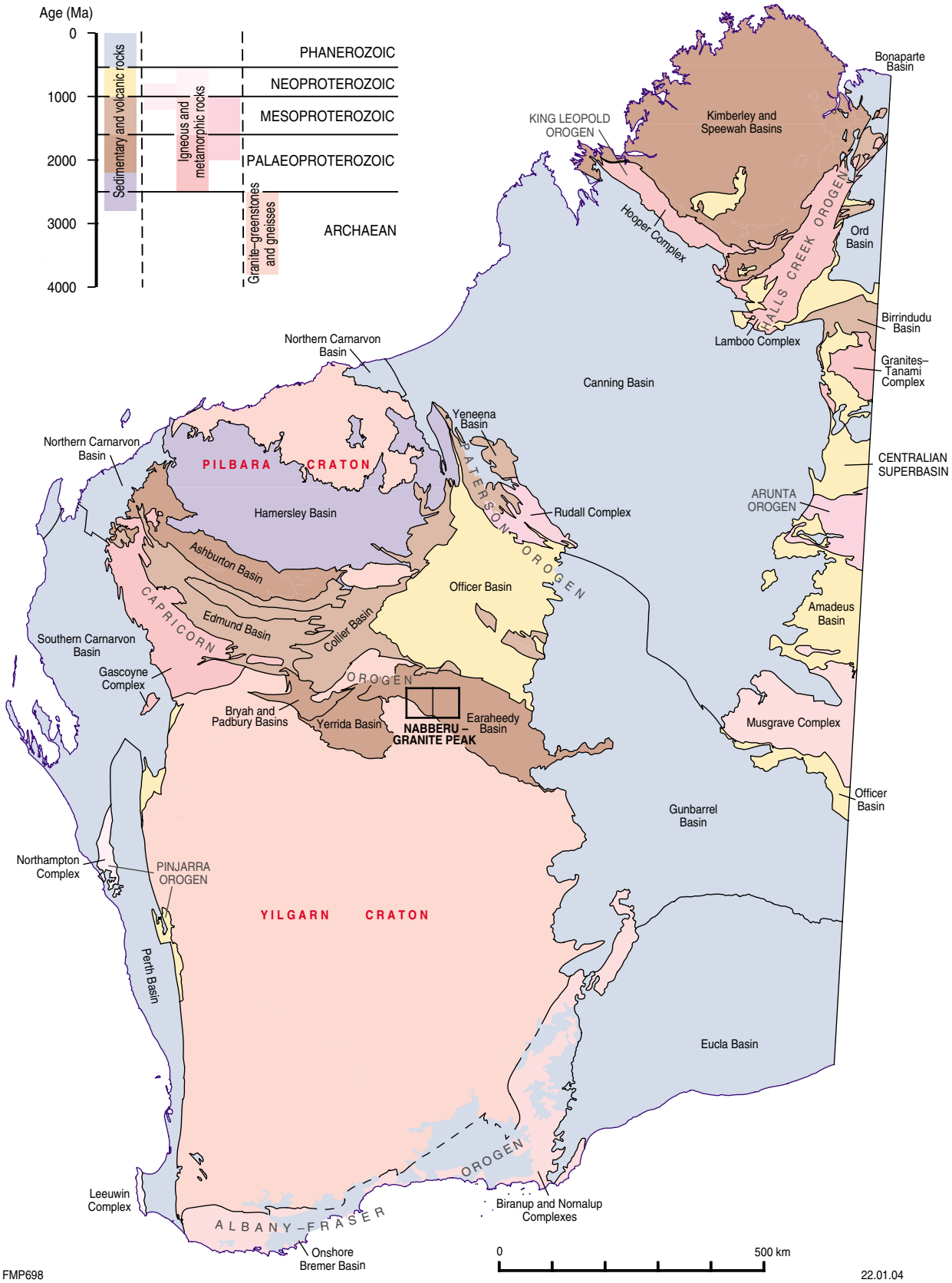

Figure 1. Tectonic units map of Western Australia, showing the position of the Earaheedy Basin and Nabberu – Granite Peak map sheets

rocks of the Earaheedy Basin (Jones et al., 2000, 2001; Pirajno et al., 2004; Fig. 2). Most of the Archaean rocks outcrop in the south of NABBERU. A major geological and physiographic feature in the area is the Shoemaker impact structure (Pirajno, 2002).

Vegetation, landform systems, and regolith

Vegetation, physiography, and geology are closely linked. Only a single major vegetation zone is present on NABBERU – GRANITE PEAK. The area is near the northern margin of Beard's (1981) Ashburton Phytogeographic District. Other than in lake systems, the area is largely covered by low mulga woodland (Beard, 1981) with stands of gums (*Eucalyptus* sp.) along major watercourses, and sparse scrub steppe on rocky ridges. There are samphire flats on and around larger, periodically wet playa areas and in the major lakes such as Lake Nabberu*. The central portion of some larger lakes remains essentially vegetation free. Similarly, NABBERU – GRANITE PEAK lies entirely within one soil-landscape (physiographic) province, the Murchison Province of the Western Region (Bettenay, 1983), although the Ayers–Canning Province of the Sandy Desert Region (Northcote and Wright, 1983) covers much of METHWIN and RHODES, immediately to the north.

The age of the landform elements and regolith on NABBERU – GRANITE PEAK is variably constrained. Regolith is shown as Quaternary (*Q*) or undifferentiated Cainozoic (*Cz*) depending on whether it is considered to have a significant component related to present-day processes, or is entirely relict (Hocking et al., 2001). In some cases, both the regolith and its associated landscape are undoubtedly older than Cainozoic. The range in possible age for some regolith and landscape components in interior areas of Western Australia is from Pleistocene to Mesozoic, and there are some land surfaces (fossil and exhumed) in Western Australia that are known to be of Mesozoic or Palaeozoic age. The Ashburton Surface in northern Australia is probably pre-Jurassic (Hays, 1967) and possibly even Cambrian–Precambrian (Stewart et al., 1986); the oldest Hamersley Surface (Pilbara region) was considered to be Mesozoic by Twidale et al. (1985), and parts of the Yilgarn Craton landscape may be Triassic (Twidale, 2000). Pillans (1998) argued for subaerial exposure as far back as the Permian over parts of the Yilgarn Craton, and Pillans and Bateman (2000) dated regolith components near Kalgoorlie as Late Cretaceous – Early Cainozoic, Jurassic, and Early Carboniferous. Permian glacial pavements are present on WONGAWOL, to the southeast.

Landform elements present on NABBERU – GRANITE PEAK are shown in Figure 3. The Lake Nabberu system cuts southeastwards across the area and separates plains developed over the Earaheedy Group to the north, from plains developed over granitoid rocks of the northern Yilgarn Craton to the south. These two plain systems differ due to the nature of the underlying rocks, but are assumed to have a similar origin, as etchplains where weathered material (regolith) has been stripped back, leaving relatively fresh rock. Ridges of resistant rock (typically silicified) form inselbergs amongst the softer, more deeply weathered rock types.

In the northern plain system, the Frere Formation is at the core of the two major ranges on NABBERU – GRANITE PEAK: the Frere Range and Mount Cecil Rhodes. Colluvium (proximal slope deposits, *Czc*) adjacent to these ranges and larger rock ridges is typically consolidated and partially dissected, suggesting that erosion of uplands is currently only minor, and that the colluvium may be coeval with the older alluvium. The colluvium is commonly ferruginous (*Czcf*) adjacent to the Frere Formation and quartz rich (*Czcq*) where derived from quartz veins. Between ridges and drainages, there is widespread thin cover of sheet-flood deposits (sheetwash, *Qw*), forming extensive tigerbush flats. Ferruginous sheetwash (*Qwf*) occurs adjacent to ironstone ranges, and quartzose wash (*Qwq*) adjacent to quartz veins and stockworks. Patches of sandplain (*Qs*) are preserved in upland areas of the southern plain, and in scattered parts of the northern plain. The sandplain is relict, and even where fires have burnt the vegetation cover, there appears to have been minimal sand movement.

Well-defined drainage systems with localized alluvial deposits *(Qa)*, grade laterally into sheet-flood areas with some patches of groundwater calcrete (*Qak*). Most creeks drain into the Lake Nabberu system, which in turn drains into the Lake Carnegie system; however, on northern GRANITE PEAK, they flow directly into Lake Carnegie. Clay and silt *(Qac)* cover non-saline pans on GRANITE PEAK.

The Lake Nabberu system marks a southeast-flowing palaeodrainage, which was active in the early to mid-Cainozoic (van de Graaff et al., 1977). Within the Lake Nabberu system, relatively small saline playas (*Ql*), fringing dunes (*Qld*), and mixed dune-and-playa terrain with underlying bedded lacustrine deposits (*Qlg*) are peripheral to the larger playas (*Ql*) at the core of the Lake Nabberu palaeodrainage system. In places, calcrete (*Qlk*) has developed within the lacustrine system, but locally this is gypsiferous (gypcrete), and is distinct from alluvial groundwater calcrete (*Qak*). Older pedogenic calcrete (*Czrk*) occurs at the margins of the lake system, and from its mode of occurrence is older than both the lacustrine and groundwater calcrete. North of Lake Teague, pedogenic calcrete contains weak uranium mineralization. There is an etched rock platform, with scattered exposure of the Earaheedy Group, beneath some playas. Scattered hills and ridges developed by headward erosion of the higher land surface north of the lacustrine area, forming a dominantly south-facing breakaway system.

Ferruginous duricrust (ferricrete, *Czrf*) and siliceous duricrust (silcrete, *Czrz*) are on and marginal to uplands. Duricrust is rarely the highest part of the landscape, and commonly on a gentle slope, suggesting development on intermediate slopes, perhaps with very local transport of material. Supergene-enriched ironstone (*Czri*) is adjacent to or above the ferricrete in situ and some Fe-enriched Frere Formation.

* MGA coordinates of localities mentioned in the text are listed in Appendix 1.

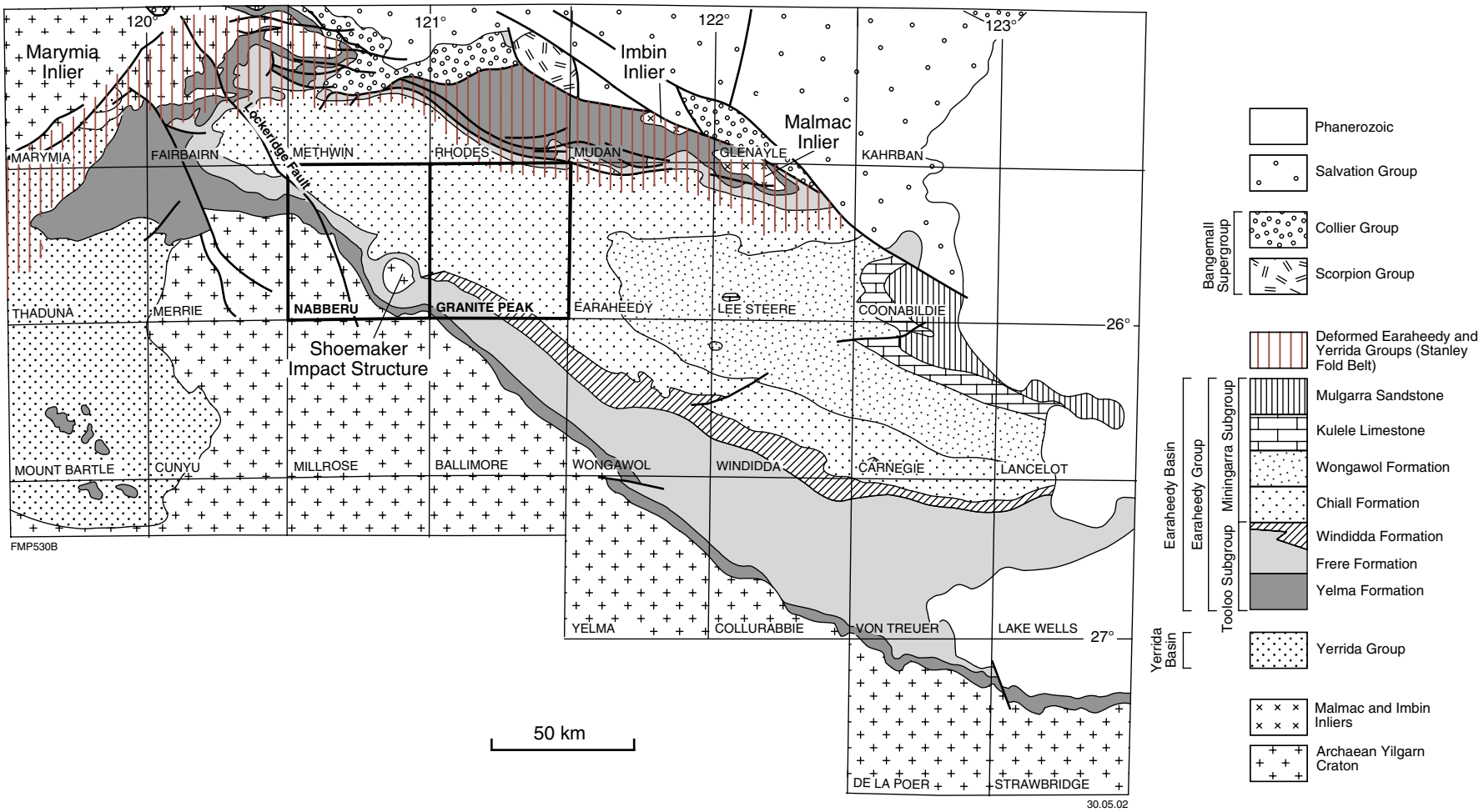

Figure 2. Simplified geology of the Earaheedy Basin and adjoining areas, and 1:100 000 map sheet index

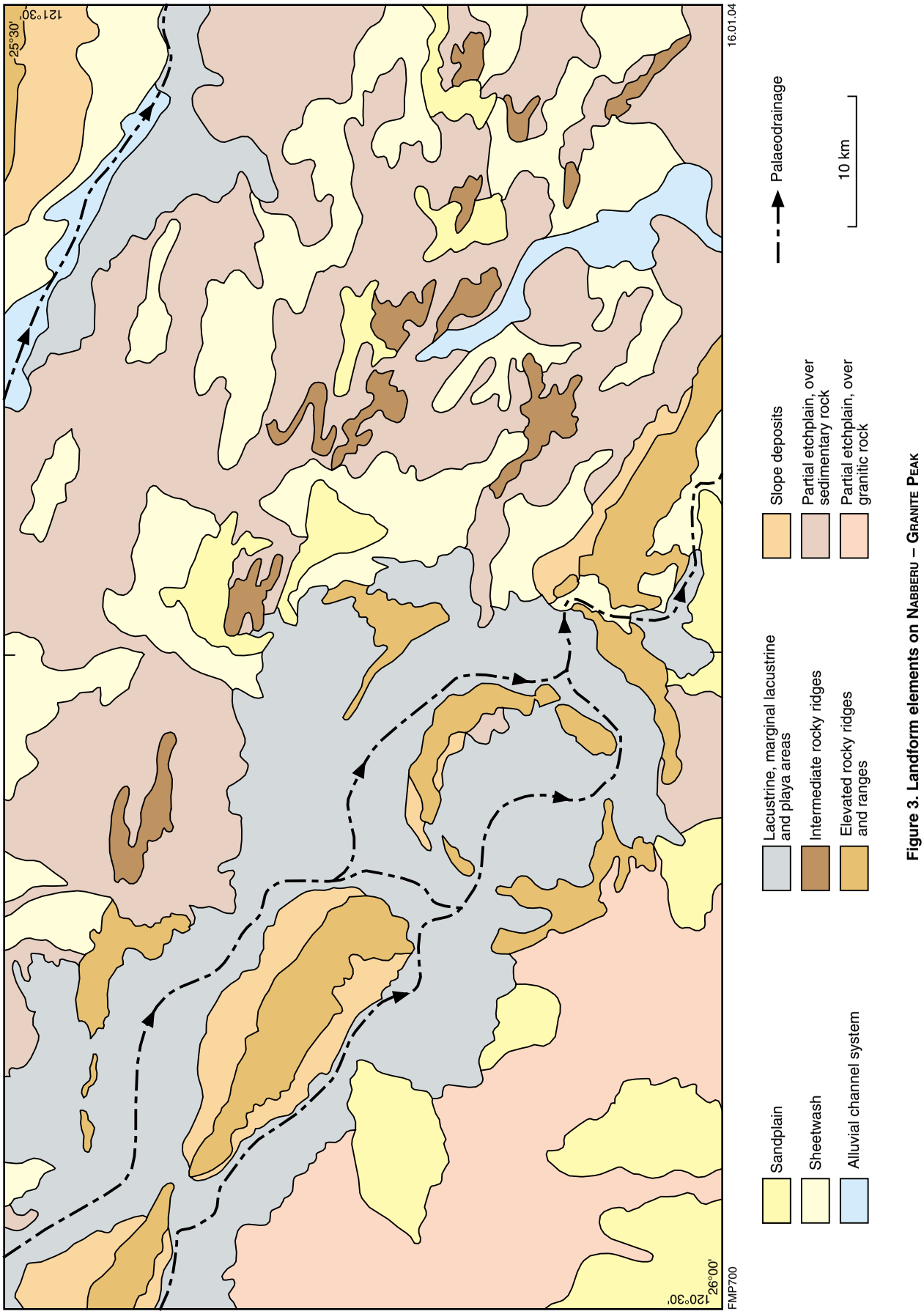

Figure 3. Landform elements on Nabberu – Granite Peak

Geological setting

NABBERU – GRANITE PEAK covers an area underlain by Archaean granitoid and greenstone rocks of the Yandal Greenstone Belt in the Yilgarn Craton (Myers and Swager, 1997), and the Palaeoproterozoic Earaheedy Basin (Jones et al., 2000, 2001; Fig. 2). The northerly to north-northwesterly trending Yandal Greenstone Belt is part of the late Archaean (2.75–2.6 Ga) Eastern Goldfields Granite–Greenstone Terrane (Griffin, 1990; Phillips and Anand, 2000; Tyler and Hocking, 2001), which has been interpreted as a tectonostratigraphic terrane that was involved in the assembly of the Yilgarn Craton (Myers, 1995). The Earaheedy Basin lies at the eastern end of the Capricorn Orogen (Tyler and Thorne, 1990; Tyler et al., 1998; Fig. 1 and Table 1), and contains the Earaheedy Group, which extends over most of the northeastern half of NABBERU and most of GRANITE PEAK. To the north, the Earaheedy Group is either overlain by, or in faulted contact with, the c. 1300–1070 Ma Collier Group (Martin and Thorne, 2001; Table 1).

Strongly deformed rocks in the northeast corner of GRANITE PEAK are part of the Stanley Fold Belt (Bunting, 1986; Pirajno et al., 2004), which is a west-northwesterly trending zone of deformation within and along the northern margin of the Earaheedy Basin. In the Stanley Fold Belt, rocks of the Earaheedy Group are weakly metamorphosed, cleaved, tightly folded, and faulted. On RHODES and MUDAN, to the north and northeast, these rocks were previously interpreted to be an older tectonic entity, the Troy Creek Beds (Bunting, 1986), but are now considered to be deformed Earaheedy Group (Hocking et al., 2000; Pirajno and Hocking, 2000, 2001; Jones et al., 2001; Pirajno et al., 2004). Deformation is less intense south of the Stanley Fold Belt, and outliers of Earaheedy Group north of the fold belt are not deformed, suggesting deformation was concentrated along a narrow easterly trending zone, possibly linked to the second phase of the Yapungku Orogeny (Smithies and Bagas, 1997; Bagas, 2004).

Archaean geology

Archaean granitoids and rocks of the Yandal greenstone belt occupy southwestern NABBERU, the central part of the Shoemaker impact structure (Pirajno, 2002), and the southwestern corner of GRANITE PEAK. The granitoids are monzogranite (*Ag*), hornblende-bearing quartz monzonite (*Agzq*), and a K-feldspar granite (*Agak*). The Teague Granite (*Ægte*) is syenitic in composition and forms the core of the Shoemaker impact structure. Greenstones comprise metamorphosed mafic and ultramafic (*Ab*) and felsic (*Af*) volcanic rocks, which belong to the Millrose domain in the Yandal greenstone belt (Farrell and Wyche, 1999; Phillips and Anand, 2000).

Granitoids (*Ag, Agzq, Agak)*

Monzogranite (*Ag*) outcrops occupy areas in the west and southwest of NABBERU. On GRANITE PEAK, a small area in the southwestern corner, around Joys Bore, is interpreted to be the continuation of monzogranite from WILUNA (1:250 000; Farrell, 1999). Monzogranite is typically very weathered, lateritized or silcretized, although small patches of comparatively fresh rock are common at the base of the ferruginous or siliceous duricrusts. The deep weathering of the monzogranite does not allow any detailed assessment of the original mineralogy; however, relict textures suggest it to be coarse-grained, biotite-rich and porphyritic, with phenocrysts of K-feldspar up to a few centimetres long. Total magnetic intensity (TMI) images indicate that the unexposed contacts of the monzogranite with the greenstone rocks are strongly foliated.

Hornblende-bearing quartz monzonite (*Agzq*) forms a massive, internally undeformed, discrete pluton cut by the north-northwesterly trending Lockeridge Fault (Fig. 2 and see **Structure** below). In outcrop it is characterized by a subhorizontal exfoliation (Fig. 4). Ion microprobe U–Pb dating of zircons from this granitoid yielded an age of 2664 ± 4 Ma (Nelson, 1999). This pluton is clearly delineated by TMI images, which suggest it was emplaced along the boundary between the monzonite and the greenstone rocks. It contains amphibolite xenoliths and is surrounded by contact-metamorphosed greenstone rocks, consisting of quartz–actinolite hornfels (*Abh*). Along the Lockeridge Fault, this granitoid is interleaved with amphibolite and cut by quartz veins subparallel to the trend of the fault. The hornblende-bearing quartz monzonite is coarse-grained, locally with K-feldspar megacrysts. The mineralogy consists of orthoclase, microcline, oligoclase, quartz, dark-green euhedral hornblende, minor biotite, and accessory titanite and epidote. The hornblende-bearing quartz monzonite is probably part of the internal granitoid suite of the Yilgarn Craton (Cassidy et al., 1991). Thin granitic dykes, too small to be represented on the geological map, intrude the greenstone rocks. The dykes have a mylonitic texture and consist of zoned plagioclase porphyroclasts surrounded by lenses and ribbons of quartz, oligoclase, and muscovite.

A medium-grained leucocratic K-feldspar granite (*Agak*) outcrops on the northwest margin of the hornblende-bearing quartz monzonite. The K-feldspar granite contains quartz, microcline, turbid plagioclase, and muscovite. Quartz and microcline form a granoblastic-like aggregate that replaced the turbid plagioclase, and these minerals are in turn cut by late-generation K-feldspar–muscovite veinlets, which may be related to a phase of potassic alteration.

Teague Granite (*Ægte, Ægtea, Ægtex)*

Granitoid rocks that outcrop in the eastern part of the 12 km-diameter inner ring of the Shoemaker meteorite impact structure are grouped under the name of Teague Granite (Pirajno, 2002). The Teague Granite and associated greenstones are interpreted as the central structural uplift of the impact structure and possibly the basement core of the original transient cavity (Pirajno, 2002).

The petrography and chemistry of the granitic rocks in the core of Shoemaker impact structure were studied in some detail by Johnson (1991), who subdivided them into syenite and alkali granite. Here, and on the basis of

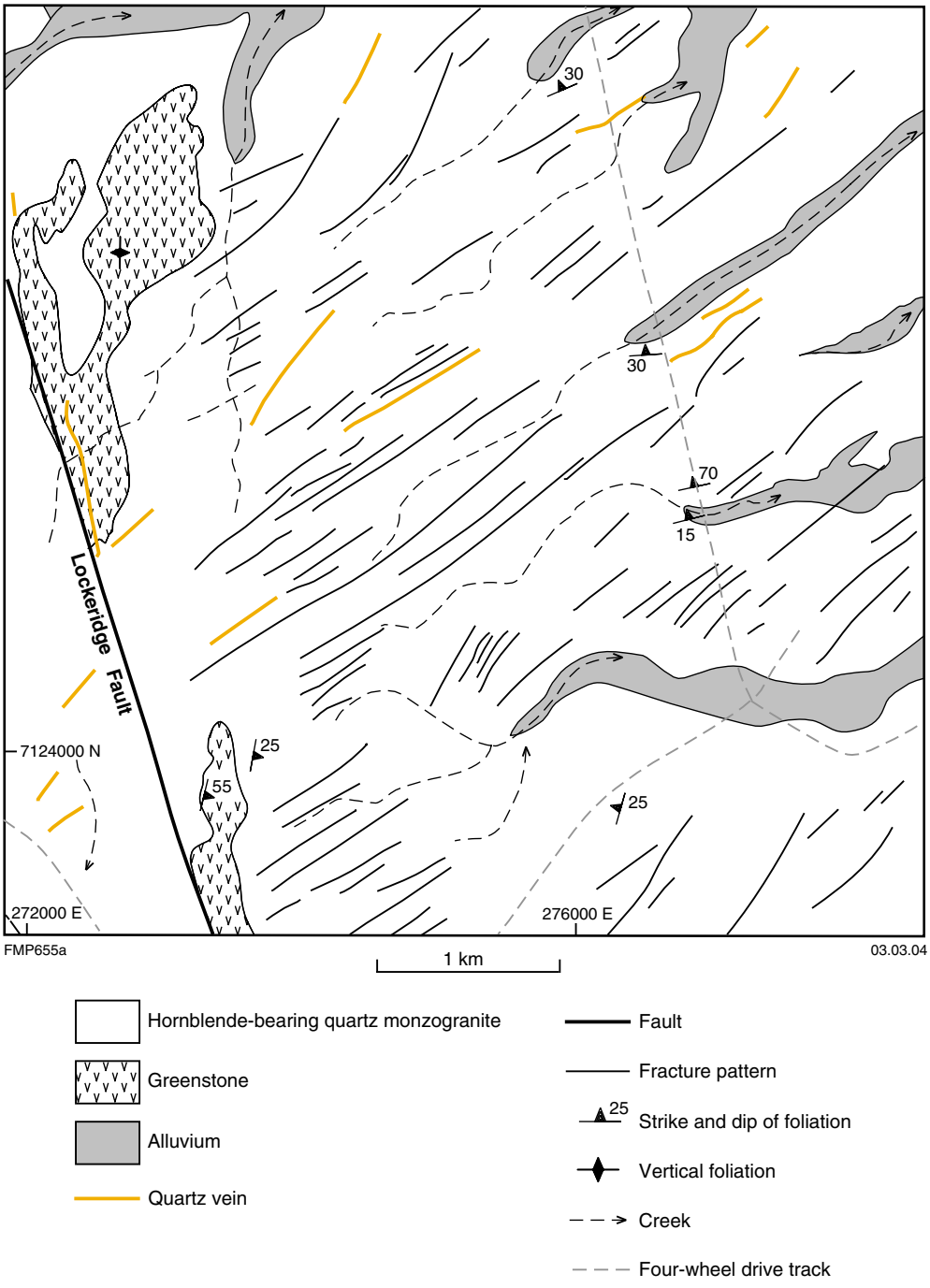

Figure 4. Fracture patterns and associated northeast-trending quartz veins in Archaean hornblende-bearing quartz monzonite, southwest of the Shoemaker impact structure

additional field and petrographic studies, the Teague Granite is subdivided into three units: leucocratic K-feldspar granite (*Ægte*), quartz–albite–microcline (–garnet–aegirine-augite) granite or syenite (*Ægtea*), and quartz–microcline(–albite–stilpnomelane) granite or quartz syenite (*Ægtex*). Field relationships between the Teague Granite and the surrounding sedimentary rocks of the Earaheedy Group are unclear due to paucity of outcrop. The lack of intrusive relationships in nearby outcrops of the Yelma Formation suggests that these rocks were originally unconformable on the Teague Granite. Although Bunting et al. (1980) considered the quartz syenite to be intrusive into the leucocratic granite, it is more likely that the boundaries between the three units are transitional. There are small xenoliths of greenstone (amphibolite) in the syenite (*Ægtea*). The petrography of the Teague Granite is described in detail by Pirajno (2002), and is summarized below.

Leucocratic K-feldspar granite (*Ægte*) is coarse to medium grained, locally brecciated, and contains the assemblage quartz – K-feldspar (microcline)–albite–

Table 1. Summary of the geological history of NABBERU – GRANITE PEAK and adjoining areas

Age (Ma)	*To west*	*Western Earaheedy Basin*	*To east and north*
Archaean, >2640 Ma		• Age of northern Yilgarn Craton and Yandal greenstone belt (basement to Earaheedy Group south of Stanley Fold Belt)	
	~ ~ ~ ~ ~ ~ ~ ~ ~ ~ ~ ~ **2100–1970 Ma** ~ ~ ~ ~ ~ ~ ~ ~ ~ ~ ~ ~		
2100–?1950	• Deposition of Windplain Group (Yerrida Basin), on Yilgarn Craton [a]		
<2015, >1802			• **Yapungku Orogeny, 1^{st} phase (D_1)**, Paterson Orogen [c]
~2000–1800	• Deposition of Bryah and Padbury Groups (Bryah–Padbury basins) [a,b]		
2000–1960	• **Glenburgh Orogeny** Convergence of Yilgarn Craton and Glenburgh Terrane of Gascoyne Complex[d]		
1990			• Extrusion of felsic volcanic rocks in Imbin Inlier (basement to Earaheedy Group north of Stanley Fold Belt) [e]
	~ ~ ~ ~ ~ ~ ~ ~ ~ ~ ~ ~ **1970–1790 Ma** ~ ~ ~ ~ ~ ~ ~ ~ ~ ~ ~ ~		
1830–1780	• **Capricorn Orogeny** • Convergence of Yilgarn and Pilbara Cratons • Deformation of Yerrida Group along Goodin Fault [a]		
~ 1830–1840	• Deposition of Mooloogool Group and eruption of flood basalts (Yerrida Basin)[a,f]		
<1840–~1800		• Deposition of Earaheedy Group (Earaheedy Basin)	• ?Continental breakup and development of passive margin along northeastern Yilgarn Craton
	~ ~ ~ ~ ~ ~ ~ ~ ~ ~ ~ ~ **1790–1760 Ma** ~ ~ ~ ~ ~ ~ ~ ~ ~ ~ ~ ~		
1790–1760		• Deformation of Earaheedy Group, formation of Stanley Fold Belt, presumably in later stages of Yapungku Orogeny	• **Yapungku Orogeny, 2^{nd} phase (D_2)**, Paterson Orogen • Convergence of Northern Australian and Western Australian (Yilgarn and Pilbara) Cratons [c]
	~ ~ ~ ~ ~ ~ ~ ~ ~ ~ ~ ~ **1760–1220 Ma** ~ ~ ~ ~ ~ ~ ~ ~ ~ ~ ~ ~		
1620	• Start of deposition of Edmund Group		• ?Start of deposition of Scorpion Group, some syndepositional normal faulting
1465	• Intrusion of dolerite sills into Edmund Group	• Folding and erosion of older rocks	
	~ ~ ~ ~ ~ ~ ~ ~ ~ ~ ~ ~ **1220–820 Ma** ~ ~ ~ ~ ~ ~ ~ ~ ~ ~ ~ ~		
<1211	• Start of deposition of Collier Group		

Table 1. (continued)

Age (Ma)	*To west*	*Western Earaheedy Basin*	*To east and north*
?1200–1100		• Deposition of Salvation Group (lower "Savory Group") in central Western Australia	
1250–900			• Deposition of Throssell Group, Paterson Orogen
~1130–800			• **Miles Orogeny**, Paterson Orogen. Folding and regional deformation due to southwest-directed compression
1070	• Emplacement of mafic sills and dykes into Collier and Edmund Groups[g]	• Intrusion of Salvation Group by mafic sills and dykes (Glen Ayle Dolerite; Prenti Dolerite). Extrusion of parts of Bentley Supergroup in Musgrave Complex (1060 Ma). ?Intrusion of Glenayle Dolerite and Prenti Dolerite into eastern Earaheedy Basin	
<1050			• Deposition of Lamil Group, Paterson Orogen
<1070, >755	• **Edmundian Orogeny** Deformation of Bangemall Supergroup[h]		
	~ **Phanerozoic** ~		
Late Mesozoic		• Development of palaeodrainage system across Western Australian interior, after some periods of ferruginous and siliceous duricrust development	
Late Eocene – Miocene		• Waning of interior palaeodrainage system, last significant flow probably late Miocene	
24000 – 15000 yrs bp	• Last major dune activity, formation and mobilisation of major dunefields across Western Australia, during arid glacial maximum		

REFERENCES:
(a) Pirajno et al. (2004)
(b) Pirajno et al. (1998)
(c) Bagas (2004)
(d) Occhipinti et al. (2004)
(e) Pirajno, unpublished data
(f) Rasmussen and Fletcher (2002)
(g) Wingate (2002; 2003)
(h) Martin and Thorne (2001)

biotite–sericite. Where least altered, it contains about 30% quartz, 40% albite, and 30% K-feldspar (Bunting et al., 1980). In some cases, the unit is partially to pervasively silicified and cut by quartz and sinuous sericite veinlets. Clay mineral phases, dominated by smectite, fill microfractures or replace early Fe–Mg silicates (e.g. biotite). In places, the overall texture is distinctly cataclastic and fractures are commonly infilled with microcrystalline or fine-grained quartz or, locally, with an unidentified dark material, or with sheafs of fibrous amphibole.

Quartz–albite–microcline(–garnet–aegirine-augite) granite or syenite (*Ægtea*) is medium-grained and pink to brick-red. This unit contains up to 55% modal volume of orthoclase crystals, up to 7 mm long, and up to 15% modal volume of zoned alkali pyroxene (sodic hedenbergite or aegirine-augite), associated with titanite and inclusions of apatite crystals up to 2.5 mm long. Albite (approximately 25% by volume) occurs as small grains (0.1 to 0.8 mm) in the groundmass. Other accessory minerals include green fibrous amphibole, zircon, and andradite garnet. Quartz is anhedral and locally exhibits deformation lamellae. In places, this granitoid has a mylonitic fabric with or without brecciated texture, in which turbid, early coarse-grained albite is embedded in a foliated quartz-rich matrix.

The quartz–microcline(–albite–stilpnomelane) granite or quartz syenite (*Ægtex*) is medium-grained, pink to brick red, fractured, and characterized by a distinct polygonal and granoblastic texture. It is transitional to the quartz–albite–microcline(–garnet–aegirine-augite) granite, discussed above. This rock is dominated by euhedral to subhedral albite and quartz, roughly in equal proportions, overprinted by microcline crystals. Accessory minerals include alkali pyroxene, probably aegirine-augite or sodic hedenbergite (brown to bright green pleochroism), fibrous amphibole (actinolite–tremolite), zircon, and titanite. The alkali pyroxene is interstitial to the albite–quartz–microcline assemblage and is commonly replaced by the fibrous amphibole. Millimetre-wide, anastomosing microbreccia zones containing grains of fractured quartz, feldspar, fibrous amphibole, prehnite, and minor epidote, cemented by iron oxides are locally present. These microbreccias are suggestive of pseudotachylite veinlets. Bunting et al. (1980) reported the presence of fluorite along fractures.

Greenstone *(Ab, Abe, Abh, Af, Afp)*

The eastern branch of the north-northwesterly trending Yandal greenstone belt extends from Millrose onto Nabberu – Granite Peak, along the Lockeridge Fault. On Nabberu, rocks of this greenstone belt are poorly exposed or are covered by ferruginous duricrust. The main rock types are metamorphosed mafic and ultramafic rocks (undivided; *Ab*), metabasalt (*Abe*), metamorphosed felsic volcanic rock (*Af*), and metamorphosed feldspar porphyry (*Afp*).

Undivided metamorphosed mafic–ultramafic rocks (*Ab*) do not outcrop on Nabberu – Granite Peak, but are interpreted from aeromagnetic data on Nabberu. Metabasalt (*Abe*) outcrops along the east side of the Lockeridge Fault and is intruded by thin, sheared, 340°-trending, granitic dykes that are probably apophyses emanating from the surrounding hornblende-bearing quartz monzonite. On the basis of aeromagnetic and subsurface data from drillholes, this metabasalt is also interpreted to flank the northern and eastern sides of the hornblende-bearing quartz monzonite. The metabasalt is fine grained, foliated, commonly chloritized, and consists of actinolite, skeletal plagioclase laths, and unidentified crystallites in a fine-grained felted groundmass composed of actinolite, chlorite, quartz, epidote, and calcite. In plane-polarized light the basaltic texture is clearly recognizable. Actinolite is interpreted as a late phase, probably pseudomorphing igneous pyroxene.

Where the metabasalt is mylonitic it consists of quartz-rich laminae or ribbons alternating with quartz–zoisite–clinozoisite–chlorite. Rotated mantled porphyroclasts of quartz suggest a possible sinistral shear sense (Passchier and Trouw, 1996). In places, the deformed metabasalt is cut by quartz vein stockworks and exhibits calc-silicate-type alteration that overprints an original foliation and is in turn deformed by a later mylonite-like fabric. There is euhedral tourmaline in some samples and it is locally abundant (e.g. at Horse Well Prospect; MGA 271223E 7130625N). It is locally overprinted by a late-stage actinolite. The calc-silicate alteration is characterized by two dominant assemblages. One consists of sericite–zoisite–clinozoisite–garnet–diopside–titanite. Granulated quartz is present in microfractures. A possible generalized paragenetic sequence, based on textural relationships, is: diopside → garnet → epidote → quartz. The other assemblage, in samples obtained from rotary air blast (RAB) holes drilled close to the northern contact with the hornblende-bearing quartz monzonite, consists of quartz, biotite, actinolite, chlorite, and feldspar, and forms the quartz–actinolite hornfels (*Abh*).

Metamorphosed felsic volcanic (*Af*) rocks are exposed in small outcrops about 2 km southeast of No 5 Well, on Nabberu. Interpretation of aeromagnetic data indicate that these units extend for at least 15 km southward along the Lockeridge Fault. Feldspar porphyry (*Afp*) outcrops in the Horse Well Prospect area to the west of the Lockeridge Fault (see **Economic geology** below). RAB drill chips of feldspar porphyry from this locality examined in the field reveal intense chloritic alteration. The only petrographic data available for the felsic rocks are from RAB chips of feldspar porphyry, which consists of albite crystals and augens of K-feldspar in a sheared matrix containing quartz, biotite, actinolite, and feldspar.

The deformation and mineral assemblages of the metabasaltic rocks on Nabberu indicate environments of brittle–ductile to ductile regimes ranging from lower-greenschist to mid-amphibolite facies. The presence of diopside and actinolite indicates proximal to intermediate alteration zones (mid-amphibolite and upper greenschist respectively), known to surround lode-gold deposits (Eilu et al., 1999; see **Economic geology** below)

Structure

Four deformation phases (D_1–D_4) have been recognized in the granite and greenstone rocks of the Yandal belt (Wyche

and Farrell, 2000). On NABBERU – GRANITE PEAK, paucity and poor quality of outcrops do not permit a detailed analysis of the deformation history of the Archaean rocks.

On NABBERU, the prominent north-northwesterly trending Lockeridge Fault is a continuation of the Celia Fault on WILUNA (1: 250 000), and may be related to the D_3 event (Wyche and Farrell, 2000). Along this fault, the greenstone and granitoid rocks are mylonitized and, locally, tectonically interleaved with each other, and exhibit a foliation fabric parallel to the fault. Foliation planes in metabasalt and felsic rocks close to the fault trend 300–340°, with either a vertical attitude or dips of about 70° to the east. Quartz veins are common along these foliation planes. A vertical foliation in metamorphosed felsic rocks (*Afp*) trends 300–320°. All of these fabrics may be associated with the D_3 event. A younger foliation (D_4) trends at 010–025° and is best exhibited by the hornblende-bearing quartz monzonite (*Agzq*). Subparallel to and west of the Lockeridge Fault are lineaments that are visible on Landsat imagery.

Several northeast-trending milky white quartz veins are associated with, and parallel to, northeasterly and north-northeasterly trending fractures in the hornblende-bearing quartz monzonite (*Agzq;* Fig. 4).

East-trending aeromagnetic linear features that crosscut the basement to the Earaheedy Group may also be of Archaean age.

Proterozoic geology

Mafic dykes (*Pdy*)

Linear aeromagnetic anomalies on the TMI images of NABBERU – GRANITE PEAK are interpreted as mafic dykes. These linear anomalies, trending north, northeast, and north-northwest, are on the eastern side of the Shoemaker impact structure. The age of these dykes is unclear, but they are interpreted to be Proterozoic by analogy with other dykes in the Eastern Goldfields Province (Hallberg, 1987).

Earaheedy Group

The Earaheedy Basin contains the clastic and chemical sedimentary succession of the Earaheedy Group. The Earaheedy Group unconformably overlies the Archaean Yilgarn Craton and, in the west, the Palaeoproterozoic Yerrida Basin (Fig. 1, Table 1). Sedimentary rocks that may be outliers of the Earaheedy Group are exposed to the south and southwest of the present margin, overlying the Yilgarn Craton and the older Yerrida Basin (2.17 Ga Windplain Group and 1.84 Ga Mooloogool Group; Pirajno et al., in press). The stratigraphy of the Earaheedy Group (Fig. 5) was introduced by Hall et al. (1977), was adopted with minor modifications by Bunting (1986), and subsequently revised by Pirajno et al. (2000) and Jones et al. (2001). The availability of drillcore from mineral exploration projects contributed considerably to the elucidation of the Earaheedy Group stratigraphy. This, together with continuing fieldwork, has led to some lithostratigraphic revision since 1986. In the revised terminology, the Chiall Formation replaces the Wandiwarra Formation and the Princess Ranges Quartzite, which now have member status (Hocking et al., 2000). The Karri Karri Member, which on NABBERU is shown as part of the Windidda Formation, is now considered to be part of the Chiall Formation, whereas the Windidda Formation is considered to be a lateral facies equivalent of the Frere Formation (Fig. 5). On GRANITE PEAK, the lithostratigraphy for the Wandiwarra and Princess Ranges Members can be equated with the usage on NABBERU.

The Earaheedy Group has an estimated maximum thickness of about 5 km, and consists of the lower Tooloo Subgroup and the upper Miningarra Subgroup. The Tooloo Subgroup includes, in ascending order, the Yelma, Frere, and Windidda Formations, and the Miningarra Subgroup comprises the Chiall and Wongawol Formations, Kulele Limestone, and the Mulgarra Sandstone. On NABBERU – GRANITE PEAK, only the Yelma, Frere, Windidda, and Chiall Formations are exposed.

Age constraints

The Earaheedy Group overlies the Mooloogool Group (c. 1.84 Ga; Rasmussen and Fletcher, 2002) and Windplain Groups (2.17 Ga; Woodhead and Hergt, 1997) on THADUNA (Pirajno and Adamides, 1998) and MOUNT BARTLE (Dawes and Pirajno, 1998). The youngest ages of detrital zircons obtained by sensitive high-resolution ion microprobe (SHRIMP) U–Pb dating are 1.8 Ga in the Mulgarra Sandstone (Fig. 2; Halilovic et al., 2004) and 2.02 Ga in the Yelma Formation at the base of the Tooloo Subgroup on NABBERU (Nelson, 1997).

Lead–lead mineralization ages of 1.65 Ga and 1.77–1.74 Ga respectively are recorded from the Magellan deposit in outliers of Yelma Formation overlying the Yerrida Basin and the Sweetwaters Well Member on MERRIE (Richards and Gee, 1985; Teen, 1996). The 1.77–1.74 Ga ages may reflect the deformation event that formed the Stanley Fold Belt, which provides a possible further minimum age constraint for the Earaheedy Basin. Deformation in the Stanley Fold Belt is tentatively attributed by Pirajno et al. (2000) and Jones et al. (2000) to the second phase of the Yapungku Orogeny (1790 to 1760 Ma; Smithies and Bagas, 1997; Bagas and Smithies, 1998; Bagas et al., 2000). This orogeny records the initial collision of the North Australian and West Australian Cratons (Myers et al., 1996; Li, 2000). Stromatolite taxa of the Earaheedy Group (Grey, 1994) are broadly similar to taxa in the Duck Creek Dolomite of the Wyloo Group (c. 1.84–1.89 Ga; Pidgeon and Horwitz, 1991).

From the above evidence, we conclude that the depositional age of the Earaheedy Group must be c. 1.8 Ga; however, these age constraints are at odds with Pb–Pb whole-rock ages of c. 2.01 Ga and 1.95 Ga (Russell et al., 1994; Karhu and Holland, 1996) obtained from carbonate units of the Sweetwaters Well Member, and the $\delta^{13}C_{carb}$ positive excursion of +2.0‰, indicating an age of about 1.9 Ga in the same carbonate rocks (Lindsay and Brasier, 2002).

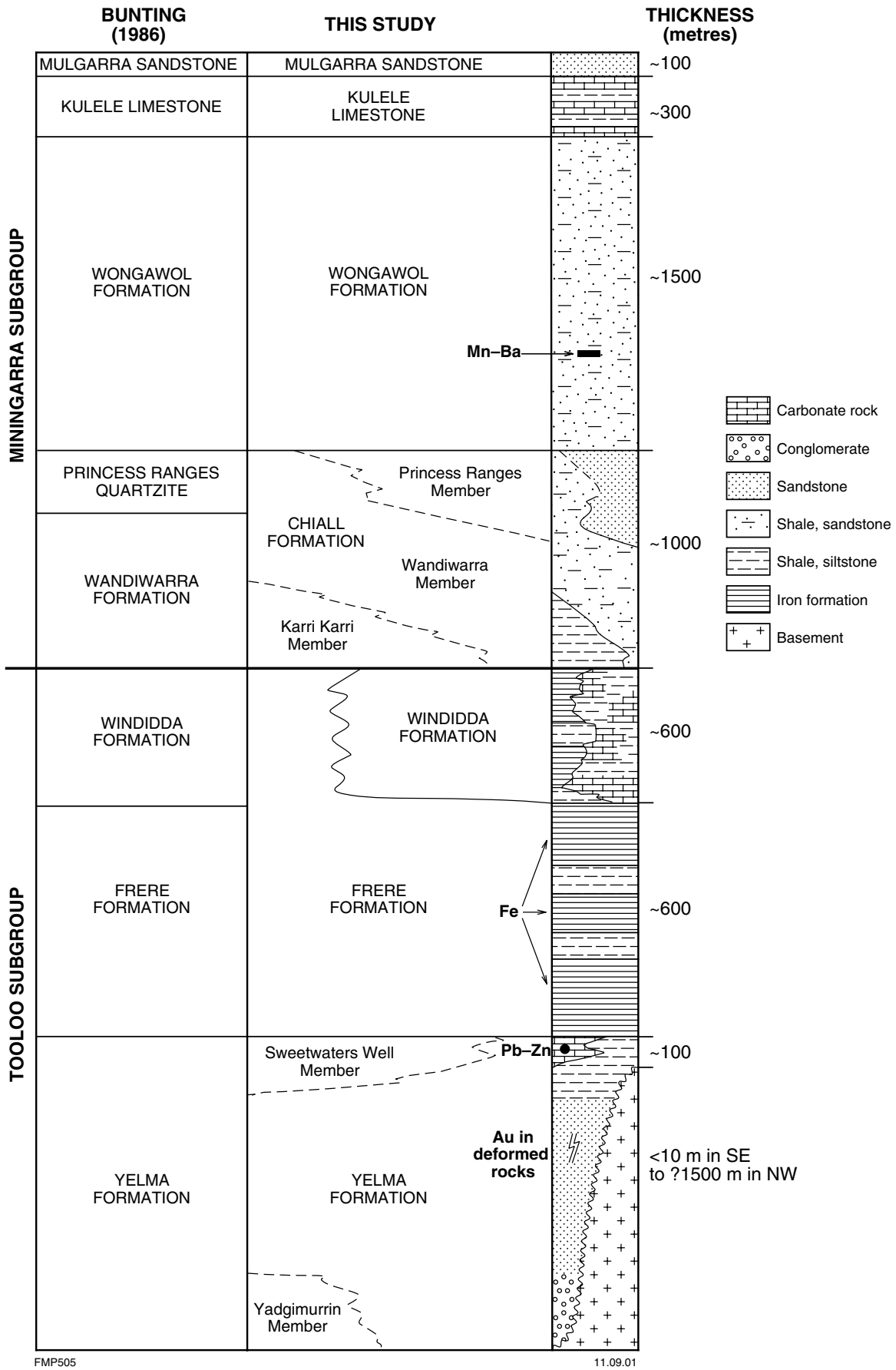

Figure 5. Simplified stratigraphy of the Earaheedy Group

Yelma Formation (*PEy*, *PEyw*, *PEya*)

The Yelma Formation is the basal unit of the Earaheedy Group and is poorly exposed in the south and central parts of Nabberu. On Granite Peak, the Yelma Formation, although unexposed, is inferred to extend from Nabberu into the southwest corner of the map sheet. The Yelma Formation is dominantly composed of sandstone and shale with lesser amounts of siltstone and conglomerate, and stromatolitic dolomite in the upper parts of the succession (Sweetwaters Well Member). At the surface, this stromatolitic dolomite is typically altered to chert. The upper contact with the Frere Formation is marked by the first major occurrence of chert or granular iron-formation (Bunting, 1986), although in places stromatolitic forms persist between granular iron beds for up to 5–6 m above the contact (e.g. drillhole TDH 26; MGA 256600E 7166400N). The thickness of the Yelma Formation is highly variable. In the southeast part of the Earaheedy Basin, the formation is only a few metres thick, but it appears to be much thicker (>350 m) to the west, on Thaduna (Pirajno and Adamides, 1998), and adjacent to the Stanley Fold Belt on the northen margin of the Basin. Bunting (1986) proposed a thickness of 1500 m on the western part of Stanley (1:250 000) and the formation is probably between 500 and 1000 m thick on Rhodes, even after allowing for considerable structural repetition (Pirajno and Hocking, 2000). On Nabberu – Granite Peak, the Yelma Formation is probably around 400 m thick.

On Nabberu – Granite Peak, undivided Yelma Formation (*PEy*) consists of interbedded shale and sandstone, and stromatolitic dolomite. The stromatolitic dolomite at the top of the Yelma Formation is designated the Sweetwaters Well Member (*PEyw*; Hocking et al., 2000). The Sweetwaters Well Member is about 100 m thick and consists mainly of stromatolitic dolomite with sandy dolomite and dolomitic feldspathic sandstone beds at top and bottom of the dolomitic succession. The dolomitic feldspathic sandstone unit at the top of the dolomite grades eastward to a micaceous sandstone and is overlain by granular iron-formation rocks of the Frere Formation. The lower contact is marked by about 15 m of transitional interbedded sandstone and dolomite passing upward to a sandy and feldspathic dolomite unit that contains quartz, microcline, albite, chert, and micritic dolomite embedded in a coarse-grained dolomite cement. The Sweetwaters Well Member dolomite is light grey to grey, massive to algal laminated, commonly with stromatolite forms. In northwest Nabberu, the Sweetwaters Well Member was intersected in a number of drillholes sunk through the Frere Formation by Renison Goldfields Consolidated (Edgar, 1994; Feldtmann, 1995; Dörling, 1998), where it is about 100 m thick. A cross section through the drillsites is shown in Figure 6 (see also section on **Economic geology** below). Samples of stromatolitic dolomite collected from drillcore show two phases or domains of dolomite; one is an aggregate of coarse-grained dolomite crystals, the other is microcrystalline (micritic) and is associated with microbial laminae. The coarser grained dolomite has intergranular microcrystalline quartz and sericite. In some cases, micritic dolomite forms peloids that are cemented by chalcedonic quartz. Locally, the carbonate material is replaced by cryptocrystalline quartz (chert) and chalcedonic quartz.

Scattered outcrops of the Sweetwaters Well Member, along the southern shore of Lake Nabberu about 9 km east-northeast of Horse Bore, are commonly chertified, except for an area along a small tributary (MGA 272359E 7145365N) where there are good exposures of subhorizontal stromatolitic dolomite. Here, the dolomite exhibits fine microbial laminae and includes the stromatolites *Murzuna nabberuensis, Omachtenia teagiana* and *Asperia digitata* (Fig. 7; Grey 1984, 1994). Drillcore sections (e.g. TDH 26, Fig. 6) indicate that stromatolites are typically present in metre-scale upward-shallowing cycles. They include *Asperia digitata* (Grey 1984, 1994), which is believed to have grown in a restricted, quiet-water environment, possibly supratidal ponds; *Pilbaria deverella* (Grey, 1984) indicative of moderately high-energy, lagoonal conditions; and *Ephyaltes edingunensis* (Grey, 1994), which formed in deeper quiet water, and *Murgurra nabberuensis* (Grey, 1984), which colonized moderate-energy patch reefs. Details of stromatolite taxa of the Earaheedy Basin are in Grey (1984, 1994).

Sandstone in the Yelma Formation is typically well sorted and composed of well-rounded quartz grains and minor detrital tourmaline and zircon. The rock is grain supported, with a diagenetic microcrystalline quartz or chalcedonic quartz cement.

Quartz sandstone (*PEya*) is in the eastern parts of the central uplift of the Shoemaker impact structure. This rock is cross-bedded and consists of a packed aggregate of rounded quartz grains showing diagenetic quartz overgrowths with minor detrital tourmaline and interstitial recrystallized quartz.

The Yelma Formation was deposited in a fluvial to coastal setting, with carbonates of the Sweetwaters Well Member developing in a saline coastal–lagoonal environment.

Frere Formation (*PEf*, *PEfg*, *PEfs*, *PEfh*, *PEfgt*, *PEfst*, *PEfi*)

The Frere Formation was formally defined and described by Hall et al. (1977). It is an important iron resource (see **Economic geology** below) and records the onset of iron oxide precipitation in the Earaheedy Basin. The formation consists of up to four major granular iron-formation intervals, separated by up to three major shale and siltstone bands (Fig. 8). Minor peloidal carbonate and chert units are also present. The shale bands increase in thickness at the expense of the granular iron-formation, towards the southeast. The upper contact with the Karri Karri Member of the Chiall Formation is transitional and defined as the uppermost major chert, jasper, or iron-formation (Hall et al., 1977). The total thickness of the Frere Formation was estimated by Bunting (1986) at about 1200–1300 m, but field evidence suggests this thickness may be exaggerated due to structural repetition. On Nabberu – Granite Peak, the Frere Formation is considered to have a maximum thickness of 600 m.

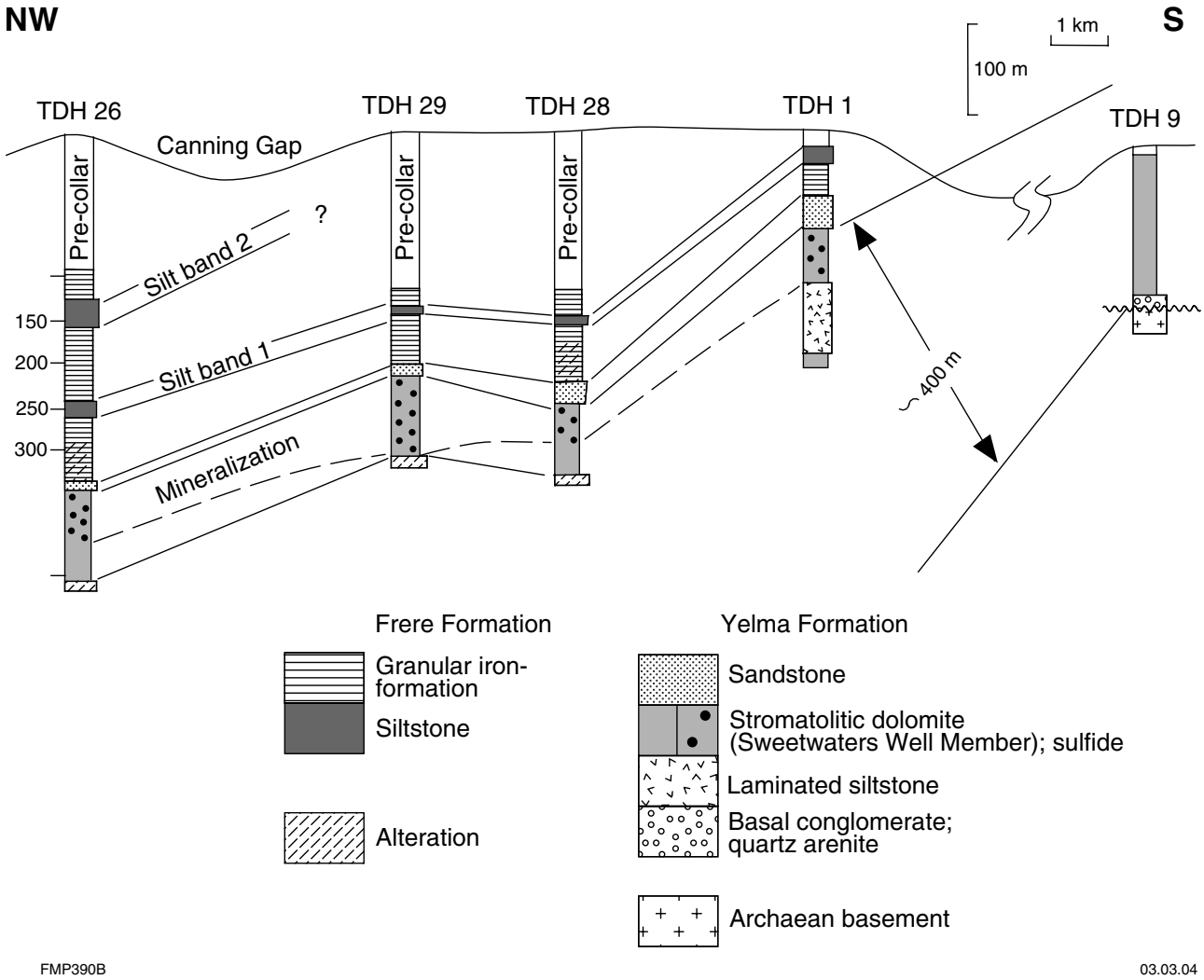

Figure 6. Cross section through TDH series drill sites that intersected mineralized dolomite of the Sweetwaters Well Member, below the Frere Formation. Information from these drillholes was obtained from relogging of core and from mineral exploration reports (references provided in text). Line of section is shown in Figure 28

The Frere Formation consists of alternating beds of hematitic shale, green chloritic siltstone, and granular iron-formation. Granular iron-formation horizons consist of granular iron beds, typically between 0.5 and 20 cm thick, interbedded with jasper, chert, shale, and siltstone (Fig. 9). Drillcore shows that chert intraclasts are common and range in size from 1.5 to 35 cm. Contact between granular iron beds and siltstone units are commonly irregular and typically marked by soft-sediment structures, such as rip-up clasts, and load and flame structures. The scale of the granular iron beds and siltstone banding ranges from millimetres to metres and up to hundreds of metres (micro-, meso-, and macroscale), and is similar to that recorded for banded iron-formations (Trendall, 2002; Fig. 10).

The textural and petrological features of granular iron-formation were described in detail by Hall and Goode (1978) and Goode et al. (1983). Granular iron-formations in the Frere Formation are texturally and mineralogically similar to those in the Lake Superior region, North America. The Gunflint Iron Formation from that region contains microfossils (Gunflint-type microbial communities) that are similar to those in the Frere Formation at Camel Well and in the Windidda Formation at Tooloo Bluff (Walter et al., 1976; Hall and Goode, 1978; Goode et al., 1983; Tobin, 1990). Gunflint-type microbiota are considered to be characteristic of marine subtidal environments (Tobin, 1990). These microfossils consist of contorted or randomly oriented filaments and include *Gunflintia minuta*, *Animikiea septata*, *Eoastrion simplex*, *Eoastrion bifurcatum*, *Huraniospora psilate*, *Kakabekia umbellata* and *Archaeorestis schreiberensis* (Walter et al., 1976; Tobin, 1990).

Granular iron-formation units are characterized by strong magnetic signatures that define major structures in the Earaheedy Basin, even through a significant thickness of overburden. Along the southern margin of the basin, northwesterly trending structures are negatively magnetized, whereas easterly and northerly trending structures, as well as the circular structures that define the Shoemaker structure, are positively magnetized. In the Stanley Fold Belt, strong positive magnetic signatures define deformational structures such as folds, reverse faults, and shear zones. These magnetic signatures help define the extent and approximate geometry of the

exposed margins of the Earaheedy Basin. On the southern margin, the Frere Formation is dominantly unmetamorphosed, undeformed to mildly deformed, and typically forms layers that are shallow-dipping (2–15°) to the north, except near major deformational structures. In the Stanley Fold Belt, the Frere Formation is intensely deformed, with tight folds, sheared limbs, and reverse faults. On Rhodes and parts of Mudan, the Frere Formation is intensely tectonized, forming mylonitic zones that resemble banded iron-formation (Pirajno and Hocking, 2000, 2001).

On Nabberu – Granite Peak, undivided Frere Formation (*PEf*) typically consists of shale, siltstone, granular iron-formation, and chert and jasper beds. The formation is subdivided into intervals dominated by granular iron-formation (*PEfg*), shale, siltstone, and mudstone (*PEfs*), and green chert (*PEfh*). The Frere Formation is typically mapped as undivided (*PEf*) where granular iron-formation is subordinate to shale and siltstone, or where the scale of the interbedded iron-formation and shale is below map resolution. Deformed granular iron-formation, siltstone, and shale are shown as *PEfgt* and *PEfst* respectively. On Nabberu, the Frere Formation is well-exposed in the Frere Range, along the northern side of Lake Nabberu, and in the Shoemaker impact structure, where it forms the inner collar (Pirajno, 2002). In the northeast corner of Granite Peak, exposures of the Frere Formation lie within the Stanley Fold Belt. Here, the granular iron-formation is tightly folded, tectonized, and well laminated, and is termed laminar iron-formation, distinguished as *PEfgt* (Fig. 11). It resembles banded iron-formation, but contains a pervasive fabric that is interpreted to be a tectonic overprint of the original bedding. Lamellae vary from continuous to discontinuous lenses and are typically between 10 and 50 mm thick. Similar laminar iron-formation also occurs on Rhodes (Pirajno and Hocking, 2000) and Methwin (Hocking and Jones, 2002). The limbs of folds in northeast Granite Peak are commonly brecciated and cut by quartz vein stockworks (e.g. about 2 km west of Yampi Well; MGA 345300E 7178295N).

Along the entire eastern sector of the inner ring of the Shoemaker structure, prominent ridges are made up of folded outcrops of massive iron oxides (*PEfi*), which are possibly due to supergene enrichment of peloidal granular iron-formation. In the southeast of the inner collar, the granular iron-formation units form a lens characterized by abundant magnetite that is well defined on TMI images (Pirajno, 2002).

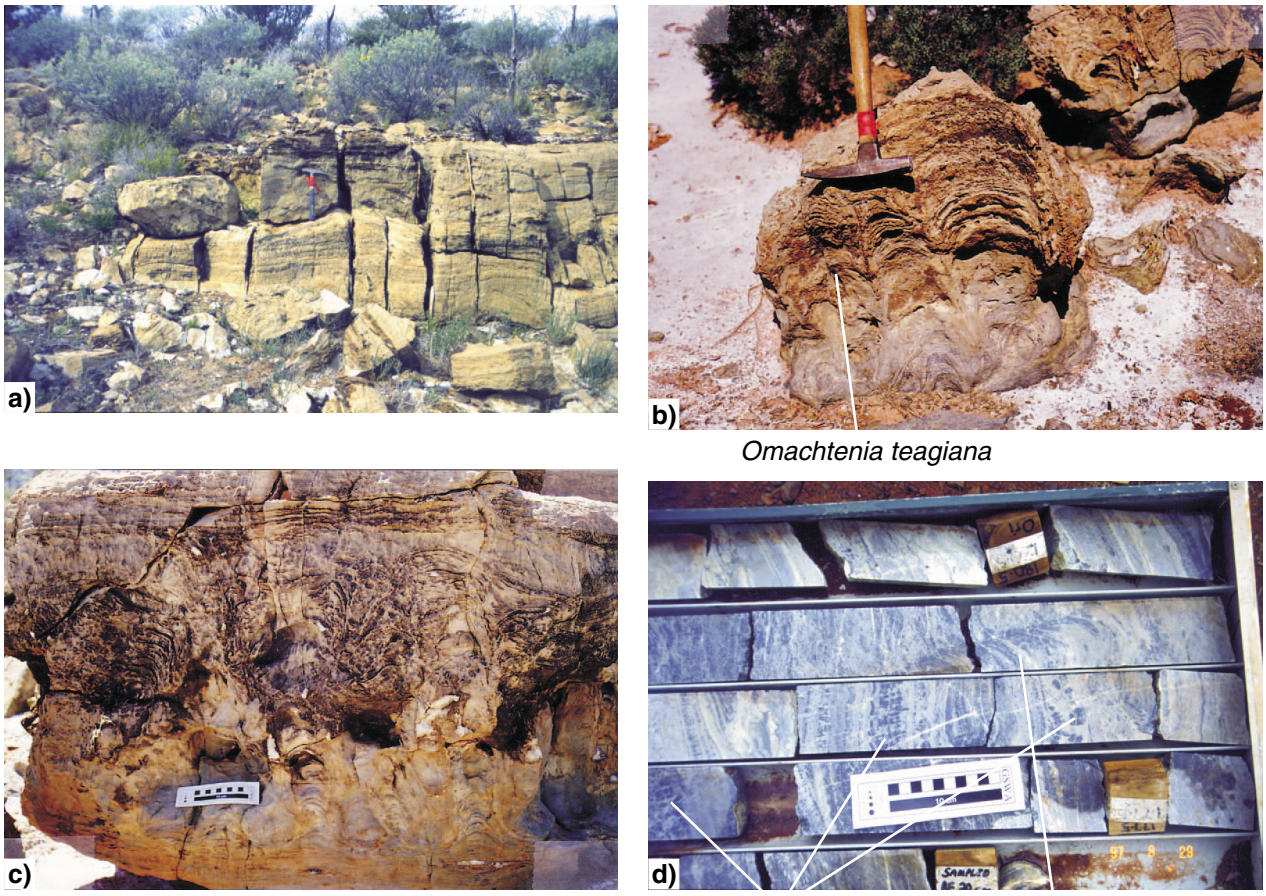

Figure 7. Outcrops of Sweetwaters Well Member stromatolitic dolomite at a locality 4 km northeast of Rabbit Well (MGA 272360E 7145370N): a) microbial laminites; b) *Omachtenia teagiana* (Grey, 1994); c) unidentified stromatolites; d) drillcore from TDH 28 with various stromatolite forms, including *Asperia digitata*, and *Pilbaria deverella* (Grey, 1994; MGA 264200E 7161250N)

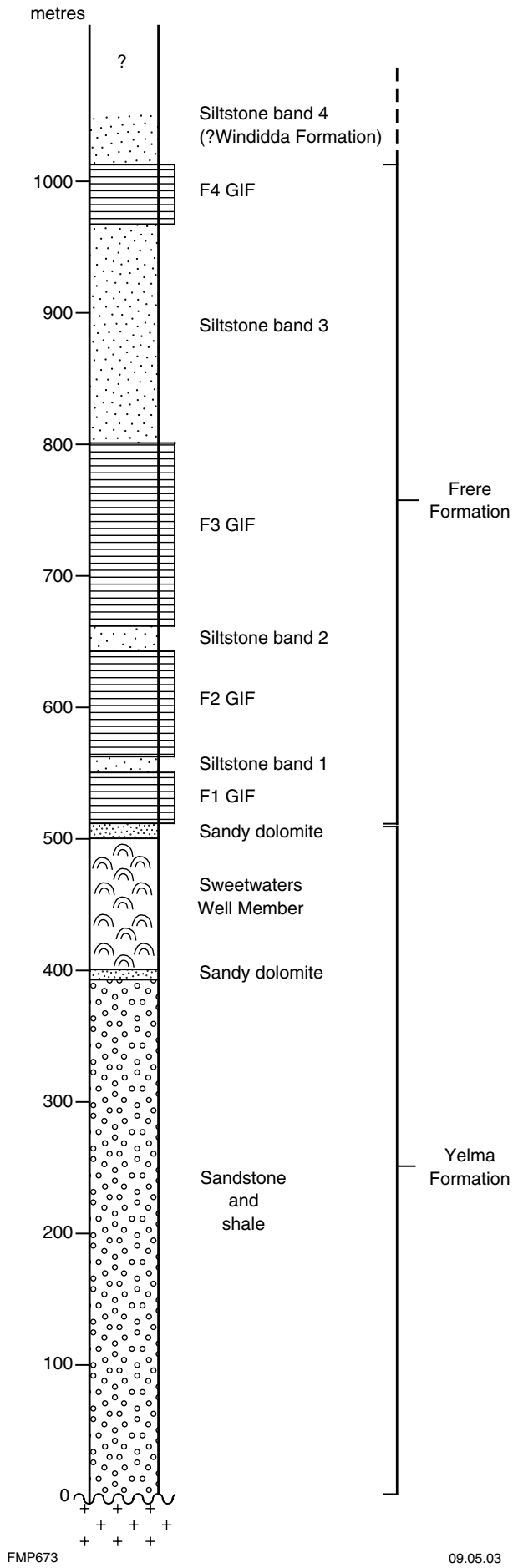

Shale and siltstone *(PEfs)* intervals that separate granular iron-formation beds are similar to those of the Yelma Formation and the Karri Karri Member of the Chiall Formation. They commonly have a bedding fissility, accentuated by weathering. Siltstone is parallel-laminated, and trough and planar cross-laminated (Fig. 12). Ripples are typically lingoidal or sinuous and interference patterns are common. Individual laminae are 1 to 10 mm in thickness. There is massive greenish chert (*PEfh*) in the southwest of Granite Peak, 3.5 km south of Oxby Well. The chert exhibits remnant peloidal textures and quartz-filled fractures, and lies parallel to a northwest trending, negatively magnetized structure. It is interpreted to be granular iron-formation that has been strongly silicified and fractured because of fluid flow along this structure (see **Structure and metamorphism** below).

On Granite Peak, a thin unit containing beds of siliceous peloids is contained within a major shale horizon. Peloids in this unit are commonly strongly attenuated. Interstitial to the peloids are cuspate features that may originally have been glass shards, and this unit may represent a waterlain volcaniclastic deposit. This unit coincides with a northwesterly trending structure. The siliceous nature of the rock and the strong attenuation of peloids may not be a primary feature, but a result of deformation and interaction with hydrothermal fluids.

Granular iron-formation petrography

A typical thin section, sketched in Figure 10c, provides a good example of microscale banding. A granular iron horizon contains a 1 cm-thick band of closely packed hematite peloids and intraclasts, cemented by orthochemical cryptocrystalline silica (chert) or allochemical chalcedony, or a combination of both. This band is overlain and underlain by 1–4 mm-thick laminae of pale green silt composed of green iron-rich chlorite (Fig. 13b), anhedral hematite, abundant disseminated euhedral magnetite crystals, and angular quartz, overprinted by carbonate, and lenticles of chlorite–quartz.

Individual granular iron-formation beds consist of chert (cryptocrystalline silica), iron oxides (hematite or magnetite or both; Figs 13c–e), microplaty hematite (Fig. 13f), and jasper (cryptocrystalline silica with finely disseminated hematite) peloids in a cherty, chalcedonic (allochemical) or jasperoidal (orthochemical) cement (Figs 13a–c). Peloids commonly exhibit concentric laminae, especially where the peloids are partially replaced by microcrystalline quartz (Figs 14a–d). Hematite is commonly replaced by magnetite in iron-formation that has been deformed in the Stanley Fold Belt, although in weathered rocks this magnetite is partially replaced and overprinted by martite–hematite and maghemite. The

Figure 8. Simplified stratigraphic column of the Yelma and Frere Formations; compiled from drillcore and outcrop information. The granular iron-formation (GIF) has four distinct bands (F1 GIF to F4 GIF, bottom to top respectively), with at least three intercalated shale–siltstone bands (siltstone band 1 to 3). The topmost siltstone band could belong to the Windidda Formation

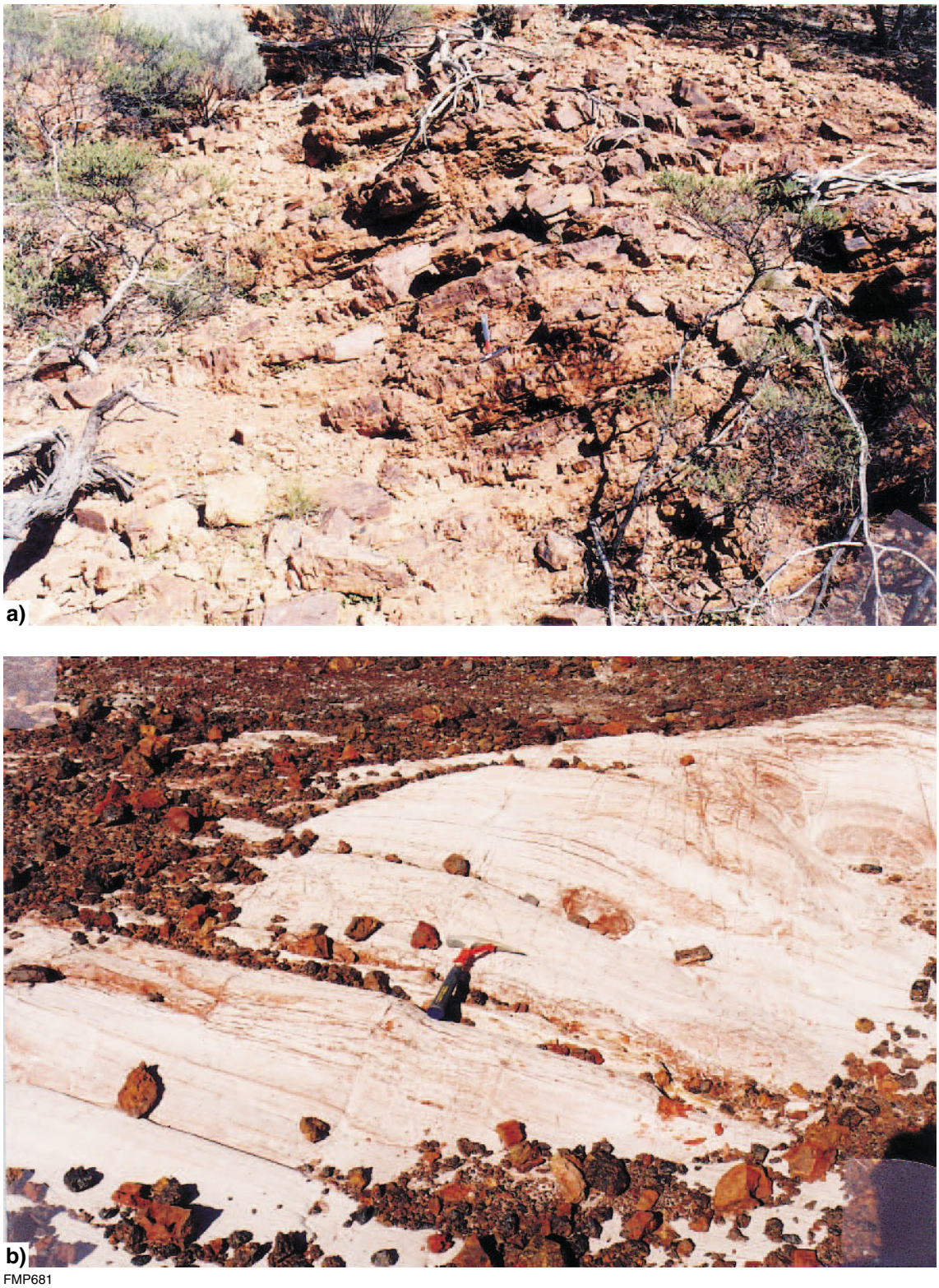

FMP681

Figure 9. Outcrops of granular iron-formation with intercalated siltstone beds: a) in the Frere Range (MGA 280500E 7133900N) and b) in the northeast inner collar of the Shoemaker impact structure (MGA 293300E 7145700N). Compare these outcrops with the granular iron-formation and intercalated siltstone intersected in drillcore shown in Figure 16

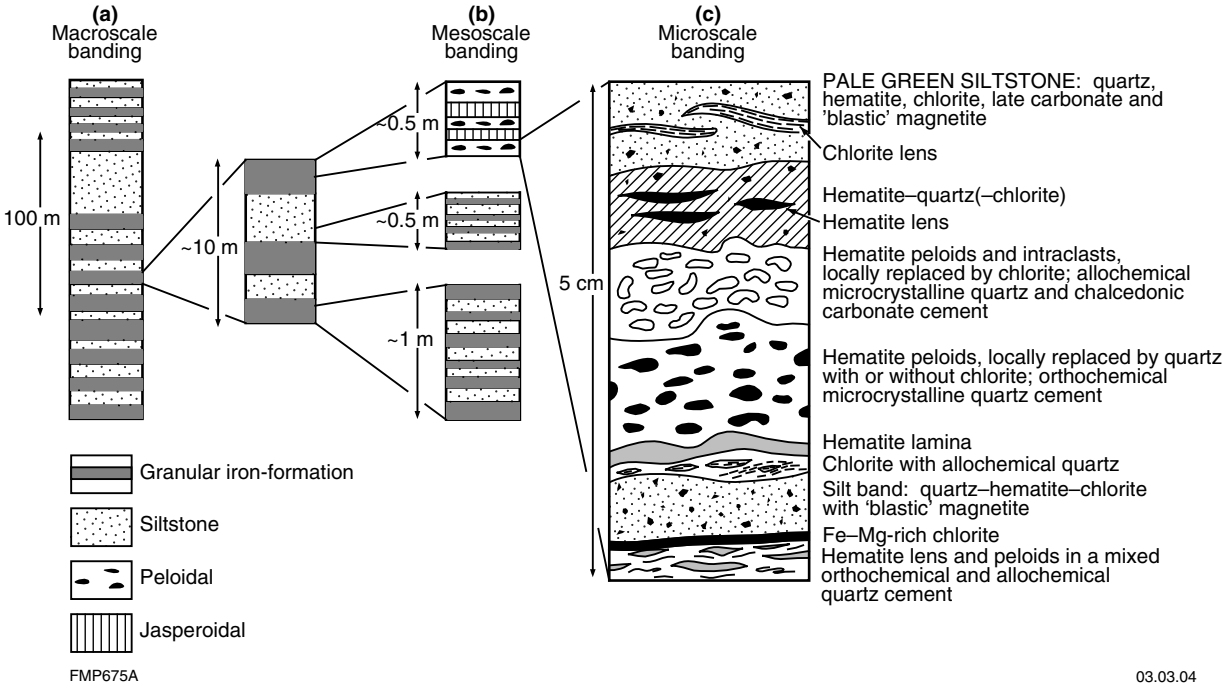

Figure 10. Macro-, meso-, and microscale banding of Frere Formation beds: a) macroscale and b) mesoscale banding illustrated schematically; c) microscale banding in a thin section of typical granular iron-formation (sample 148363; long side is about 5 cm; (from the bottom) hematite peloids cemented by quartz, closely-packed hematite peloids cemented by quartz and carbonate, a siltstone band composed of pale-green chlorite, carbonate, and quartz grains

Figure 11. Outcrop of laminar granular iron-formation in northeast GRANITE PEAK (MGA 343350E 7177830N). Light-coloured bands are chert

FMP691

Figure 12. Cross-laminated siltstone interbedded with shale–siltstone horizon in the Frere Formation on Granite Peak (MGA 316380E 7126720N)

sphericity of peloids is highly variable and generally depends on the degree of early diagenetic compaction and lithification. The average spherical dimensions of over one hundred peloids indicate the long axes of the ellipse average 0.52 mm, whereas the short axes average 0.26 mm, with a length to width ratio of 2.0. Peloids commonly contain syneresis cracks infilled with quartz or chalcedony.

Examination of drillcore (e.g. TDH 26) reveals that thin bands (a few centimetres in thickness) of peloidal carbonate are locally intercalated with the granular iron-formation. Typically, carbonate peloids exhibit close packing, are plastically deformed, and are commonly replaced by stilpnomelane with or without euhedral magnetite (Figs 14d–f).

Reflected-light petrographic studies of the granular iron beds reveal that the main iron minerals are hematite (microplaty, blades, and irregularly-shaped blebs), magnetite, maghemite, martite, and goethite (Figs 13e,f). Maghemite and martite are products of the oxidation of magnetite, whereas goethite is related to recent weathering. Magnetite crystals are especially common along faults and in deformed Frere Formation.

A possible paragenesis of the iron minerals is:
Hematite → magnetite → martite–hematite → maghemite → goethite

This sequence is interpreted to have resulted from the deposition of primary hematite, followed by formation of hydrothermal magnetite along fault zones, subsequent oxidation to produce martite and maghemite, and late supergene redistribution of iron to precipitate the goethite.

Alteration of granular iron-formation

Alteration of the Frere Formation is common, especially along faults and in fractures around the Shoemaker impact structure and close to the Lockeridge Fault (Fig. 2). This alteration is manifested by cryptocrystalline (chert), microcrystalline and chalcedonic quartz, and carbonate that replace the iron oxide peloids and the orthochemical ferruginous or jasperoidal matrix. Stilpnomelane and minnesotaite are locally abundant. In places, stilpnomelane forms pervasive replacements. Some of the more typical alteration features are illustrated in Figures 15 and 16.

West-northwest of the Shoemaker structure, diamond drillholes intersected Frere Formation rocks that exhibit varying degrees of stratabound alteration. This alteration consists of more than one phase of pervasive silicification and replacement by stilpnomelane and carbonate (probably dolomite). The paragenesis of this alteration is difficult to gauge because the same alteration minerals appear in more than one event; however, in general, the following paragenetic sequence can be reconstructed, on the basis of petrographic studies:
Hematite peloids → stilpnomelane → chert → carbonate → chlorite–carbonate–magnetite

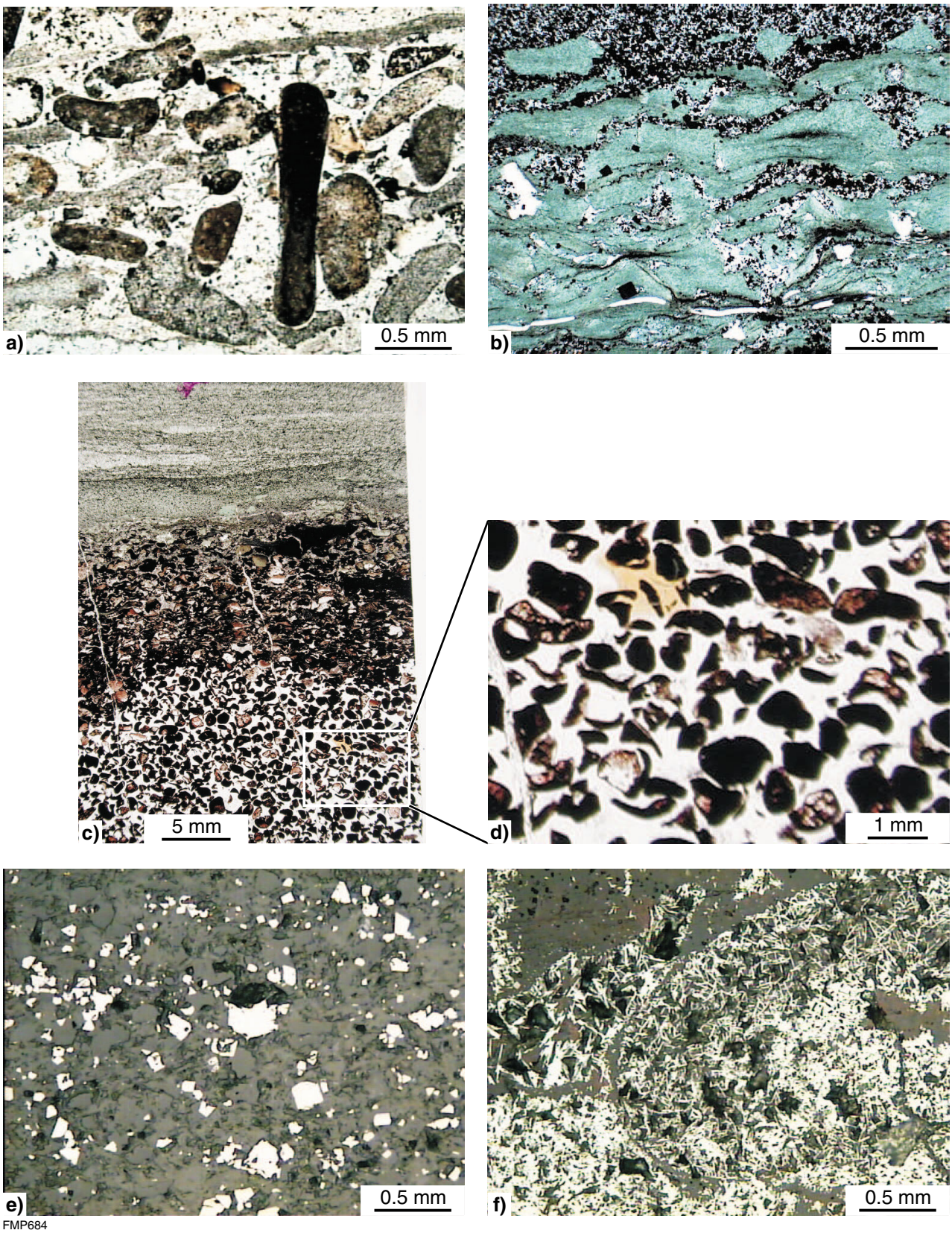

Figure 13. Photomicrographs of granular iron-formation in the Frere Formation: a) sample 153593, intraclast and jasperoidal peloids in a siliceous matrix; b) sample 171735, chloritic shale intercalated with peloidal iron-formation. The pale-green chlorite is a ferroan clinochlore (X-ray diffraction analysis) associated with quartz, kaolinite, and opaque; c) peloidal ironstone; d) detail of (c); e) sample 148363, disseminated euhedral magnetite crystals in chloritic siltstone band; f) sample 148363, detail of peloid composed of microplaty hematite minerals. a) to d) plane-polarized light; e) and f) reflected light

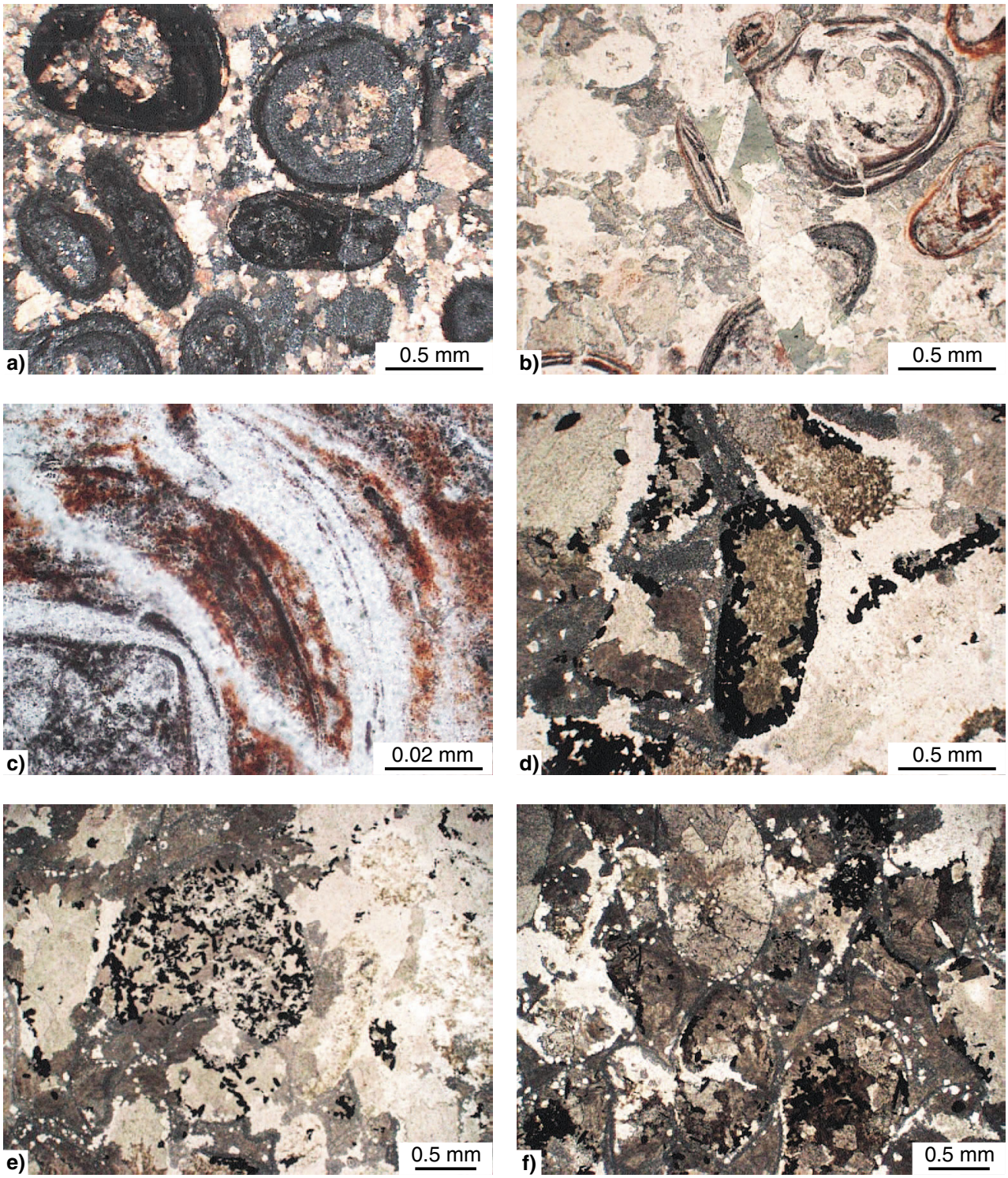

Figure 14. Photomicrographs showing aspects of alteration of granular iron-formation in the Frere Formation: a) sample 148369, peloids partly replaced by cryptocrystalline quartz (chert) and cemented by allochemical dolomite; b) sample 148369, with cross-cutting quartz–chlorite–carbonate veinlet; dark concentric laminae in the peloids are composed of hematite; c) sample 148369, detail of replacement of peloid by cryptocrystalline quartz; d) sample 148368, peloidal carbonate intercalated with granular iron-formation; here the peloid in centre of photomicrograph is replaced by chlorite (core) and microplaty hematite along the margins, surrounding material is dolomite, chlorite, and microcrystalline quartz; e) and f) carbonate peloids partly replaced by hematite and cemented by chlorite, ?orthochemical dolomite and locally stilpnomelane (not visible in this section). All in plane-polarized light, except for a) which is with crossed polars

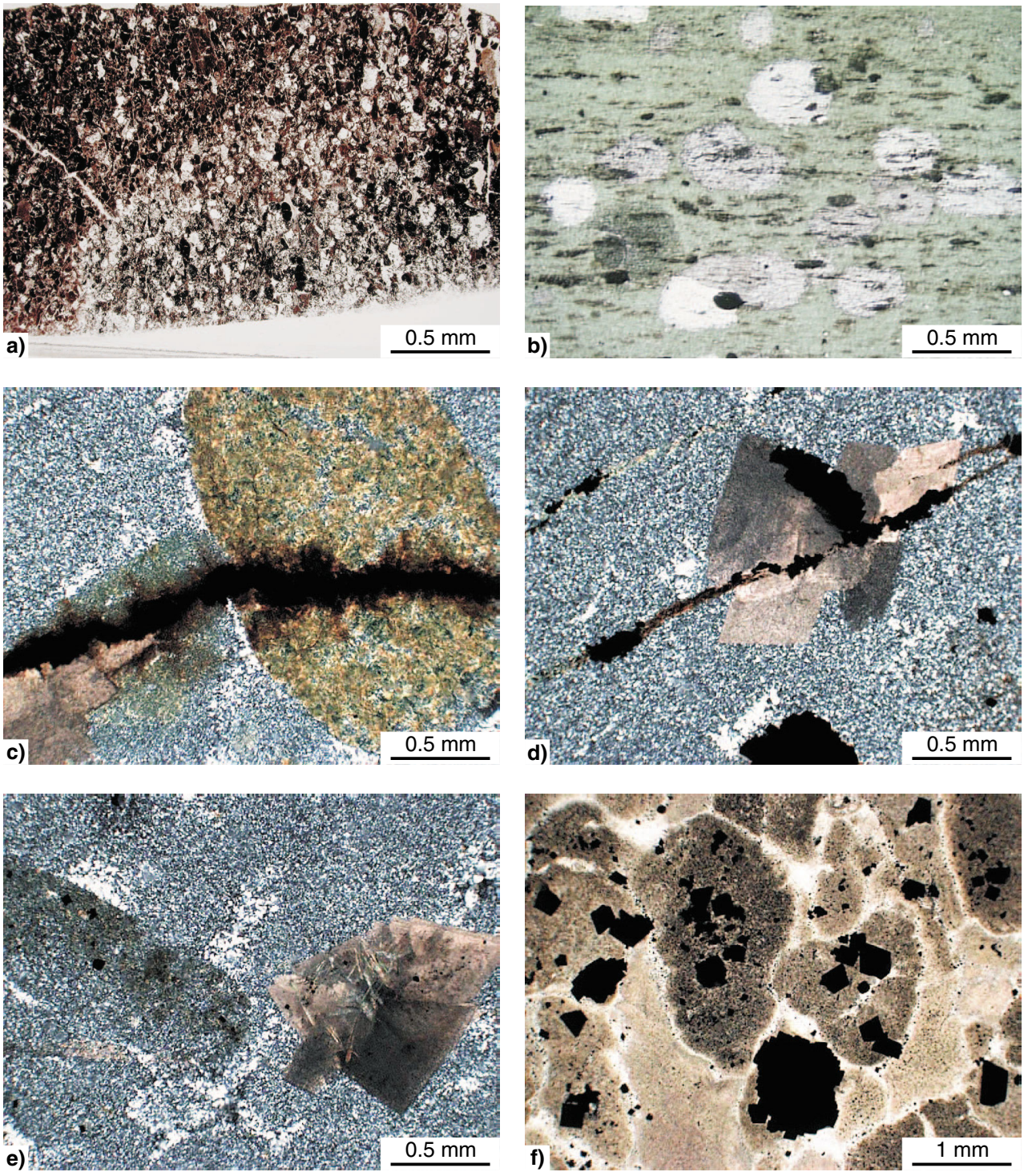

Figure 15. **Photomicrographs showing aspects of alteration of granular iron-formation in the Frere Formation: a) sample 148371, transitional boundary between hematite peloids (lower right) and carbonate replacement (left); b) sample 148359, chloritic shale intercalated with granular iron-formation, showing disseminated carbonate blebs (up to 2 mm across) that overprint the chlorite minerals; c) sample 148366, peloid entirely replaced by stilpnomelane and cut by a veinlet of iron oxides (?magnetite); the matrix is crypto- and microcrystalline quartz; d) sample 148366, pervasively silicified (crypto- and microcrystalline quartz) granular iron-formation overprinted by euhedral dolomite, which is in turn cut by a veinlet of iron oxides and stilpnomelane; e) sample 148366, granular iron-formation pervasively replaced by crypto- and microcrystalline quartz (light-coloured areas), overprinted by euhedral dolomite. Note ghost of peloid on left of image; f) sample 148366, complex alteration patterns are represented in this section; iron oxide peloids are replaced by stilpnomelane and perhaps minnesotaite, the matrix is entirely silicified (chalcedonic quartz is brown and microcrystalline quartz is white), and both are overprinted by euhedral magnetite. a), b), and f) plane-polarized light; c–e) crossed polars**

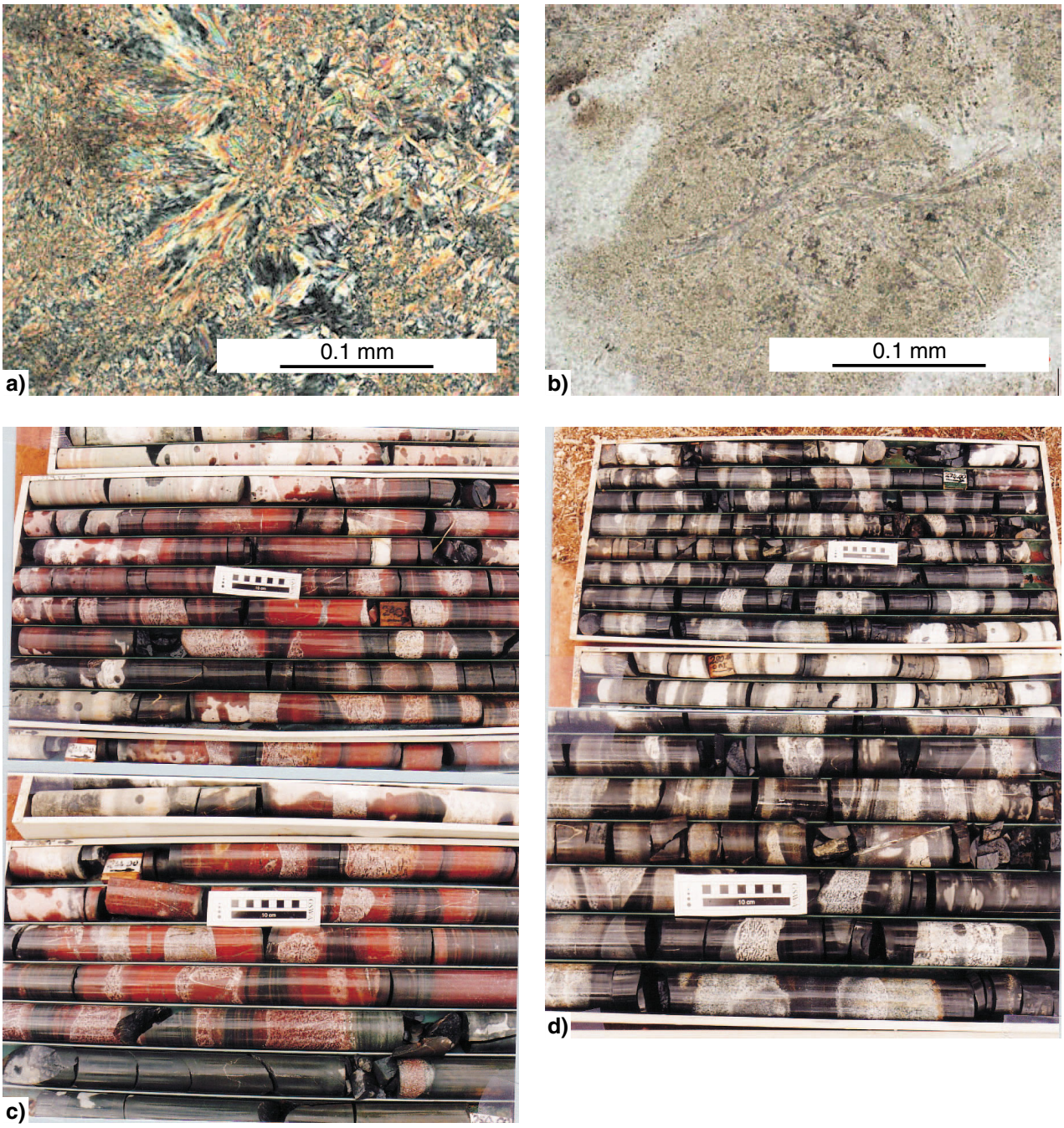

FMP687

Figure 16. Stilpnomelane alteration of granular iron-formation in the Frere Formation: a) photomicrograph showing sheafs of acicular stilpnomelane (crossed polars; sample 148367); b) photomicrograph showing green-pleochroic stilpnomelane crystals cutting through chalcedonic quartz (brown; plane-polarized light; sample 148367); c) drillcore showing typical granular iron-formation beds (red bands with chert intraclasts), intercalated with dark-coloured shale; d) drillcore of silicified and stilpnomelane-altered granular iron-formation and shale interbeds; e) close-up of core showing massive stilpnomelane (dark material) and partially silicified and stilpnomelane-altered peloidal iron-formation

In places, there is evidence of only one event (e.g. carbonatization, Figs 15a,b; or total replacement of the chloritic siltstone by stilpnomelane, Figs 16a,b). In other instances, two or more alteration events are evident, such as partial silicification overprinting peloids that had been earlier replaced by stilpnomelane (Fig. 15e), and by late magnetite (Figs 15d,f). Similarly, all stages of carbonatization are present, from localized development of carbonate rhombs (Figs 15b,c) to more pervasive carbonate alteration. Late alteration phases include magnetite, which overprints dolomite (Fig. 15f) or magnetite–stilpnomelane–chlorite in late fractures that cut across all phases. Peloidal carbonate is also altered, to microcrystalline silica, chlorite, and stilpnomelane, with a late overprint by euhedral magnetite (Figs 15e,f).

Carbonate porphyroblasts and dolomitization are also associated with the sulfide mineralization in the Sweetwaters Well Member stromatolitic dolomite (Yelma Formation), as discussed in more detail in **Economic geology** below**.**

Stilpnomelane, a complex K, Ca, Na, Fe, Mg, Al, hydrous silicate, is common in iron-formation world-wide, (Deer et al., 1965). Stilpnomelane-rich beds have been reported from the banded iron-formation of the Transvaal Supergroup in South Africa (LaBerge, 1966a; Beukes and Klein, 1990) and the Hamersley province in Western Australia (LaBerge, 1966b; Trendall, 2002). At those locations, the stilpnomelane beds are interpreted as products of low-grade metamorphism of volcanic ash (LaBerge, 1966a,b; Beukes and Klein, 1990). The stilpnomelane, silica, and carbonate replacement of beds of granular iron-formation rocks in the Earaheedy Basin is interpreted to be related to K–Si–Ca–CO_2-rich basinal fluids. Stilpnomelane preferentially replaces Fe-chlorite-rich siltstone interbeds and a possible reaction to explain the change from Fe-rich chlorite-dominated siltstone beds to stilpnomelane-dominated beds is (Deer et al., 1965, p. 111):

Fe-rich chlorite (granular iron-formation) + SiO_2 + $K_2O \rightarrow$ stilpnomelane + MgO + Al_2O_3

Depositional setting of granular iron-formation

The deposition of granular iron-formation in the Earaheedy Basin coincided with a decrease in the supply of sand-sized siliciclastic detritus into the basin. Granular iron-formation beds probably formed in shallow waters on a continental shelf. According to Beukes and Klein (1992), ferruginous peloids form by accretion in wave- and current-agitated iron-rich waters and following reworking are deposited with variable amounts of terrigenous contamination. In modern clastic-starved marine shelves, amorphous iron oxide with or without oxyhydroxide peloids (or ooids) appear to form as concretions a few centimetres below the sea floor, as a result of iron- and silica-rich exhalative fluids that rise from the substrate (Heikoop et al., 1996; Donaldson et al., 1999). An alternative view is that the ooids grow from the precipitation of Fe-rich clays that become oxidized to goethite at the sediment–water interface (Donaldson et al., 1999). In either case, the iron oxide – oxyhydroxides alternate with silica to form the concentric laminae. The reason for the iron oxide – silica alternations is not understood, but it may relate to pulses of fluid emission based on episodic temperature variations (high temperature, iron precipitation; lower temperature silica precipitation). Dehydration and diagenesis would produce hematite and, at higher temperatures, magnetite, and the formation of these ooidal or peloidal structures would occur in a geologically short time. Mechanical reworking by wave action with or without strong currents would account for the classic shape of the ooids (Heikoop et al., 1996).

Cross-bedding, locally recognized in granular iron-formation beds, indicates dominantly moderate-energy conditions. Local, peloidal carbonate beds that are intercalated with beds of iron-formation do not show evidence of current transport and may represent a particulate sediment that accumulated in situ (Blatt et al., 1980, p. 469); however, the intercalated shale and siltstone horizons show tractional structures, from Granite Peak southwards.

The granular iron beds, shale, and siltstone all have different iron and silica contents, both within and between units (see **Economic geology** below). This points to a complex, varying interrelationship between clastic influx, dissolved silica, and dissolved iron. The supply of dissolved silica appears to have been variable at all scales, and can be interpreted as a result of fluctuating concentrations. The supply of iron is also interpreted as the result of fluctuating concentrations but with a high proportion of iron remaining in suspension throughout deposition of the Frere Formation. The shale interbedded with granular iron-formation and in major shale horizons may indicate periods where the rates of silica and iron precipitation were low.

Both iron-rich and silica-rich fluids are interpreted to have a distal source. The supply of iron and silica is ultimately related to distal hydrothermal effluents such as a mid-ocean ridge or other subaqueous hot springs (e.g. Isley, 1995; Trendall, 2002). Upwelling currents would transport Fe^{2+} and Mn^{2+} away from the discharge vents and precipitation would occur just above the oxic–anoxic interface, where Fe^{2+} and Mn^{2+} are oxidized to Fe^{3+} and Mn^{4+} respectively (Pirajno and Adamides, 2000). A depositional and tectonic model for the Yelma and Frere Formations (Tooloo Subgroup), based on the stratigraphic, sedimentological, and genetic attributes of the granular iron-formation (Beukes and Klein, 1992; Isley, 1995; Trendall, 2002) is shown in Figure 17.

Detailed studies of field and textural features of granular iron-formation in the Earaheedy Group (Hall and Goode, 1978; Goode et al., 1983; Bunting, 1986) clearly show similarities with the iron-formations of the Superior Province of North America (e.g. Kimberley, 1989). Peloidal and oncolytic textures, orthochemical and allochemical cements, iron-rich chlorite, and the presence of mineral phases such as minnesotaite and stilpnomelane, are common in both. These characteristic features have been interpreted as the result of chemical deposition, followed by mechanical reworking of the sediment, whilst still plastic (gel state; Beukes and Klein, 1990, 1992). Microfossils from the Frere Formation were described by

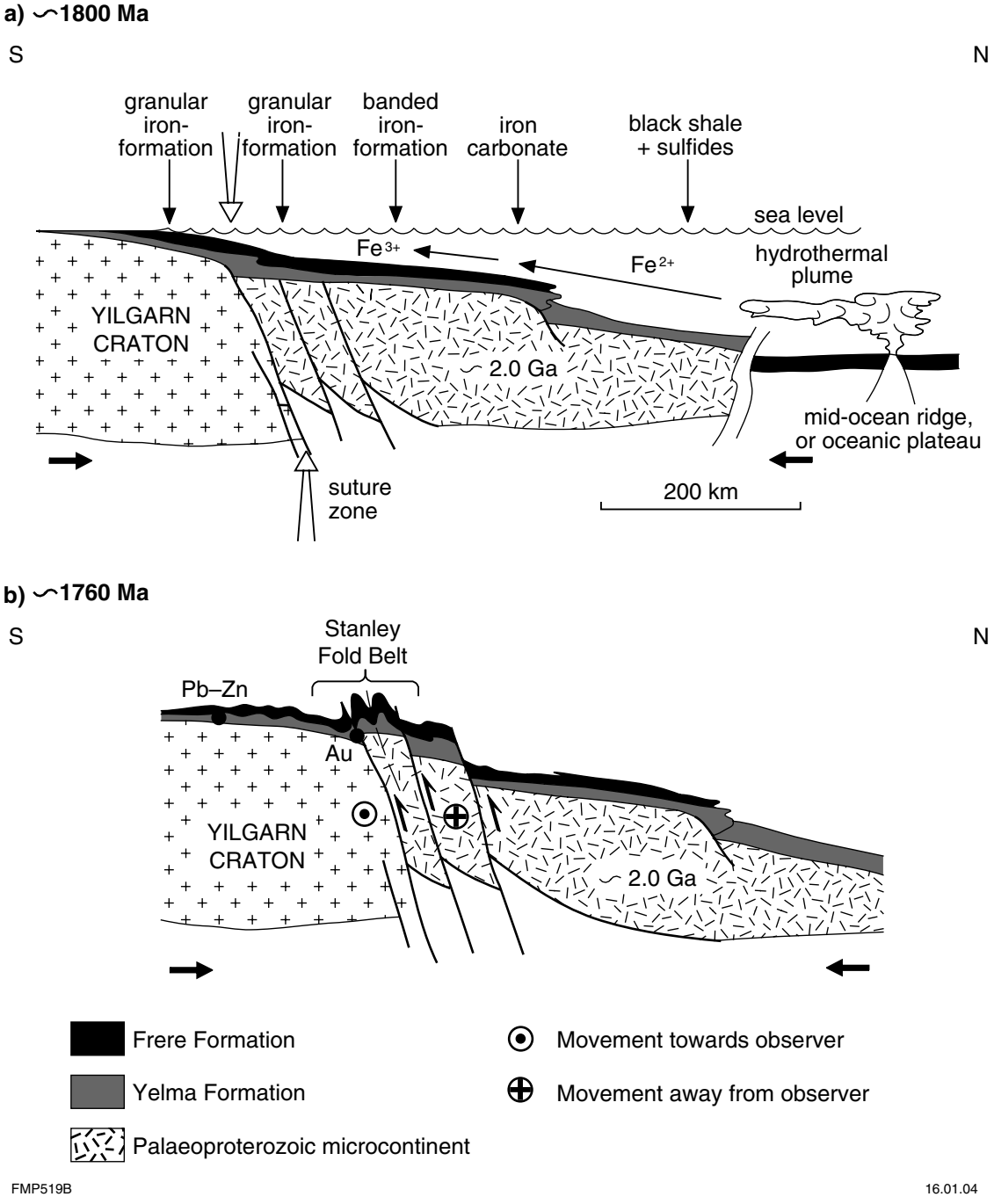

Figure 17. Depositional and tectonic model for the Tooloo Subgroup of the Earaheedy Basin and its contained mineralization: a) at about 1800 Ma iron oxides were deposited on a continental shelf, with granular iron-formation in shallower depths and banded iron-formation deposited further down the continental slope. Lateral equivalents deposited in deeper settings consist of carbonate and sulfide facies. Iron was possibly sourced from a spreading centre; b) at about 1760 Ma, deformation related to far-field tectonics (?Yapungku Orogeny) formed the Stanley Fold Belt and caused southward flow of basinal fluids which resulted in the formation of Mississippi Valley-type (MVT) deposits hosted in shelf carbonates. Minor orogenic-style gold lodes are present in the deformed rocks of the fold belt. After Pirajno and Adamides (2000), modified from Isley (1995)

Walter et al. (1976) and Tobin (1990). The latter author recognized eight microbial assemblages, similar to those in the Gunflint iron-formation of North America and the Duck Creek Dolomite in Western Australia. The model for the origin of the iron-formation proposed by Beukes and Klein (1990; 1992) and Isley (1995) accounts for the large volumes of iron, but it does not explain the association of iron and silica in grains of possible biogenic origin. Some of the grains classified as peloids (Fig. 13d) may have been originally oncolites (Figs 14a–f; Brown et al., 1995). If this is correct, then it is possible that biogenic activity may have played a major role in the development of the granular iron-formation, through a mechanism of bacterial iron oxidation (Nealson, 1982; Brown et al., 1995).

Windidda Formation (*PEd, PEdj*)

The Windidda Formation (*PEd*) contains stromatolitic carbonate, peloidal jasper, jasper, shale, and siltstone. The Karri Karri Member was mapped on NABBERU as part of the Windidda Formation (*PEdk*), but later work, which includes mapping of GRANITE PEAK, interpreted the member as part of the Chiall Formation (*PEck*); however, it is still unclear whether the Karri Karri Member is part of the Chiall Formation or part of the underlying Tooloo Subgroup (Jones, in prep.). To be consistent with current work the Karri Karri Member is discussed here as part of the Chiall Formation (see below). Bunting (1986) considered the Windidda Formation to overlie the Frere Formation. Work subsequent to mapping of both NABBERU and GRANITE PEAK has interpreted the Windidda Formation as stratigraphically equivalent to the upper part of the Frere Formation in the northern part of the exposed Earaheedy Group (e.g. Hocking and Jones, 2002; Jones, in prep.). The contact with the overlying Chiall Formation is defined as the upper carbonate horizon (Hall et al., 1977). The thickness of the Windidda Formation varies laterally. Bunting (1986) estimated the thickness of the type area to be about 800 m. On GRANITE PEAK, the maximum thicknesss is considered to be about 60 m.

The Windidda Formation is typically characterized by poorly defined low relief outcrops. Carbonate beds are commonly less than 50 cm thick. Stromatolite forms range up to 30 cm in diameter and include *Carnegia wongawolensis, Nabberubia tooloooensis, Windidda granulosa,* and *Kulparia* (Grey, 1984). Locally, peloidal jasper is interstitial to stromatolites and is incorporated within stromatolite laminae (Fig. 18; *PEdj*).

The Windidda Formation is interpreted to reflect the development of a carbonate bank along the southern margin of the basin during deposition of the upper part of the Frere Formation (Fig. 5). Interstitial peloidal jasper in stromatolitic carbonate represents washover of granular iron, possibly during storm events.

Chiall Formation (*PEc, PEca, PEcaa, PEck, PEckt, PEcp, PEcs, PEdk, PEcw*)

The Chiall Formation (*PEc*; defined by Hocking et al., 2000) incorporates the Princess Ranges Quartzite and the

FMP692

Figure 18. Domical stromatolite in Windidda Formation with peloidal jasper matrix (MGA 318267E 7134000N)

Wandiwarra Formation of Hall et al. (1977) as members, together with the Karri Karri Member. Both the Princess Ranges Quartzite and Wandiwarra Formation were assigned member status after recognition that they are part of a single depositional package within the Chiall Formation. The boundaries between those two members and the Karri Karri Member is interpreted to be diachronous (Fig. 5). The Wandiwarra and Princess Ranges Members (*PEcw* and *PEcp*) are only used on NABBERU. They were considered inappropriate on GRANITE PEAK because of the lack of stratigraphic control.

The thickness of the Chiall Formation was considered by Bunting (1986) to be up to 1500 m. We suggest that there has been more structural repetition than was estimated by Bunting (1986), and that the maximum thickness of the formation may only be 1000 m. On NABBERU – GRANITE PEAK, the contact between the Chiall Formation and the underlying Frere Formation is transitional and taken as the top of the last major chert bed or iron-formation. Where the Chiall Formation overlies the Windidda Formation, the contact is taken as the top of the last carbonate bed. The top of the Chiall Formation is not present on NABBERU – GRANITE PEAK.

Karri Karri Member (PEdk, PEck, PEckt)

The Karri Karri Member is included in the Windidda Formation (*PEdk*) on NABBERU. However, stratigraphic revision that has taken place since NABBERU was published has meant that it is now included within the Chiall Formation (*PEck*). The stratigraphic relationship of the Karri Karri Member to the Chiall Formation is, however, still unclear (Jones, in prep).

The Karri Karri Member consists of shale, siltstone, and mudstone, with minor development of phyllite (*PEckt)* in the Stanley Fold Belt in the northeast corner of GRANITE PEAK. The Karri Karri Member is interpreted as having a maximum thickness of 600 m. The contact with the underlying Frere Formation is exposed near No. 8 Bore, and is transitional. The boundary with the Windidda Formation is not exposed on GRANITE PEAK.

Lithologically, the Karri Karri Member closely resembles the shale and siltstone in the underlying Frere and Yelma Formations and without other stratigraphic control may be difficult to separate. These rocks are typically thinly parallel laminated, with individual laminae between 1 to 10 mm or cross laminated. The iron-rich nature of the rocks indicates that some iron remained in suspension or solution even after deposition of the last granular iron-formation.

Wandiwarra Member (PEcw, PEca)

The Wandiwarra Member (*PEcw* on NABBERU; undivided) consists dominantly of siltstone and shale, with intercalated sandstone intervals. Fine- to medium-grained sandstone-dominated units on GRANITE PEAK (*PEca*) are probably equivalent to the sandstone-rich part of the Wandiwarra Member on NABBERU. Siltstone and shale horizons are typically well exposed in breakaways, whereas sandstone intervals form resistant cappings on hills.

Sandstone intervals (*PEcw, PEca*) consist of fine- to medium-grained sandstone, which is locally conglomeratic, interbedded with siltstone, mudstone, and shale. Sandstone is poorly to moderately sorted and consists dominantly of rounded to subrounded quartz grains and minor chert fragments. Mudchip intraclasts are common (Fig. 19), especially at the base of individual beds. Sedimentary structures in the sandstone include tabular and trough cross-bedding, flute clasts, and current lineation. Quartz grains may be coated by hematite granules (Fig. 20a); in other places iron oxides replace both quartz and interstitial matrix, and can be an important component at some stratigraphic levels (Fig. 20b). Glauconite peloids vary from spherical to elliptical, with an average size of 0.22 mm. Locally, glauconite is oxidized to brown-coloured iron oxides. It varies from colourless to light-green or brown when weathered, or blue-green when fresh, and is locally replaced by a mosaic of quartz grains, which are not in crystallographic continuity with the surrounding authigenic silica. Glauconite is generally deposited in shallow-marine continental shelves (water depths of 50–500 m), and has a spatial association with iron and manganese formations (Kimberley, 1989; Ostwald and Bolton, 1992; Chafetz and Reid, 2000).

Mudstone dominantly consists of quartz and chlorite, the latter being a replacement product after detrital muscovite (Figs 20e,f).

On NABBERU, rocks of the Wandiwarra Member outcrop in a series of breakaways along the northern edge of the Lake Nabberu system (Fig. 21). Here, the rocks are gently dipping and deformed into mesoscale folds with easterly trending doubly plunging fold axes and with local reverse faults (Figs 21 and 22). There are spectacular mega-ripples in sandstone beds 6.5 km southeast of Bitter Pool, on outcrops of the outer collar of the Shoemaker impact structure (Fig. 23). Three kilometres southwest of Kennedy Bore, brecciated beds of glauconitic sandstone are exposed, which may represent ancient tsunami or seismic shock deposits (Figs 24a,b).

Princess Ranges Member (PEcp, PEcaa, PEcs).

The Princess Ranges Member (*PEcp*) consists of shale, siltstone, and mature quartz arenite and outcrops along the margin of the Shoemaker impact structure on NABBERU. On GRANITE PEAK, mature quartz arenite-dominated horizons (*PEcaa*) are mostly interpreted to be stratigraphically equivalent to the Princess Ranges Member. Sedimentary structures within the sandstone include symmetrical sharp-crested low-amplitude ripples (Fig. 25), current lineation, and tabular cross bedding.

Shale- and siltstone-dominated units (*PEcs* on GRANITE PEAK) in the Chiall Formation are parallel laminated and cross laminated and the laminae are typically 0.5 to 5 cm thick. These units are similar to shale and siltstone horizons in the Frere Formation and Karri Karri Member, except that they commonly contain thin very fine grained sandstone and coarse-grained siltstone beds. The sedimentary structures mentioned above, in both the shale and sandstone intervals, suggest that the Wandiwarra Member and stratigraphically equivalent lower Chiall

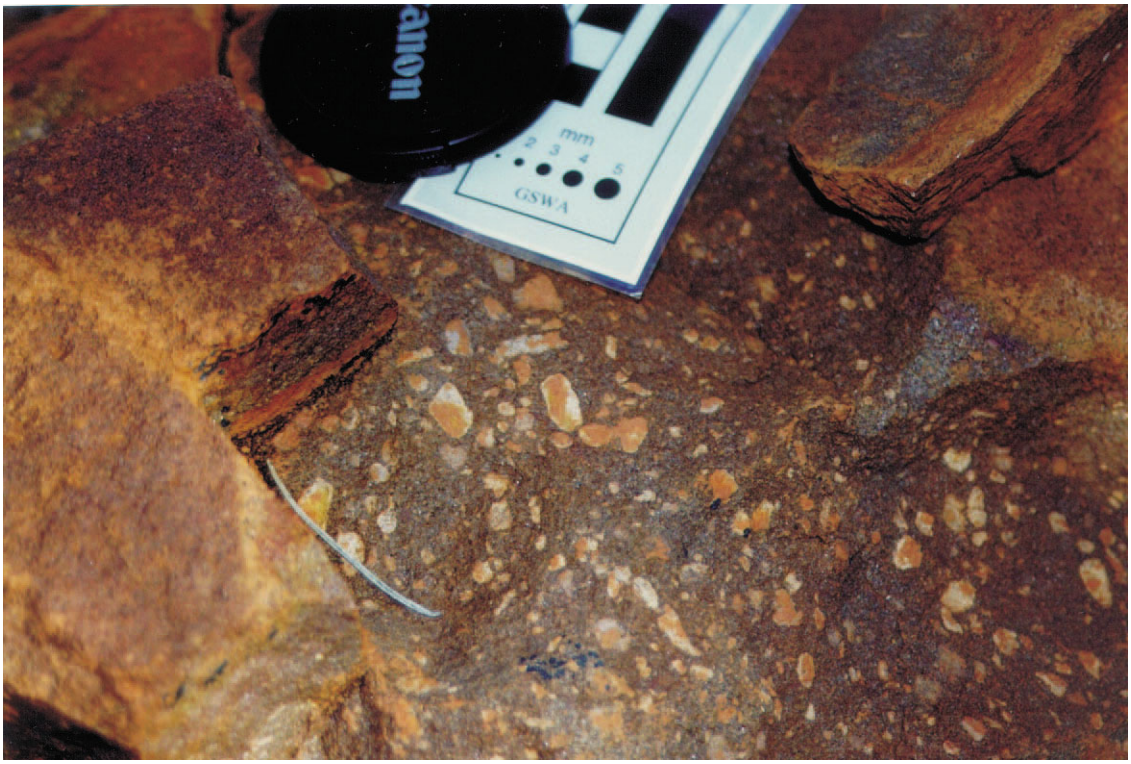

FMP693

Figure 19. Intraclasts of shale in quartz sandstone towards the base of the Chiall Formation on Granite Peak (MGA 38351E 7124574N). Clasts are typically angular and parallel to bedding

Formation on Granite Peak were mostly deposited below wavebase and that shallowing occurred to the south and up the stratigraphic sequence. The Princess Ranges Member and stratigraphically equivalent mature quartz arenite in the upper part of the Chiall Formation on Granite Peak were deposited in an upper shoreface environment. Sandstone beds are probably either tempestites (storm related) or seismites (related to earthquakes; Seilacher, 1969; Rodriguez-Pascua et al., 2000), or both. Conglomeratic beds may be related to tsunamis.

Depositional setting of the Earaheedy Basin

The Earaheedy Group consists of both chemical and clastic sedimentary rocks indicative of a shallow marine to coastal environment, which deepened to the north and northeast (Jones et al., 2000; Pirajno et al., 2000, 2004). The exposed rocks represent only the coastal to upper shelf portion of the continental shelf within the basin. Sedimentary deposits of the continental slope and rise are not exposed, suggesting that much of the original depositional system is buried. Two depositional sequences can be clearly distinguished: the Tooloo Subgroup, which is characterized by granular iron-formation, and reflects the intermittent influx of iron and silica into the basin in a dominantly clastic-starved environment; and the overlying Miningarra Subgroup, which is characterized by fine- to coarse-grained sandstone and reflects an abundant supply of clastic material.

The source of iron and silica for the granular iron-formations in the Frere Formation is a key element in the understanding of the basin, as is the lack of evidence of contemporaneous volcanism and major deformation. Beukes and Klein (1992) and Isley (1995) considered granular iron-formation to be a shallow-water, higher energy equivalent of deeper water banded iron-formation. The northwards-deepening, passive-margin model for the Earaheedy Basin of Pirajno et al. (2000, 2004) and Jones et al. (2000) is consistent with this interpretation. In the case of the Earaheedy Basin, the iron could have been sourced from a hydrothermal effluent, such as a mid-ocean ridge, which was located north or northeast of the presently exposed margin of the basin (Jones et al., 2000; Pirajno et al., 2000, 2004).

The exact cause of the change in depositional dynamics at the boundary between the Tooloo and Miningarra Subgroups is poorly understood and may reflect either sedimentary processes, or tectonism, or a combination of the two. It is interpreted here to have been, at least initially, tectonically driven.

On Wongawol and Windidda, the contact between the Chiall Formation (Miningarra Subgroup) and the underlying Windidda Formation (Tooloo Subgroup) is defined by a pebble- to cobble-sized conglomerate. Deposition of the Miningarra Subgroup therefore reflects an increased influx of fine- to coarse-grained sand-sized detritus. SHRIMP U–Pb dating of detrital zircons by Halilovic et al. (in press) suggests that sandstone in the Earaheedy Group was probably sourced predominantly

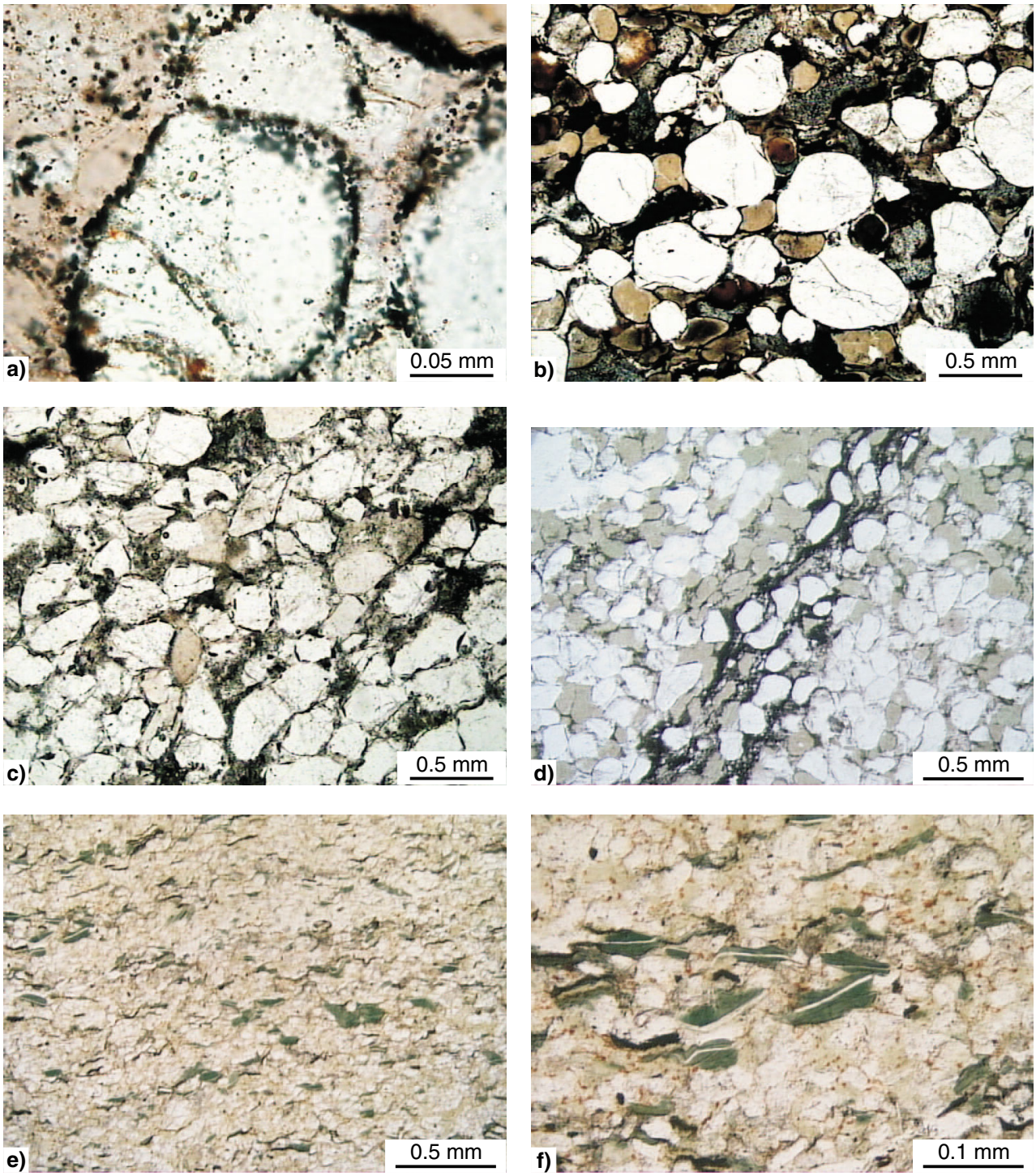

Figure 20. Photomicrographs of rocks from the Princess Ranges Member, Chiall Formation: a) sandstone with rounded quartz grains coated by hematite granules, a feature that is typical of red beds; b) sample 153554, glauconitic sandstone. Glauconite grains are about 0.6 mm across and are partially oxidized (brown); c) sample 153551, grain-supported sandstone. Quartz grains with interstitial clay, quartz, muscovite, and iron oxides; d) sample 152609, glauconitic sandstone of the Wandiwarra Member from the outer ring of the Shoemaker impact structure, composed of quartz grains and glauconite (pale green). Dark vein is probably pseudotachylite; e) and f) sample 152619, chloritic mudstone composed of quartz and iron-rich chlorite (green). The chlorite has replaced ?detrital muscovite. All in plane-polarized light

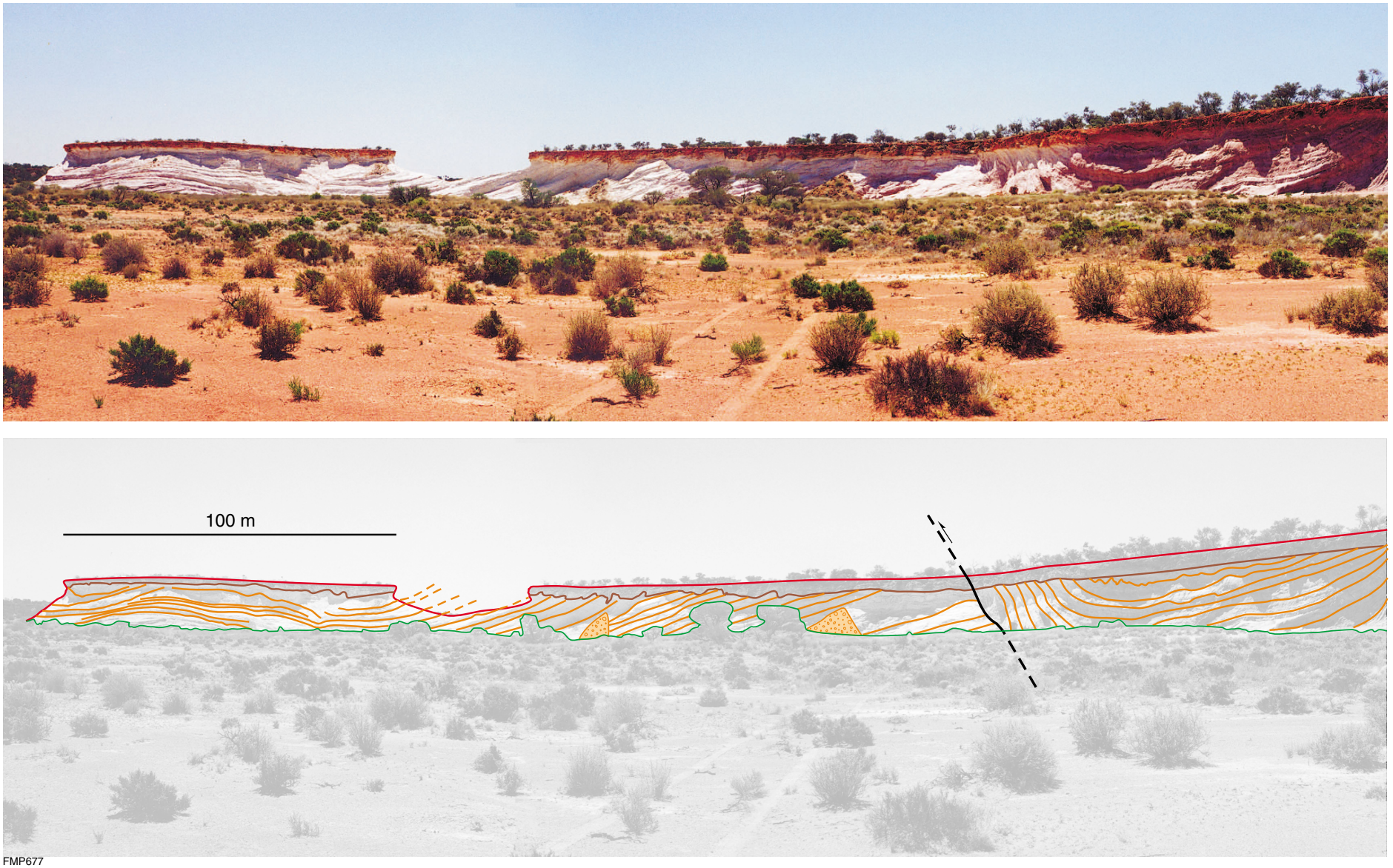

Figure 21. Breakaways in Wandiwarra Member quartz sandstone and siltstone at the northern margin of NABBERU between MGA 274903E 7175735N and 272641E 7176689N, showing mesoscale folding and thrusting. The beds are capped by iron-rich weathered residual quartz sandstone and siltstone in situ

FMP678

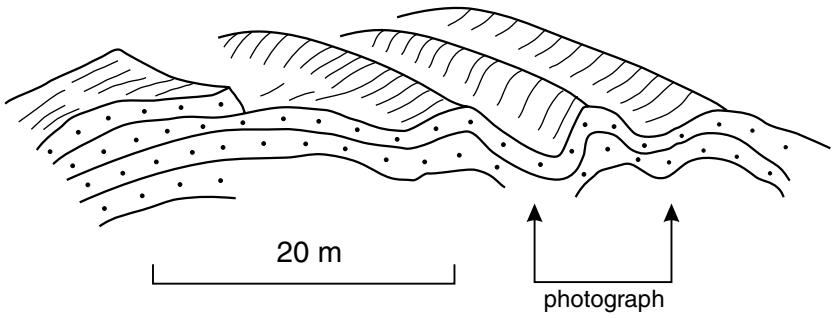

Figure 22. Doubly plunging mesoscale fold in Wandiwarra Member quartz sandstone (MGA 265056E 7176598N). Sketch below shows the overall style of folding in this area

from the Yilgarn Craton and the Gascoyne Complex to the west. It also suggests that this siliciclastic detritus was sourced from progressively younger sources during the evolution of the basin. In addition, ball-and-pillow deformation is common higher in the succession in the Wongawol Formation (Bunting, 1986). A tectonically driven model is certainly consistent with current age constraints that suggest deposition of the Earaheedy Group may have been more or less synchronous with the Capricorn Orogeny. Thus, the Miningarra Subgroup is interpreted to reflect rapid uplift in the west, causing influx of siliciclastic material that overwhelmed the proportion of iron and silica in solution and consequently terminated the deposition of granular iron-formation, while favouring the deposition of glauconite peloids. Glauconite peloids, associated with clastic grains, are particularly common in shale, siltstone, and very fine grained sandstone horizons, and at the base of medium- to coarse-grained sandstone horizons in the Chiall Formation. There is an association between glauconite and ferruginous sandstone, with alternations of glauconite-rich and ferruginous layers.

Structure and metamorphism of the Earaheedy Group

The exposed Earaheedy Basin is deformed into a regional easterly to east-southeasterly trending, south-verging, asymmetric syncline, which plunges gently towards the southeast. The northern limb is steeply dipping to locally overturned, and forms the Stanley Fold Belt, a 110°-trending structural domain, which is about 200 km long and up to 35 km wide, and which is characterized by strike–slip faulting, foliation fabrics, tight folding, and reverse faulting. Folding varies in scale, with fold limbs commonly truncated by faults. Faults trend easterly, and

FMP695

Figure 23. Mega-ripple marks in Chiall Formation (Princess Ranges Member) sandstone, along the northestern part of the outer collar of the Shoemaker impact structure (MGA 297690E 7150193N)

include both dip–slip (dipping north), and sinistral strike–slip components.

Deformed rocks of the fold belt are exposed in the northeast corner of Granite Peak (Muir Range) in the vicinity of Yampi Well. The degree of deformation in the Stanley Fold Belt decreases southward resulting in open, typically gentle folds, locally with an associated axial-plane cleavage. These features are expressed on aeromagnetic images as a series of broad, low-amplitude, easterly trending ridges and swales. Doubly plunging mesoscale folds with wavelengths of 10–20 m (Fig. 22) are well exposed along the breakaways north of Lake Edith Withnell and Lake Karri Karri. Breccias and quartz vein stockworks are commonly associated with the folded rocks.

In the transition zone between the Stanley Fold Belt and folded southern margin of the Earaheedy Basin, small-scale disharmonic folding and normal faulting is common (Fig. 26).

Sedimentary rocks of the Earaheedy Group are commonly weakly metamorphosed, only locally attaining lower greenschist facies. Typical metamorphic minerals in fine-grained rocks are sericite and chlorite.

Centimetre-thick veins of syntaxial fibrous quartz are common in the sandstone units of the Chiall Formation. The stress field present at the time the veins were emplaced can be gauged by the orientation of the veins and syntaxial quartz fibres. There are two sets of quartz veins on Nabberu – Granite Peak: the older vein set (strike 270°) in which the fibres are oriented 355° (s_3; least compressive stress); and the younger vein set (strike 060°) in which the fibres are oriented 150° (s_3; strike 060°).This implies that the veins may have formed as a result of northeast–southwest directed compression (Fig. 27). This compression event is interpreted to reflect the tectonic compression associated with the Yapungku Orogeny (Smithies and Bagas, 1997; Bagas and Smithies, 1998; Bagas, 2004), which resulted in the formation of the Stanley Fold Belt.

Shoemaker impact structure

The Shoemaker impact structure has an outer diameter of about 30 km (Fig. 28) and consists of two well-defined concentric ring syncline and anticline structures, formed in rocks of the Chiall and Frere Formations, surrounding Archaean basement rocks (Teague Granite and greenstone rocks; Pirajno and Glikson, 1998; Pirajno, 2002). The structure is discussed in detail by Pirajno (2002) and only a brief review is given here.

Evidence for an impact origin of the Shoemaker impact structure includes:

1. a well-defined circular structure with surrounding rings of synclinal and anticlinal structures, which enclose a core of Archaean basement interpreted as a central uplift (Teague Granite and greenstone rocks);
2. shatter cones in sedimentary rocks in both inner and outer rings;

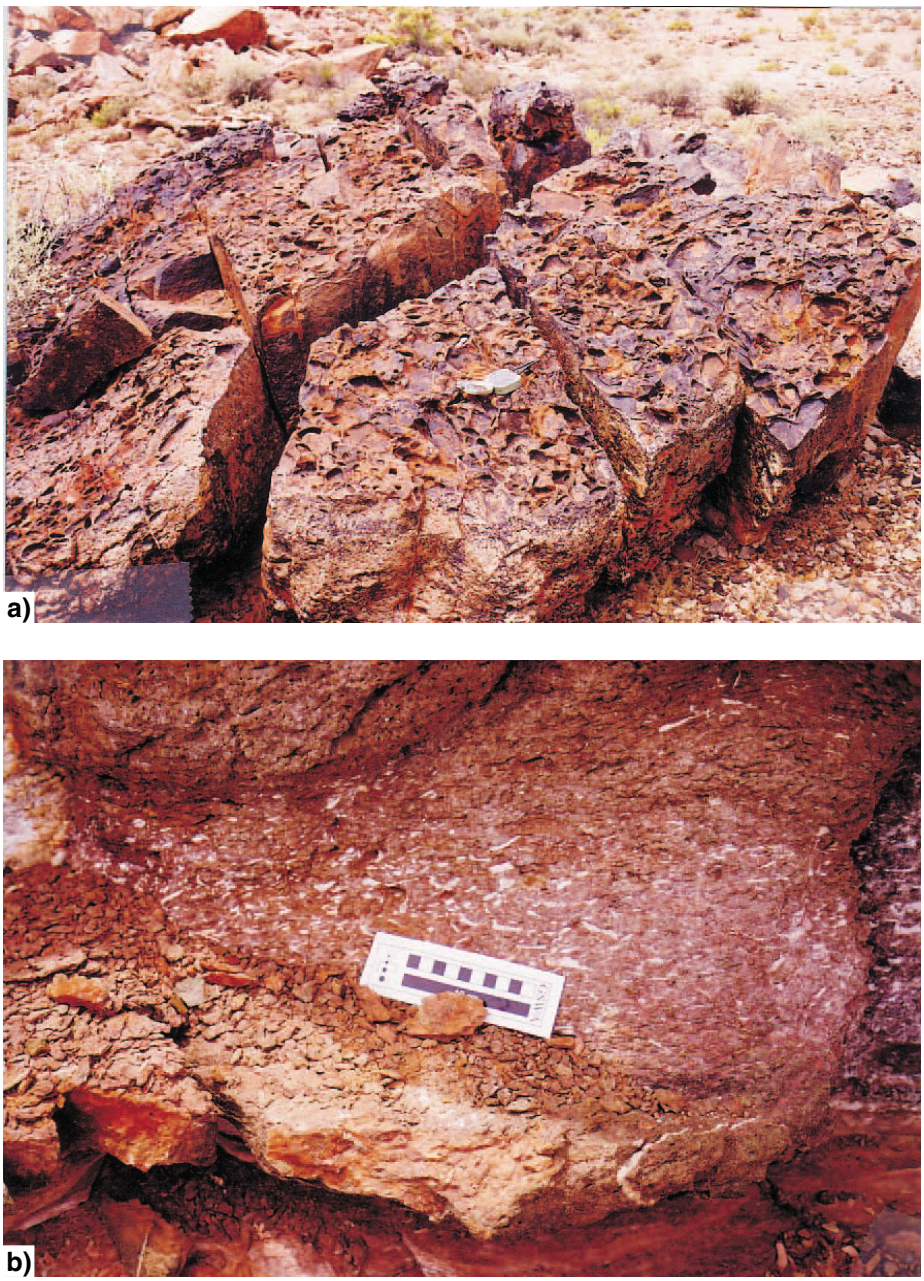

Figure 24. Mass flow deposits at the base of the Wandiwarra Member (MGA 275900E 7160780N): a) sedimentary mass-flow deposit and b) fluidized arenite, representing possible tsunamite or seismite

3. planar deformation features (PDFs) in quartz crystals in the Teague Granite.

The central basement uplift, with a diameter of 12 km, consists of fractured Archaean granitoids of syenitic composition (Teague Granite). Shock metamorphic features include shatter cones in sedimentary rocks and planar deformation features in quartz crystals of the Teague Granite. The syenitic composition of the Teague Granite suggests that it could either belong to a late Archaean suite of alkaline plutons that intrude the Yilgarn Craton (Johnson, 1991; Smithies and Champion, 1999), or instead be the product of alteration of a precursor granitoid by alkali metasomatism related to an impact-generated heat source. Locally, the Teague Granite is partially to pervasively silicified, fractured, and contains hydrothermal minerals, such as fibrous amphibole, garnet, sericite and prehnite, consistent with metasomatism.

The age of the Shoemaker structure is not known with certainty. A K–Ar age of 568 Ma was determined on illite–smectite mineral separates from the Teague Granite (Pirajno, 2002). This age is likely to represent hydrothermal activity triggered by impact-related heat energy.

FMP688

Megabreccia (*Px*)

About 5 km from the eastern shore of Lake Teague are scattered, centimetre- to metre-sized round and angular boulders of sandstone (*Px*). This could be a lag deposit of Permian age (Paterson Formation; Bunting et al., 1982; Commander et al., 1982). Alternatively, because of their position close to the outermost ring and the absence of any such lithology elsewhere in the Earaheedy Group in the region, it is also possible that they are either remnants of reworked lithic breccia ejecta, or crater-fill allochthonous breccia (Pirajno, 2002).

Dolerite sill (*Pd*)

A dolerite ?sill outcrops on the northeast inner collar of the Shoemaker impact structure on NABBERU (MGA 294076E 7145194N). This dolerite (*Pd)* is undeformed (possibly post-impact) and composed of plagioclase, augite, brown hornblende, biotite, and accessory quartz, sericite, and ilmenite. The optically determined plagioclase composition is about An_{50} (andesine–labradorite). Hornblende replaces augite along the crystal margins and biotite replaces hornblende. Minor and interstitial granophyric intergrowths (quartz–feldspar) are also present.

Figure 25. Asymmetric, straight-crested ripples in mature fine-grained quartz arenite in the Chiall Formation (MGA 297876E 71466026N)

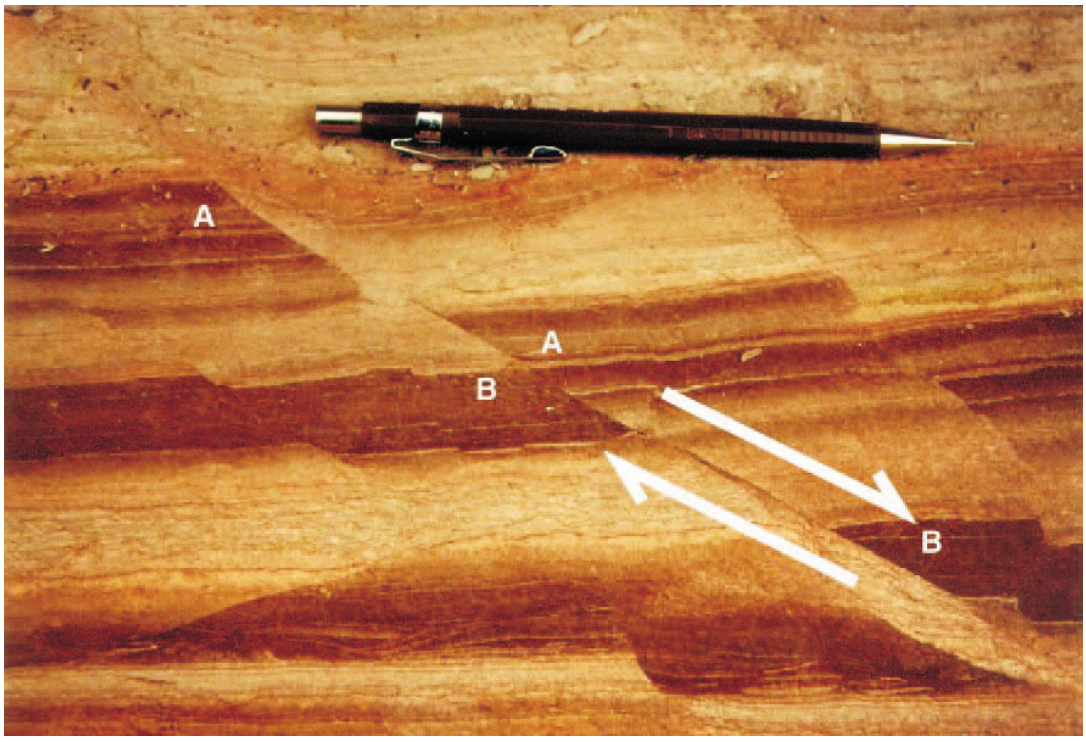

FMP694

Figure 26. Small-scale normal faulting in siltstone of the Chiall Formation (MGA 300076E 7155324N)

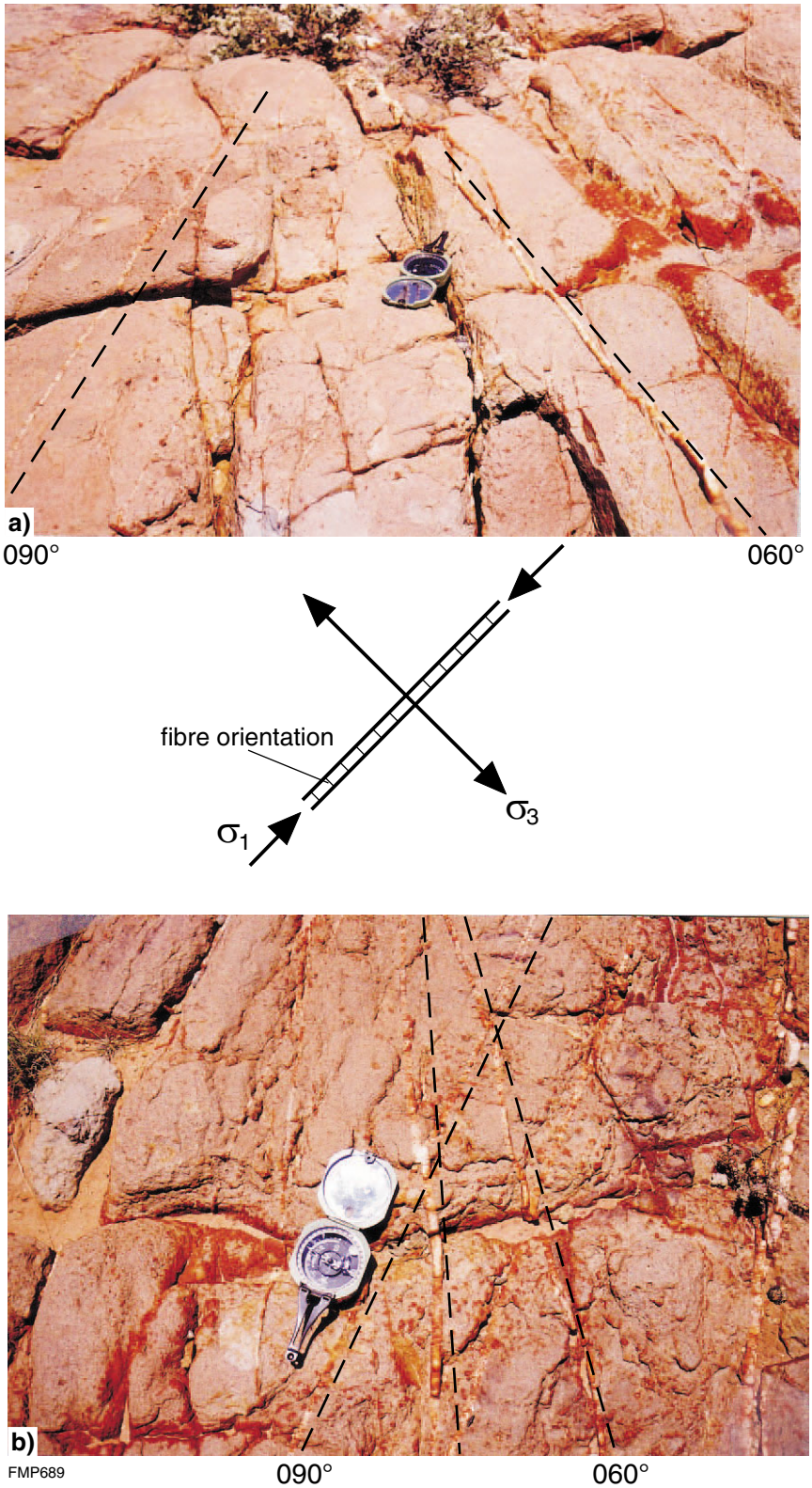

Figure 27. a) and b): Fibrous quartz veins crosscutting the Wandiwarra Member outcrop about 3.5 km southwest of Kennedy Bore (MGA 277790E 7160400N). These are indicative of brittle failure and the orientation of the quartz fibres, perpendicular to the fracture walls, represents the least compressive stress direction. The fractures resulted from a maximum compressive stress oriented northeast–southwest (see text for more details)

Quartz veins and hydrothermal chert (*q, qc*)

To the southwest of the Shoemaker impact structure, northeasterly trending milky white quartz veins (*q*) are associated with, and parallel to, northeasterly and north-northeasterly trending fractures in hornblende-bearing quartz monzonite (*Agzq*; Fig.4). The attitude of the veins and associated fractures suggest a pattern that converges towards the centre of the Shoemaker impact structure. The quartz veins post-date the hornblende-bearing quartz monzonite, which was emplaced at 2664 ± 4 Ma (Nelson, 1999), and are evidence of hydrothermal activity in the area. Other Archaean granitoid rocks in the region do not display the same regular pattern of quartz veins and fractures. It is possible, therefore, that the northeasterly trending fractures are impact-related, and that their local infilling with quartz may have resulted from impact-induced circulation of hydrothermal fluids.

Pods of chert and jasperoidal quartz (*qc*) are present along the eastern margin of the central uplift of the Shoemaker structure (e.g. MGA 295300E 7139500N). The chert material consists mainly of brecciated microcrystalline quartz cemented by chalcedonic quartz. Open spaces are filled with euhedral quartz crystals. Dark grey to opaque patches are possibly carbonaceous matter, and are associated with opaque spherules, 0.07 to 0.1 mm in diameter, and vermicular shapes, 0.25 to 0.2 mm long. Colourless and nearly isotropic rhombohedral crystals may be either dolomite or anglesite. These chert pods were probably formed by precipitation from hydrothermal fluids that circulated along the boundaries, or along faults in the eastern sector of the Shoemaker impact structure.

Economic geology

Although there is no reported mineral production on Nabberu – Granite Peak, considerable exploration activity has been reported for the Earaheedy Basin and adjoining Archaean rocks. Open-file statutory mineral exploration reports (WAMEX database) and mineral resource information (MINEDEX database) are held at the Western Australian Department of Industry and Resources and are accessible online from the Department's website (www.doir.wa.gov.au).

Archaean rocks

The Yandal greenstone belt is well endowed with gold mineralization, for which a resource of about 4.5 t was established during exploration in the 1990s (Phillips and Anand, 2000). Jundee–Nimary, Bronzewing, Mount Joel, and Darlot are some of the prominent gold deposits in the belt (Phillips and Anand, 2000).

Greenstone rocks, representing the northward continuation of the Yandal belt onto Nabberu, are exposed along the Lockeridge Fault, where much of the mineral exploration in the area has been focused. One of the areas investigated is the Celia prospect (Hallmark Gold, 1988), in the vicinity of Rabbit Well. This prospect consists of a 300 m-long zone of 'iron–silica' (possibly banded iron-formation), in which rock-chip samples assayed up to 0.3 g/t gold. South of the prospect, an area of stockwork quartz veins in felsic volcanic rocks (*Af*) was considered prospective during exploration (Hallmark Gold, 1988).

The Horse Well prospect is spatially associated with the Lockeridge Fault in the south of Nabberu (Fig. 28). Gold mineralization in the prospect is hosted by a west-dipping shear zone system, and inferred resources of 0.24 Mt at 4.3 g/t have been reported over a strike length of about 200 m (Morris et al., 1997).

Earaheedy Basin

Iron

The Frere Formation was considered to be highly prospective for iron ore of the Hamersley type (Broken Hill Proprietary, 1978). Several Temporary Reserves were granted within the basin between 1973 and 1978, and zones of iron enrichment within granular iron-formation were located.

Least-weathered granular iron-formation within the Frere Formation contains various amounts of iron. Bunting (1986) reported Fe enrichment in some units, ranging from 27–47% Fe, with less than 0.06% P_2O_5. Analyses of grab samples of granular iron-formation rocks range from 20 to 39% Fe, with P_2O_5 from 0.05 to 0.9%. Enrichment of secondary iron oxides is common in areas close to faults as a result both of hydrothermal fluids and weathering processes. Such enriched zones may have economic potential. To the northwest on Fairbairn, platy hematite is in a predominantly shaly sequence near the top of the Frere Formation in the Miss Fairbairn Hills area (Adamides et al., 2000). Iron enrichment was interpreted as the result of localized chemical weathering (Robinson and Gellatly, 1978) and drilling indicated that the high-grade zones encountered during surface sampling were both small and sulfurous. The decrease in iron content with depth indicates that much of the high iron content resulted from surface lateritization.

Zinc, lead, and copper

Zinc–lead–copper mineralization occurs in stromatolitic dolomite rocks of the Sweetwaters Well Member of the Yelma Formation (Hocking et al., 2000; Pirajno, 2002). On Merrie (Adamides, 2000), Zn–Pb-sulfide mineralization is in the interstices of stromatolite columns in the Sweetwaters Well area.

On Nabberu, carbonate-hosted sulfide and sulfate mineralization is known from a number of localities near to and west of the Shoemaker impact structure (Fig. 28), along at least 50 km of strike length. Except for the Iroquois prospect close to the Shoemaker structure, the mineralization does not outcrop, but was intersected in drillholes (TDH 1 to TDH 28; see cross section in Fig. 6) at depths ranging from 100 to 350 m, beneath the Frere Formation. These base metal prospects, 6 km west-

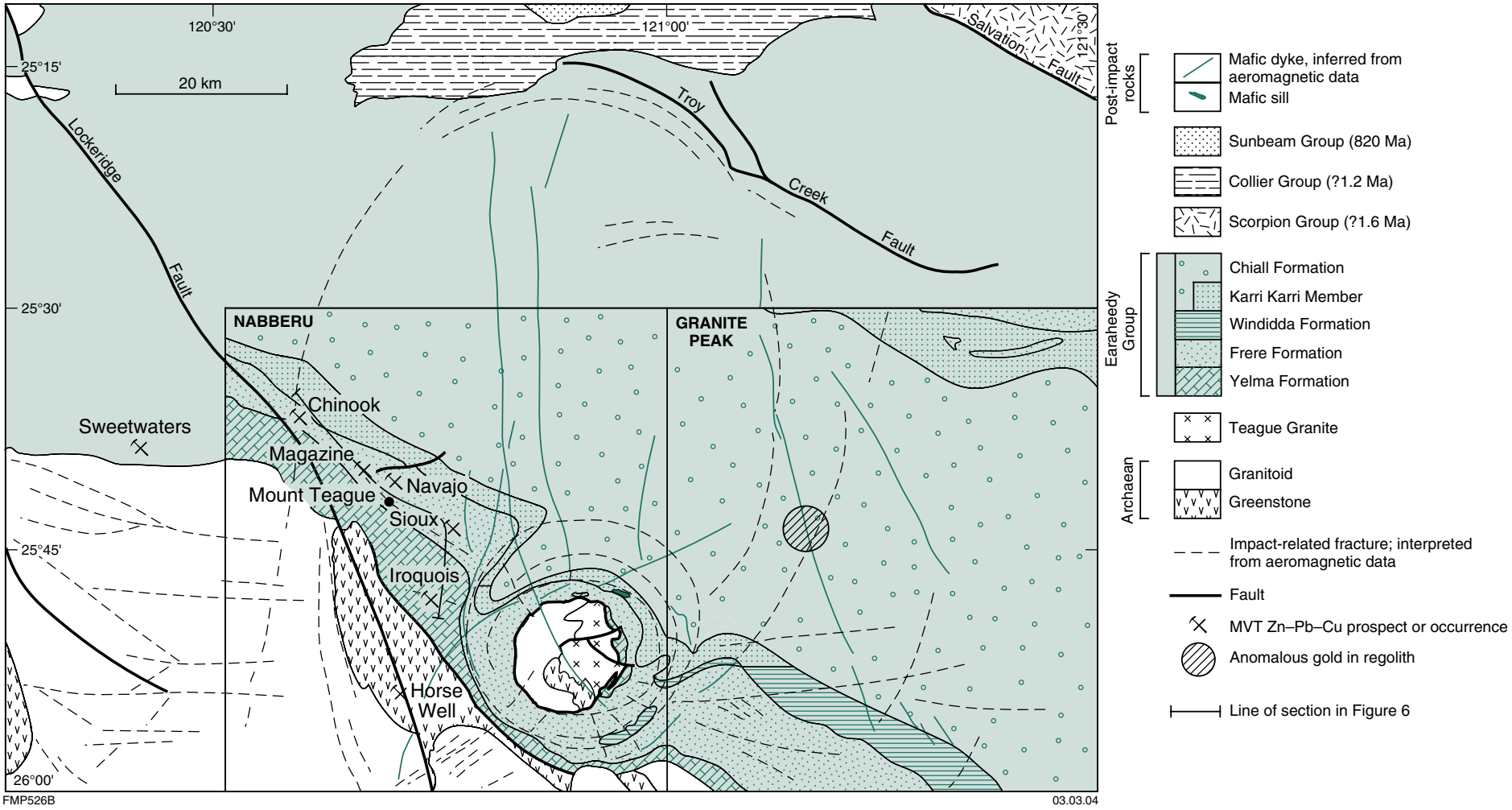

Figure 28. Simplified geology of part of the western Earaheedy Basin and the Shoemaker impact structure showing distribution of known Mississippi Valley-Type (MVT) Zn–Pb–Cu and Au prospects on Nabberu – Granite Peak and adjacent areas (after Pirajno, 2002)

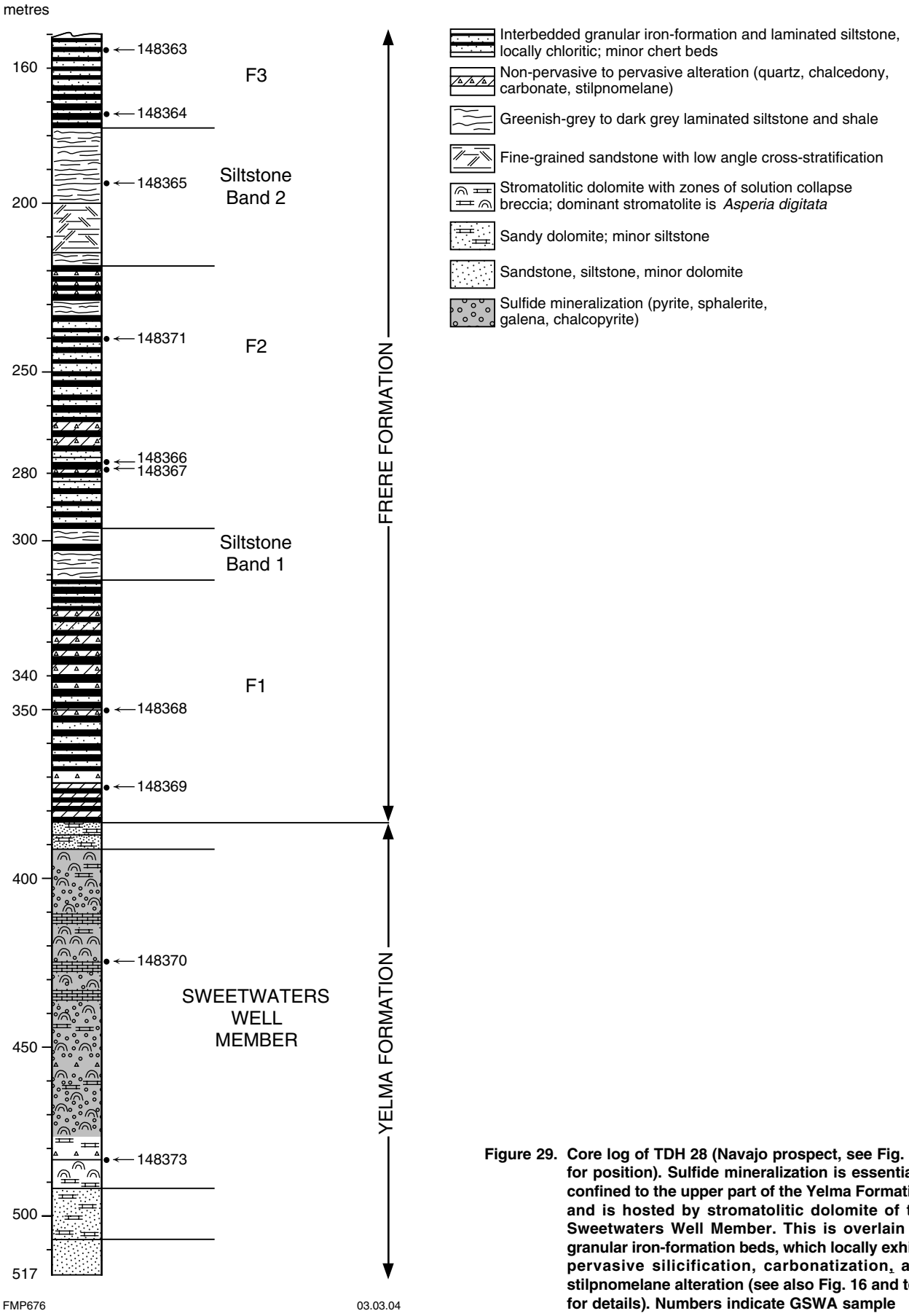

Figure 29. Core log of TDH 28 (Navajo prospect, see Fig. 28, for position). Sulfide mineralization is essentially confined to the upper part of the Yelma Formation and is hosted by stromatolitic dolomite of the Sweetwaters Well Member. This is overlain by granular iron-formation beds, which locally exhibit pervasive silicification, carbonatization, and stilpnomelane alteration (see also Fig. 16 and text for details). Numbers indicate GSWA sample

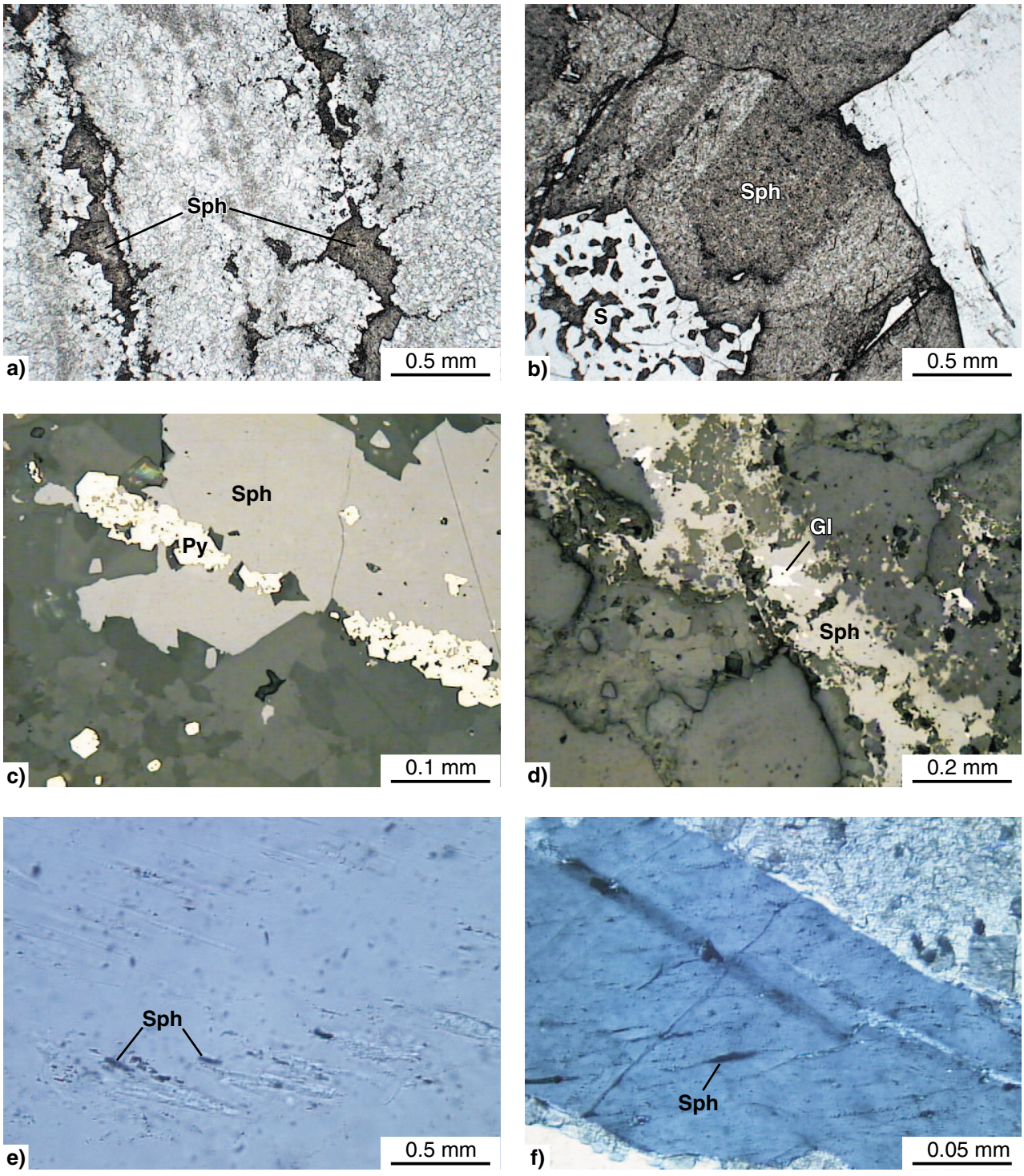

FMP690

Figure 30. Photomicrographs of mineralized Sweetwaters Well Member stromatolitic dolomite: a) sample 148360 showing sphalerite along microbial laminae; b) sample 148361 zoned sphalerite and simplectic quartz (S) + sphalerite texture; c) sample 148361 euhedral pyrite overprinting sphalerite; d) sample 148362 sphalerite veinlet with galena inclusions; e) and f) sample 148362 sphalerite infilling microcracks in quartz grains of dolomitic sandstone; the microcracks are possibly planar deformation features. a–d) reflected light; e–f) plane-polarized light. Sph — sphalerite; Py — pyrite; Gl — galena

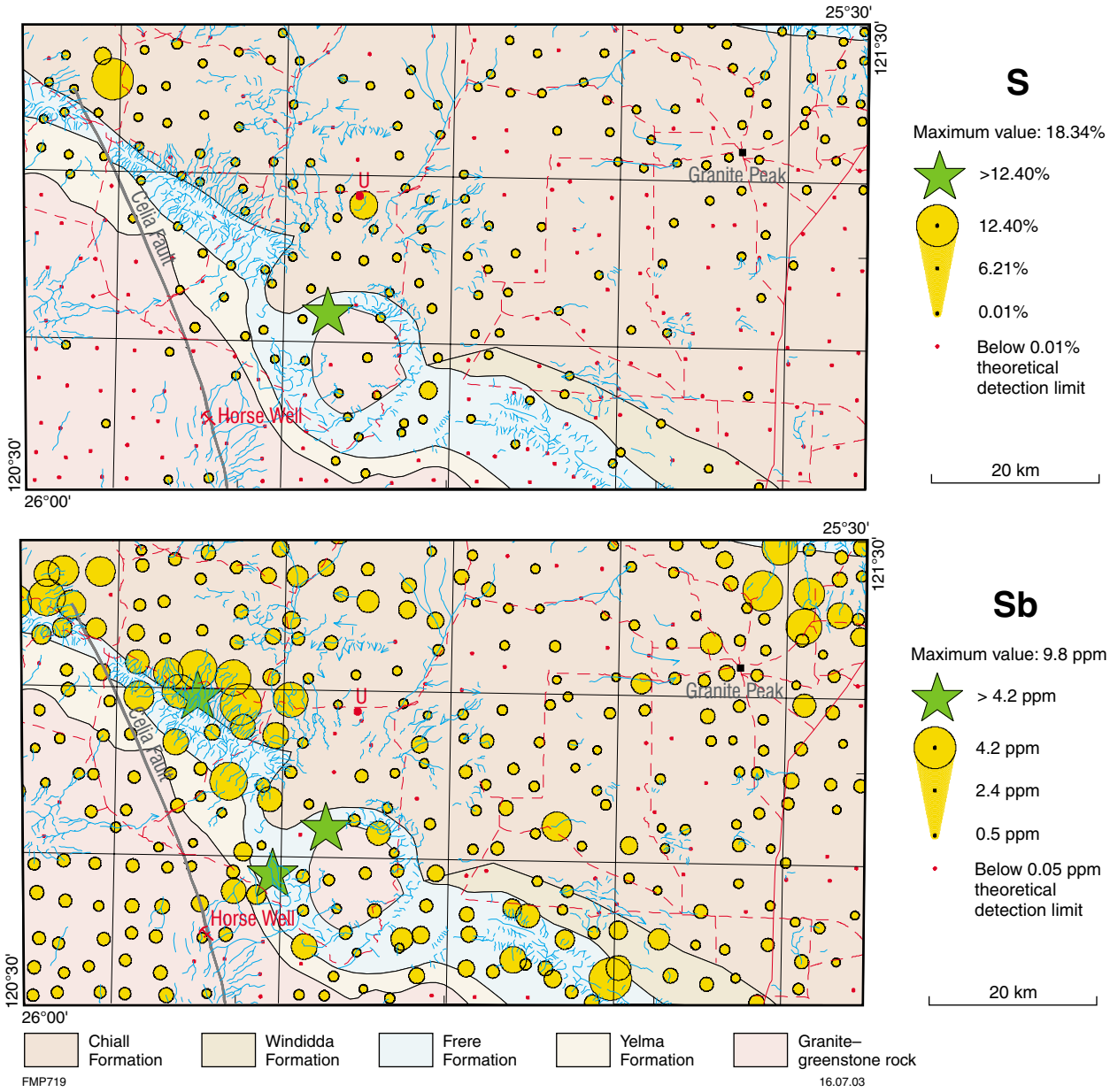

Figure 31. Sulfur (S) and antimony (Sb) distribution in regolith materials on Nabberu (1:250 000; Morris et al., 1997). Note anomalous Sb in the Frere Formation and peak values north of Horse Well and in the northwest of the Shoemaker structure's inner collar. The latter is coincident with elevated S and As, suggesting possible presence of sulfides in that area

northwest of Mount Teague (Fig. 28), were named and investigated in detail by Renison Goldfields Consolidated following a systematic diamond and reverse-circulation (RC) drilling program (Edgar, 1994; Feldtmann, 1995; Dörling, 1998). Best assay results of reported drillcore intersections gave 11 m at 1.3% Zn and 0.2% Pb, 3 m at 2.3% Zn and 0.2% Pb, 6 m at 1.86% Zn and 0.23% Pb, 20 m at 0.88% Zn and 0.1% Pb. Best assay results reported from RC drilling gave 13 m at 2.36% Zn and 0.72% Pb. Barium values from mineralized rock-chip samples range from 1000 to 4000 ppm (Dörling, 1996, 1997, 1998; Feldtmann, 1995).

Ore minerals include pyrite and sphalerite, with minor amounts of galena, chalcopyrite, bornite, and tetrahedrite (Figs 30a,b). These sulfides are associated with jig-saw breccias, open spaces, microfracture infills, and microbial laminae. Cross-cutting barite veins are locally present, commonly in silicified dolomite. Minor amounts of pyrobitumen, associated with sulfides, were identified by Teen (1996).

Textural relationships indicate three stages of mineralization paragenesis (Teen, 1996). They are: I) pyrite–dolomite; II) microcrystalline quartz–chalcedony–quartz–pyrite–sphalerite–galena–chalcopyrite–bornite–tetrahedrite; III) dolomite–quartz–pyrite–sphalerite–galena. Sphalerite is typically zoned (Fig. 30b), banded or colloform, dark in colour and therefore iron-poor, and commonly contains inclusions of galena. Typically,

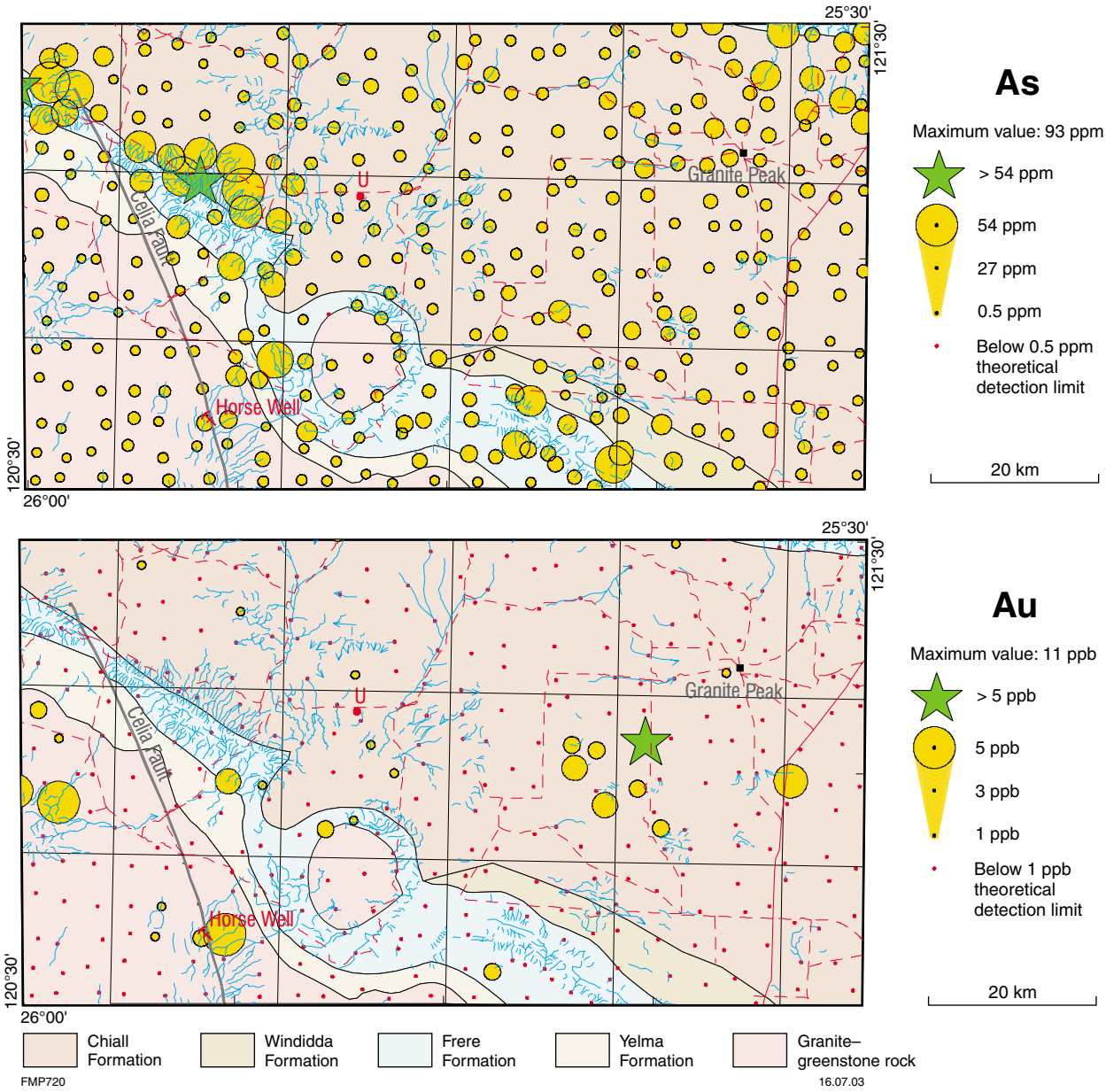

Figure 32. Arsenic (As) and gold (Au) distribution in regolith materials for Nabberu (1:250 000; Morris et al., 1997). Of relevance here is the anomalous As along the Frere Formation, which could be explained by either presence of As-bearing phases in granular iron-formation rocks or sulfides in the underlying Sweetwaters Well Member. Note the cluster of Au anomalies south of Granite Peak station. Also of interest is the weakly anomalous Au in the northwest inner collar of the Shoemaker impact structure, because it is coincident with Sb and S peak values

sphalerite either replaces microbial laminae or columnar stromatolites (*Asperia digitata*), or fills open space (Figs 30c,d). The mineralization in open-space cavities indicates that sphalerite is the oldest ore mineral, and was followed by dolomite and late pyrite. The euhedral calcite shows growth zones rich in fluid inclusions, for which homogenization-temperature measurements indicate relatively high temperatures (c. 250°C; Teen, 1996).

In one sample of dolomitic feldspathic sandstone (GSWA 148362) from the base of the succession in the Navajo prospect, sericite, iron sulfides, and sphalerite infill microfractures. Pyrite is always of late generation, both as euhedral crystals that replace sphalerite and as fine disseminations. In other cases, pyrite infills dissolution seams. Hydrothermal dolomite is associated with the mineralization and is typically characterized by large anhedral to euhedral crystals, up to 2 mm long, that infill open spaces.

The Sweetwaters Well Member base metal mineralization has many features that are consistent with carbonate-hosted Mississippi Valley-type ore deposits (MVT), namely: colloform textures, shelf carbonate host at the margins of a sedimentary basin (Garven and Raffensperger, 1997), and low-temperature and moderate-salinity fluids (Teen, 1996).

Uranium

On NABBERU, about 6 km north of Lake Teague, pedogenic calcrete (*Czrk*), 12 to 15 m thick, hosts carnotite mineralization, with values of between 10 and 700 ppm U (average 45 ppm; Butt et al., 1977; Bunting, 1986; Morris et al., 1997).

Rare earth elements (REE)

The Teague Granite, because of its alkaline nature, was investigated for REE mineralization by Metals Exploration (Metals Exploration NL, 1983). Results of this work indicated Ce and La values of up to 1550 and 570 ppm, respectively, in the more syenitic components of the Teague Granite; however, these results could not be substantiated during subsequent studies (Metals Exploration NL, 1984). Average Ce and La abundances in the Teague Granite are 150 and 100 ppm respectively (Pirajno, 2002).

Regolith geochemistry

The NABBERU regolith geochemistry and its relation to bedrock geology have been reported and discussed by Morris et al. (1998). Anomalous abundances in regolith materials are recorded for As, Sb, and S to the west and west-northwest of the Shoemaker impact structure (Figs 31 and 32). These anomalies probably reflect a combination of iron-formation rocks and lead, zinc, iron, and copper sulfides in the underlying Sweetwater Well Member stromatolitic dolomite; however, of some interest are weakly anomalous abundances of As, Au, Pb, and W, and a peak Sb value of 18.34 ppm located in the northwestern part of the inner rim of the Shoemaker impact structure (Figs 31 and 32). This Sb value is coincident with a peak S value of 8 ppm, suggesting the presence of sulfides (Fig. 32). A further gold anomaly was recorded in an area south of the Granite Peak Homestead (Fig. 32). This anomaly is difficult to explain due to the paucity of outcrops in the area, which is thought to be largely underlain by quartz arenite, shale, and siltstone of the Chiall Formation.

References

ADAMIDES, N. G., 2000, Geology of the Merrie 1:100 000 sheet: Western Australia Geological Survey, 1:100 000 Geological Series Explanatory Notes, 37p.

ADAMIDES, N. G., PIRAJNO, F., and HOCKING, R. M., 2000, Geology of the Fairbairn 1:100 000 sheet: Western Australia Geological Survey, 1:100 000 Geological Series Explanatory Notes, 26p.

BAGAS, L., 2004, Proterozoic evolution and tectonic setting of the northwest Paterson Orogen, Western Australia: Precambrian Research, v. 128, p. 475–496.

BAGAS, L., and SMITHIES, R. H., 1998, Geology of the Connaughton 1:100 000 sheet, Western Australia: Western Australia Geological Survey, 1:100 000 Geological Series, Explanatory Notes, 38p.

BAGAS, L., WILLIAMS, I. R., and HICKMAN, A. H., 2000, Rudall, Western Australia (2nd Edition): Western Australia Geological Survey, 1:250 000 Geological Series Explanatory Notes, 50p.

BEARD, J. S., 1981, The vegetation of Western Australia at the 1:3 000 000 scale explanatory notes: Forests Department of Western Australia, 32p.

BETTENAY, E., 1983, Chapter 13, Western Region (II), *in* Soils — an Australian Viewpoint: CSIRO Division of Soils, CSIRO, Melbourne, Academic Press, London, p. 179–187.

BEUKES, N. J., and KLEIN, C., 1990, Geochemistry and sedimentology of a facies transition — from microbanded to granular iron-formation — in the early Proterozoic Transvaal Supergroup, South Africa: Precambrian Research, v. 47, p. 99–139.

BEUKES, N. J., and KLEIN, C., 1992, Models of iron-formation deposition, *in* The Proterozoic biosphere: a multidisciplinary study, *edited by* W. SCHOPF and C. KLEIN: Cambridge University Press, New York, p. 147–151.

BLATT, H., MIDDLETON, G., and MURRAY, R., 1980, Origin of sedimentary rocks: Prentice-Hall, Englewood Cliffs, New Jersey, 782p.

BROKEN HILL PROPRIETARY, 1978, Final report on Temporary Reserves 6492H, 6493H, 6494H, 6495H, 6496H, 6497H, Western Australia: Western Australia Geological Survey, Statutory mineral exploration report, Item 590 A7739 (unpublished).

BROWN, D. A., GROSS, G., A., and SAWICKI, J. A., 1995, A review of the microbial geochemistry of banded iron-formations: Canadian Mineralogist, v. 33, p. 1321–1333.

BUNTING, J. A., 1986, Geology of the eastern part of the Nabberu Basin: Western Australian Geological Survey, Bulletin 131, 130p.

BUNTING, J. A., BRAKEL, A. T., and COMMANDER, D. P., 1982, Nabberu, Western Australia: Western Australia Geological Survey, 1:250 000 Geological Series Explanatory Notes, 27p.

BUNTING, J A., de LAETER , J. R., and LIBBY, W. G., 1980, Evidence for the age and cryptoexplosive origin of the Teague ring structure, Western Australia: Western Australia Geological Survey, Annual Report for 1980, p. 125–129.

BUTT, C. R. M., HORWITZ, R. C., and MANN, A. W., 1977, Uranium occurrences in calcrete and associated sediments in Western Australia: CSIRO Minerals Reseach Laboratories, report FP16, 67p.

CASSIDY, K. F., BARLEY, M. E., GROVES, D. I., PERRING, C. S., and HALLBERG, J. A., 1991, An overview of the nature, distribution and inferred tectonic setting of granitoids in the late-Archaean Norseman–Wiluna belt: Precambrian Research, v. 51, p. 51–83.

CHAFETZ, H. S., and REID, A., 2000, Syndepositional shallow-water precipitation of glauconitic minerals: Sedimentary Geology, v. 136, p. 29–42.

COMMANDER, D. P., MUHLING, P. C., and BUNTING, J. A., 1982, Stanley, Western Australia: Western Australia Geological Survey, 1:250 000 Geological Series Explanatory Notes, 19p.

DAWES, P. R., and PIRAJNO, F., 1998, Geology of the Mount Bartle 1:100 000 sheet: Western Australia Geological Survey, 1:100 000 Geological Series Explanatory Notes, 26p.

DEER, W. A., HOWIE, R. A., and ZUSSMAN, J., 1965, Rock-forming minerals, volume 3: Longmans, Green and Company, London; p. 103–114.

DONALDSON, W. S., PLINT, A. G., and LONGSTAFFE, F. J., 1999, Tectonic and eustatic control on deposition and preservation of Upper Cretaceous ooidal ironstone and associated facies: Peace River Arch area, NW Alberta, Canada: Sedimentology, v. 46, p. 1159–1182.

DÖRLING, S., 1996. Teague Project, E69/562, 856, 857, 858, 975, 987, 988, 1012, 1014, 1036, 1059, 1060: Western Australia Geological Survey, Statutory mineral exploration report, Item 10603 A49642 (unpublished).

DÖRLING, S. L., 1997, Partial surrender report, Canning Gap Project, E69/597: Western Australia Geological Survey, Statutory mineral exploration report, Item 9769 A51110 (unpublished).

DÖRLING, S. L., 1998, Teague Project, E69/562, 856, 857, 858, 975, 987, 988, 1012, 1014, 1036, 1059, 1060: Western Australia Geological Survey, Statutory mineral exploration report, Item 10603 A53279 (unpublished).

EDGAR, W.,1994, Teague Project, Annual Report, E69/562, 855, 856, 857, 858, 975, vols. 1 and 2: Western Australia Geological Survey, Statutory mineral exploration report, Item 10603 A42560 (unpublished).

EILU, P. K., MATHISON, C. I., GROVES, D. I., and ALLARDYCE, W. J., 1999, Atlas of alteration assemblages, styles and zoning in orogenic lode-gold deposits in a variety of host rock and metamorphic settings: Geology and Geophysics Department (Centre for Strategic Mineral Deposits) and UWA Extension, The University of Western Australia Publication No. 30, 50p.

FARRELL, T. R., 1999, Wiluna, W. A. Sheet SG 51-9 (2nd Edition): Western Australia Geological Survey, 1:250 000 Geological Series.

FARRELL, T. R. and WYCHE, S., 1999, Geology of the Millrose 1:100 000 sheet: Western Australia Geological Survey, Geological Series Explanatory Notes, 29p.

FELDTMANN, R., 1995, Teague Project, E69/562, 855, 856, 857, 858, 975, 987, 988, 1012, 1013, 1014, 1031, 1059, 1060, 1036: Western Australia Geological Survey, Statutory mineral exploration report, Item 10603 A45916 (unpublished).

GARVEN, G. and RAFFENSPERGER, J. P., 1997, Hydrogeology and geochemistry of ore genesis, in sedimentary basins, *in* Geochemistry of Hydrothermal Ore Deposits *edited by* H. L. BARNES: 3rd Edition, John Wiley and Sons, p. 125–190.

GOODE, A. D. T., HALL, W. D. M., and BUNTING, J. A., 1983, The Nabberu Basin of Western Australia, *in* Iron-formation: Facts and problems *edited by* A. F. TRENDALL and R. C. MORRIS: Developments in Precambrian Geology, Elsevier, Amsterdam, Monograph 6, p. 295–323.

GREY, K., 1984, Biostratigraphic studies of stromatolites from the Proterozoic Earaheedy Group, Nabberu Basin, Western Australia: Western Australia Geological Survey, Bulletin 130, 123p.

GREY, K., 1994, Stromatolites from the Palaeoproterozoic Earaheedy Group, Earaheedy Basin, Western Australia: Alcheringa, v. 18, p. 187–218.

GRIFFIN, T. J., 1990, Eastern Goldfield Province, *in* Geology and mineral resources of Western Australia: Western Australia Geological Survey, Memoir 3, p. 77–119.

HALILOVIC, J., CAWOOD, J. A. JONES, PIRAJNO, F., and NEMCHIN, A. A., 2004, Provenance of the Earaheedy Basin: implications for assembly of the Western Australia Craton: Precambrian Research, v. 128, p. 343–366.

HALL, W. D. M., and GOODE, A. D. T., 1978, The early Proterozoic Nabberu Basin and associated iron formations of Western Australia: Precambrian Research, v. 7, p. 129–184.

HALL, W. D. M., GOODE, A. D. T., BUNTING, J. A., and COMMANDER, D. P., 1977, Stratigraphic terminology of the Earaheedy Group, Nabberu Basin: Western Australia Geological Survey, Annual Report 1976, p. 40–43.

HALLBERG, J. A., 1987, Postcratonization mafic and ultramafic dykes of the Yilgarn Block: Australian Journal of Earth Sciences, v. 34, p. 135–149.

HALLMARK GOLD N. L., 1988, Annual report for E69/234, Celia Prospect, Warburton Mineral Field: Western Australia Geological Survey, Statutory mineral exploration report, Item 5753 A25598 (unpublished).

HAYS, J., 1967, Surfaces and laterites in the Northern Territory, *in* Landform studies from Australia and New Guinea *edited by* J. N. JENNINGS and J. A. MABBUTT: Canberra, Australian National University Press, p. 182–210.

HEIKOOP, J. M., TSUJITA, C. J., RISK, M. J., TOMASCIK, T., and MAH, A. J., 1996, Modern iron ooids from a shallow-marine volcanic setting: Mahengetang, Indonesia: Geology, v. 24, p. 759–762.

HOCKING, R. M., and GREY, K., 2000, Stacked Proterozoic basins in central Western Australia: Geological Society of Australia Abstracts no. 59, 15th Australian Geological Convention, Sydney, July 3–7, p. 231.

HOCKING, R. M., and JONES, J. A., 2002, Geology of the Methwin 1:100 000 Sheet: Western Australia Geological Survey, 1:100 000 Geological Series Explanatory Notes, 35p.

HOCKING, R. M., JONES, J. A., PIRAJNO, F., and GREY, K., 2000, Revised lithostratigraphy for Proterozoic rocks in the Earaheedy Basin and nearby areas: Western Australia Geological Survey, Record 2000/16, 22p.

HOCKING, R. M., LANGFORD, R. L., THORNE, A. M., SANDERS, A. J., MORRIS, P .A., GOZZARD, J. R., and STRONG, C. A., 2001, A classification system for regolith in Western Australia: Western Australia Geological Survey, Record 2001/4, 22p.

ISLEY, A. E., 1995, Hydrothermal plumes and the delivery of iron to banded iron formation: Journal of Geology, v. 103, p. 169–185.

JOHNSON, G. I., 1991, The petrology, geochemistry and geochronology of the felsic alkaline suite of the eastern Yilgarn block, Western Australia: University of Adelaide, PhD thesis (unpublished), p. 192.

JONES, J. A., in prep., Geology of the Wongawol 1:100 000 sheet: Western Australia Geological Survey, 1:100 000 Geological Series Explanatory Notes.

JONES, J. A., 2000, Granite Peak W. A. Sheet 3146: Western Australia Geological Survey, 1:100 000 Geological Series.

JONES, J. A., PIRAJNO, F., and HOCKING, R. M., 2000, Stratigraphy, tectonic evolution, and mineral potential of the Earaheedy Basin: Western Australia Geological Survey, Record 2000/8, p. 11–13.

JONES, J. A., PIRAJNO, F., and HOCKING, R. M., 2001, A revised stratigraphic framework for the Earaheedy Group: implications for the tectonic evolution and mineral potential of the Earaheedy Basin: Western Australia Geological Survey Annual Review 1999–2000, p. 57–63.

KARHU, J. A., and HOLLAND, H. D., 1996, Carbon isotopes and the rise of atmospheric oxygen: Geology, v. 24, p. 867–870.

KIMBERLEY, M. M., 1989, Exhalative origin of iron formations: Ore Geology Reviews, v. 5, p. 13–145.

LaBERGE, G. L., 1966a, Altered pyroclastic rocks in South African iron-formation: Economic Geology, v. 61, p. 572–581.

LaBERGE, G. L., 1966b, Altered pyroclastic rocks in iron-formation in the Hamersley Range, Western Australia: Economic Geology, v. 61, p. 147–161.

LI, Z. X., 2000, Palaeomagnetic evidence for unification of the North and West Australian cratons by ca 1.7 Ga: new results from the Kimberley Basin of northwestern Australia: Geophysical Journal International, v. 142, p. 173–180.

LINDSAY, J. F., and BRASIER, M., 2002, Did global tectonics drive early biosphere evolution? Carbon isotope record from 2.6 to 1.9 Ga carbonates of Western Australia: Precambrian Research, v. 114, p. 1–34.

MARTIN, D. McB., and THORNE, A. M., 2001, New insights into the Bangemall Supergroup: Western Australia Geological Survey, Record 2001/5, p. 1–2.

METALS EXPLORATION LTD, 1983, Annual report, year ended 4th September 1983, Nabberu Project: Western Australia Geological Survey, Statutory mineral exploration report, Item 1836 A12894 (unpublished).

METALS EXPLORATION LTD, 1984, Final report year ended 3rd September 1984, Nabberu Project: Western Australia Geological Survey, Statutory mineral exploration report, Item 1836 A14554 (unpublished).

MORRIS, P. A., SANDERS, A. J., and FAULKNER, J. A., 1997, Geochemical mapping of the Nabberu 1:250 000 sheet: Western Australia Geological Survey Explanatory Notes, 63p.

MORRIS, P. A., SANDERS, A. J., PIRAJNO, F., FAULKNER, J. A., and COKER, J., 1998, Regional scale regolith geochemistry: identification of metalloid anomalies and the extent of bedrock in the Archaean and Proterozoic of Western Australia: Proceedings of Regolith '98, 3rd Australian Regolith Conference, Kalgoorlie; CRC LEME, Perth, p. 101–108.

MYERS, J. S., 1995, The generation and assembly of an Archaean supercontinent: evidence from the Yilgarn Craton, Western Australia: The Geological Society, London, Special Publication No. 95, p. 143–154.

MYERS, J. S., SHAW, R. D., and TYLER, I. M., 1996, Tectonic evolution of Proterozoic Australia: Tectonics, v. 15, p. 1431–1446.

MYERS, J. S., and SWAGER, C. P., 1997, The Yilgarn Craton, *in* Greenstone Belts *edited by* M. J. DE WITT and L. D. ASHWAL: Clarendon Press, Oxford, p. 640–656.

NEALSON, K. H., 1982, Microbiological oxidation and reduction of iron, *in* Mineral Deposits and the Evolution of the Biosphere *edited by* H. D. HOLLAND and M. SCHIDLOWSKI: Springer-Verlag, p. 51–66.

NELSON, D. R., 1997, Compilation of SHRIMP U–Pb zircon geochronology data, 1996: Western Australia Geological Survey, Record 1997/2, 196p.

NELSON, D. R, 1999, Compilation of SHRIMP U–Pb zircon geochronology data, 1998: Western Australia Geological Survey, Record 1999/2, 222p.

NORTHCOTE, K. H., and WRIGHT, M. J., 1983, Chapter 12, Sandy Desert Region (I), *in* Soils—an Australian Viewpoint: CSIRO Division of Soils, Academic Press, Melbourne, p. 179–187.

OCCHIPINTI, S. A., SHEPPARD, S., PASSCHIER, C., TYLER, I. M., and NELSON, D., 2004, Palaeoproterozoic crustal accretion and collision in the southern Capricorn Orogen: the Glenburgh Orogeny: Precambrian Research, v. 128, p. 237–255.

OSTWALD, J., and BOLTON, B. R., 1992, Glauconite formation as a factor in sedimentary manganese deposit genesis: Economic Geology, v. 87, p. 1336–1344.

PASSCHIER, C. W., and TROUW, R. A. J., 1996, Micro-tectonics: Springer-Verlag, Berlin, 287p.

PHILLIPS, G. N., and ANAND, R. R. (editors), 2000, Yandal greenstone belt; regolith, geology and mineralization: Australian Institute of Geoscientists, Bulletin no. 32, 400p.

PIDGEON, R.T., and HORWITZ, R.C., 1991, The origin of olistoliths in Proterozoic rocks of the Ashburton Trough, Western Australia, using zircon U–Pb isotopic characteristics: Australian Journal of Earth Sciences, v. 38, p. 55–63.

PILLANS, B., 1998, Ancient weathering in an ancient landscape?: Australian National University, Research School of Earth Sciences, Annual Report 1998, p. 107.

PILLANS, B., and BATEMAN, R., 2000, Palaeomagnetic dating of Phanerozoic weathering imprints, Mount Percy Mine, Kalgoorlie, Western Australia: Geological Society of Australia 15th Australian Geological Convention, Sydney, N.S.W., 2000, Proceedings, Abstract Series, no. 59, p. 390.

PIRAJNO, F., 1999, Nabberu, W.A. Sheet 3046: Western Australia Geological Survey, 1:100 000 Geological Series.

PIRAJNO, F., 2002, Geology of the Shoemaker impact structure: Western Australia Geological Survey, Report 82, 52p.

PIRAJNO, F., and ADAMIDES, N. G., 1998, Geology of the Thaduna 1:100 000 sheet: Western Australia Geological Survey, 1:100 000 Geological Series Explanatory Notes, 24p.

PIRAJNO, F., and ADAMIDES, N. G., 2000, Iron–manganese oxides and glauconite-bearing rocks of the Earaheedy Group: implications for the base metal potential of the Earaheedy Basin: Geological Survey of Western Australia, Annual Review 1999–2000, p. 65–71.

PIRAJNO, F., and GLIKSON, A. Y., 1998, Shoemaker Impact Structure, Western Australia: Celestial Mechanics and Dynamical Astronomy, v. 69, p. 25–30.

PIRAJNO, F., and HOCKING, R. M., 2000, Rhodes W.A. Sheet 3147: Western Australia Geological Survey, 1:100 000 Geological Series.

PIRAJNO, F., and HOCKING, R. M., 2001, Mudan W.A. Sheet 3247: Western Australia Geological Survey, 1:100 000 Geological Series.

PIRAJNO, F., JONES, J. A., and HOCKING, R. M., 2000, Revised stratigraphy of the Palaeoproterozoic Earaheedy Group: implications for the tectonic evolution of the Earaheedy Basin, Western Australia: Geological Society of Australia 15th Australian Geological Convention, Sydney, N.S.W., Proceedings, Abstract Series, no. 59, p. 391.

PIRAJNO F., JONES J. A., HOCKING R. M., and HALILOVIC, J., 2004, Geology and tectonic evolution of Palaeoproterozoic basins of the eastern Capricorn Orogen, Western Australia: Precambrian Research, v. 128, p. 315–342.

PIRAJNO, F., OCCHIPINTI, S.A., and SWAGER, C.P., 1998, Geology and tectonic evolution of the Palaeoproterozoic Bryah, Padbury and Yerrida Basins (formerly Glengarry Basin), Western Australia: implications for the history of the south-central Capricorn Orogen: Precambrian Research, v. 90, p. 119–140.

RASMUSSEN, B., and FLETCHER, I. R., 2002, Indirect dating of mafic intrusions by SHRIMP U–Pb analysis of monazite in contact metamorphosed shale: an example from the Palaeoproterozoic Capricorn Orogen, Western Australia: Earth Planetary Science Letters, v. 197, p. 287–299.

RICHARDS, J. R., and GEE, R. D., 1985, Galena lead isotopes from the eastern part of the Nabberu Basin: Australian Journal of Earth Sciences, v. 32, p. 47–54.

ROBINSON, K., and GELLATLY, D. C., 1978, Final report on iron ore exploration, Nabberu Basin, Western Australia; AMAX Exploration (Australia), Inc: Western Australia Geological Survey, Statutory mineral exploration report, Item 769 A7448 (unpublished).

RODRIGUEZ-PASCUA, M. A., CLAVO, J. P., DE VICENTE, G., and GOMEZ-GRAS, D., 2000, Soft-sediment deformation structures interpreted as seismites in lacustrine sediments of the Prebetic Zone, SE Spain, and their potential use as indicators of earthquake magnitudes during the Late Miocene: Sedimentary Geology, v. 135, p. 117–135.

RUSSELL, J., GREY, K., WHITEHOUSE, M., and MOORBATH, S., 1994, Direct Pb/Pb age determination of Proterozoic stromatolites from the Ashburton and Nabberu basins, Western Australia, *in* 8th International Conference on Geochronology, Cosmochronology and Isotope Geology, Berkeley, California, Abstracts: United States Geological Survey, Circular 1107, 275p.

SEILACHER, A., 1969, Fault graded beds interpreted as seismites: Sedimentology, v. 13, p. 155–159.

SMITHIES, R. H., and BAGAS, L., 1997, High pressure amphibolite–granulite facies metamorphism in the Paleoproterozoic Rudall Complex, central Western Australia: Precambrian Research, v. 83, p. 243–265.

SMITHIES, R. H., and CHAMPION, D. C., 1999, Late Archean felsic alkaline igneous rocks in the Eastern Goldfields, Yilgarn Craton, Western Australia: a result of lower crustal delamination?: Journal of the Geological Society, London, v. 156, p. 561–576.

STEWART, A. J., BLAKE, D. H., and OLLIER, C. D., 1986, Cambrian river terraces and ridge tops in central Australia—oldest persisting landforms?: Science, v. 233, p. 758 –761.

TEEN, M. T., 1996, Silicification and base metal mineralization within the Earaheedy Basin, Western Australia: Centre for Ore Deposit and Exploration Studies, University of Tasmania, BSc honours thesis (unpublished), 128p.

TOBIN, K. J., 1990, The paleoecology and significance of the Gunflint-type microbial assemblages from the Frere Formation (Early Proterozoic), Nabberu Basin, Western Australia: Precambrian Research, v. 47, p. 71–81.

TRENDALL, A., 2002, The significance of banded iron formation in the Precambrian stratigraphic record, *in* Precambrian sedimentary environments *edited by* W. ALTERMANN and P. L. COROCRAN: Blackwell, Oxford, p. 33–66.

TWIDALE, C. R., 2000, Early Mesozoic (?Triassic) landscapes in Australia: evidence, argument, and implications: Journal of Geology, v. 108, p. 537–552.

TWIDALE, C. R., HORWITZ, R. C., and CAMPBELL, E. M., 1985, Hamersley landscapes of the northwest of Western Australia: Revue de geologie dynamique et de geographie physique, v. 26, fasc. 3, p. 173–186.

TYLER, I. M., and HOCKING, R. M., 2001, Tectonic units of Western Australia (scale 1: 2 500 000): Western Australia Geological Survey.

TYLER, I. M., and THORNE, A. M., 1990, The northern margin of the Capricorn Orogen, Western Australia — an example of an early Proterozoic collision zone: Journal of Structural Geology, v. 12, p. 685–701.

TYLER, I. M., PIRAJNO, F., BAGAS, L., MYERS, J. S., and PRESTON, W., 1998, The geology and mineral deposits of the

Proterozoic in Western Australia: AGSO Journal of Geology and Geophysics, v. 17, p. 223–224.

van de GRAAFF, W. J. E., CROWE, R. W. A., BUNTING, J. A., and JACKSON, M. J., 1977, Relict early Cainozoic drainages in arid Western Australia: Zeitschrift fur Geomorphologie, v. 21, p. 379–400.

WALTER, M. R., GOODE, A. D. T., and HALL, J. A., 1976, Microfossils from a newly-discovered Precambrian stromatolitic iron formation in Western Australia: Nature, v. 261, p. 221–223.

WINGATE, M. T. D., 2002, Age and paleomagnetism of dolerite sills of the western Bangemall basin: Western Australia Geological Survey, Record 2002/4, 48p.

WINGATE, M. T. D., 2003, Age and palaeomagnetism of dolerite intrusions of the southeastern Collier Basin, Western Australia: Western Australia Geological Survey, Record 2003/3, 34p.

WOODHEAD, J. D., and HERGT, J. M., 1997, Application of the 'double spike' technique to Pb-isotope geochronology: Chemical Geology, v. 138, p. 311–321.

WYCHE, S., and FARRELL, T., 2000, Regional geological setting of the Yandal greenstone belt, northeast Yilgarn Craton: Australian Institute of Geoscientists, Bulletin no. 32, p. 41–49.

Appendix

Gazetteer of localities

Locality	*1:100 000 map sheet*	*Easting*	*Northing*
Bitter Pool	Nabberu	292500	7154500
Camel Well	Granite Peak	328500	7107000
Chinook Prospect (TDH 26)	Nabberu	256600	7166400
Granite Peak Station	Granite Peak	334700	7163600
Horse Bore	Nabberu	263500	7142150
Horse Well Prospect	Nabberu	271223	7130625
Iroquois Prospect (TDH 9)	Nabberu	270300	7147600
Joys Bore	Granite Peak	302350	7123950
Kennedy Bore	Nabberu	278600	7162600
Lake Edith Withnell	Nabberu	268000	7168400
Lake Karri Karri	Nabberu	273000	7166500
Lake Nabberu	Nabberu	278000	7145000
Mount Teague	Nabberu	267600	7156300
Muir Range	Granite Peak	345500	7178500
Navajo Prospect (TDH 28)	Nabberu	264400	7161250
No. 8 Bore	Nabberu	269900	7159000
No. 5 Well	Nabberu	266000	7145250
Oxby Well	Granite Peak	312800	7136050
Rabbit Well	Nabberu	268900	7140600
Yampi Well	Granite Peak	347700	7177850

The Nabberu and Granite Peak 1:100 000 sheets lie within the southern portion of the Nabberu 1:250 000 sheet, and cover the sedimentary sequences of the Paelaeozoic Earaheedy Group of the Earaheedy Basin, and the northern part of the Archaean Yandal greenstone belt and granitoid rocks of the Yilgarn Craton. A prominent feature in the area is the Shoemaker impact structure, which is characterized by two annular collars of Earaheedy Group with the Teague Granite at the core. The Yandal greenstone belt is host to orogenic-style gold mineralization. Other mineralization in the area includes sulfides in stromatolitic dolomite, and uranium in calcrete. Potential also exists for iron deposits, and for gold in rocks of the Chiall Formation of the Earaheedy Group.

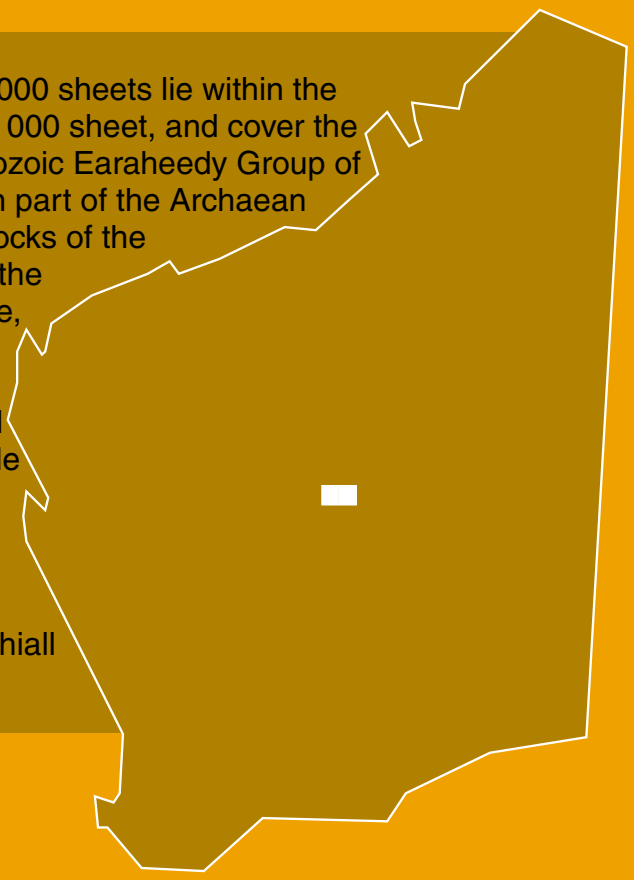

These Explanatory Notes are published in digital format (PDF) and are available online at: www.doir.wa.gov.au/gswa.
This copy is provided for reference only. Laser-printed copies can be ordered from the Information Centre for the cost of printing and binding.

Further details of geological publications and maps produced by the Geological Survey of Western Australia can be obtained by contacting:

Information Centre
Department of Industry and Resources
100 Plain Street
East Perth WA 6004
Phone: (08) 9222 3459 Fax: (08) 9222 3444
www.doir.wa.gov.au/gswa

PIRAJNO et al.

Geology of the Nabberu and Granite Peak 1:100 000 sheet

EXPLANATORY NOTES

GRANITE PEAK

GEOLOGICAL SURVEY OF WESTERN AUSTRALIA

SHEET 3146

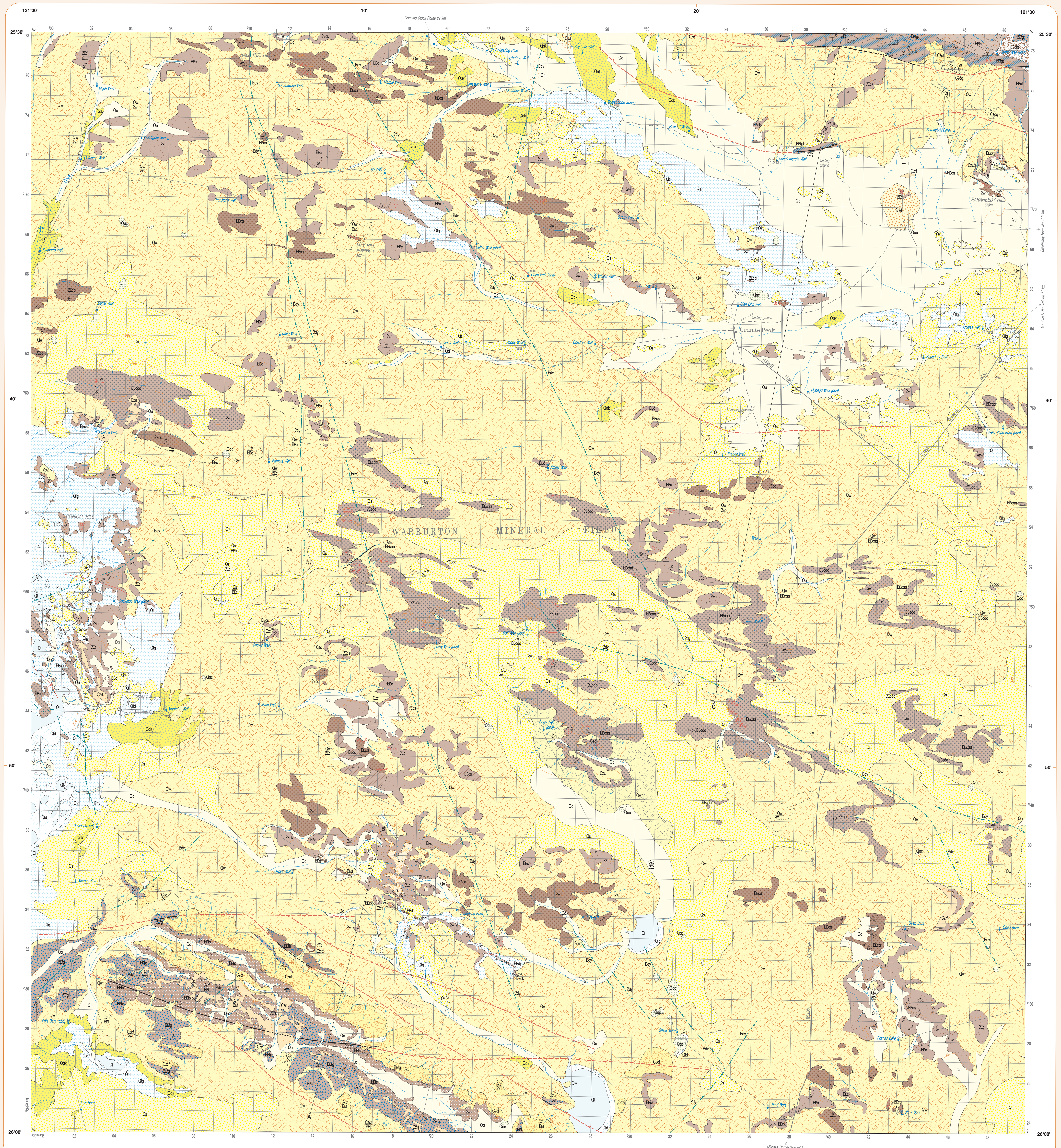

Ql	Qld	Qlg	Qa	Qak	Qac	Qw	Qwf	Qwq	Qs		

PHANEROZOIC — CAINOZOIC — QUATERNARY

- Ql — Lacustrine deposits — mud, silt, and minor sand in playa lakes, commonly saline; primarily associated with palaeodrainage systems
- Qld — Sand in dunes on and around playa lakes; in places gypsiferous
- Qlg — Gypsiferous and saline bedded deposits, generally associated with major lake systems
- Qa — Alluvium — sand, silt, and gravel in channels and channel systems; poorly consolidated
- Qak — Calcrete associated with palaeodrainage and active drainage systems
- Qac — Clay and silt in non-saline claypans
- Qw — Sheetwash deposits — sand, silt, and gravel in areas that lack clearly defined drainage channels
- Qwf — Ferruginous gravel
- Qwq — Quartz rubble adjacent to and washed from quartz veins
- Qs — Sandplain and dunes — sand and minor silt; largely eolian; minor residual component

- Czc — Colluvium — gravel, sand, and silt, commonly consolidated and dissected
- Czcf — Ferruginous rubble and colluvium, dominantly ferruginized pisoliths and nodules with ferruginized rock and ironstone rubble; degraded lateritic duricrust
- Czcq — Rubble and colluvium derived from quartz veins

- Czrf — Ferruginous duricrust — nodular, pisolitic, and massive ferricrete, and associated debris
- Czrz — Siliceous duricrust — nodular, pisolitic, and massive silcrete, and intensely silicified rock

- q — Quartz vein

Stanley Fold Belt (?1760 Ma)

PROTEROZOIC — PALAEOPROTEROZOIC — Earaheedy Group — EARAHEEDY BASIN

Miningarra Subgroup

- PEc — **CHIALL FORMATION:** siltstone and sandstone, coarsening upwards; marine shelf to coastal
- PEcaa — Mature quartz arenite, commonly silicified; minor shale and siltstone
- PEca — Sandstone, variable textural and compositional maturity; stratigraphic position uncertain
- PEcs — Siltstone and minor sandstone
- PEckt — Phyllite; restricted to the Stanley Fold Belt
- PEck — **Karri Karri Member:** laminated shale and siltstone, and minor sandstone; generally evenly laminated

Tooloo Subgroup

- PEd — **WINDIDDA FORMATION:** shale, siltstone, and minor sandstone
- PEdj — Red jasper horizon; locally containing stromatolites

FRERE FORMATION:
- PEf — Granular and laminar iron-formation, granular siliceous iron-formation, siltstone, shale, and chert; marine to near-shore
- PEfgt — Laminar granular iron-formation; deformed and metamorphosed in the Stanley Fold Belt
- PEfg — Granular iron-formation and granular siliceous iron-formation, in places peloidal; minor siltstone, shale, and chert
- PEfh — Massive green chert
- PEfst — Phyllite and phyllitic shale; minor deformed and metamorphosed iron-formation; restricted to the Stanley Fold Belt
- PEfs — Siltstone and shale; minor iron-formation

- PEy — **YELMA FORMATION** (Diagrammatic Sections and Interpreted Bedrock Geology only)

YILGARN CRATON

- Pdy — Dolerite dyke, concealed; interpreted from aeromagnetic data
- Ag — Granitoid rock (Diagrammatic Sections and Interpreted Bedrock Geology only) — ARCHAEAN

INTERPRETED BEDROCK GEOLOGY

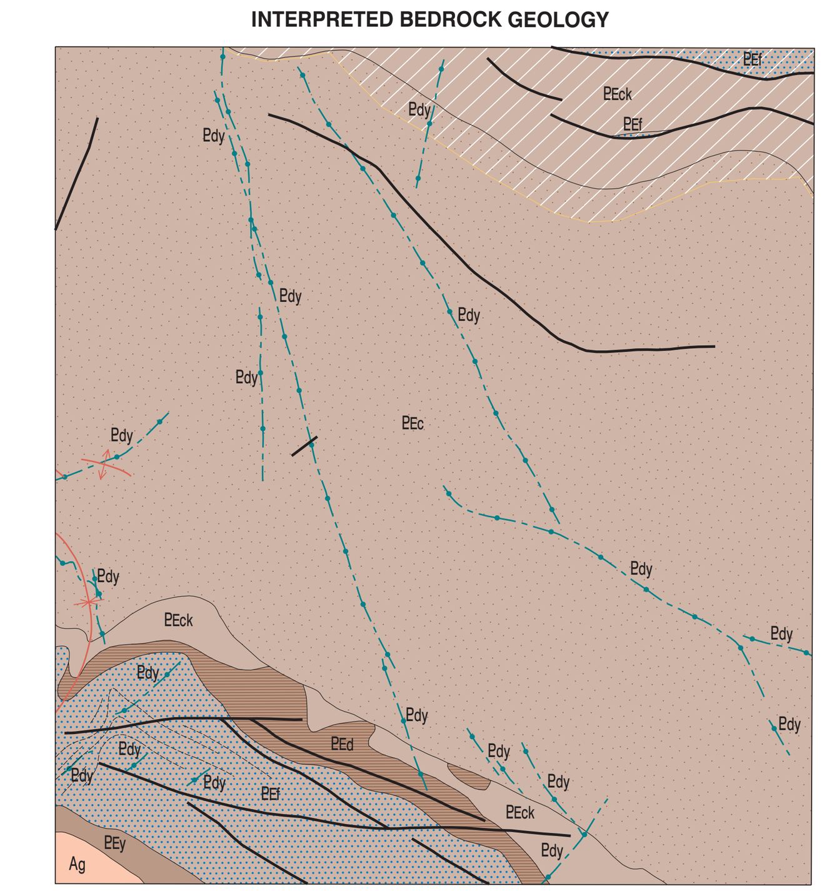

- Overprint indicates deformation in Stanley Fold Belt
- PEc — Chiall Formation
- PEck — Karri Karri Member
- PEd — Windidda Formation
- PEf — Frere Formation
- PEy — Yelma Formation

(Earaheedy Group — EARAHEEDY BASIN)

- Pdy — Mafic dyke within Yilgarn Craton
- Ag — Granitoid rock

(YILGARN CRATON)

SCALE 1:500 000 — 0 5 10 15 20 Kilometres

Geological boundary
- exposed
- concealed

Fault
- exposed
- concealed
- concealed, interpreted from aeromagnetic data

Fold
- anticline; exposed, concealed
- syncline; exposed, concealed

Small-scale fold axis showing trend and plunge
- anticline
- syncline
- meso-scale folding

Bedding, showing strike and dip
- inclined
- vertical
- trend of bedding

Cleavage, showing strike and dip
- inclined
- vertical

Palaeocurrent, showing trend and sense of direction
- from asymmetrical ripple marks
- from cross-bedding
- from symmetrical ripple marks, sense not known
- from current lineation, sense not known

Breccia

Stromatolite fossil locality

Airphoto lineament
- structural trend, unspecified

Formed road

Track

Fence, generally with track

Homestead — Granite Peak

Building

Yard

Microwave repeater station

Horizontal control; minor

Breakaway

Sand dune

Contour line, 20 metre interval — 540

Watercourse

Spring

Bore, well

Windpump

Abandoned — (abd)

Mineral occurrence
- Iron — Fe

SHEET INDEX

FAIRBAIRN 2947	METHWIN 3047 NABBERU	RHODES 3147	MUDAN 3247	GLENAYLE 3347 STANLEY	KAHRBAN 3447
MERRIE 2946	SG 51-5 NABBERU 3046	GRANITE PEAK 3146	EARAHEEDY 3246	SG 51-6 LEE STEERE 3346	COONABILDIE 3446
CUNYU 2945	MILLROSE 3045 WILUNA	BALLIMORE 3145	WONGAWOL 3245	WINDIDDA 3345 KINGSTON	CARNEGIE 3445
WILUNA 2944	SG 51-9 LAKE VIOLET 3044	SANDALWOOD 3144	YELMA 3244	SG 51-10 COLLURABBIE 3344	VON TREUER 3444

1:100 000 maps shown in black

1:250 000 maps shown in brown

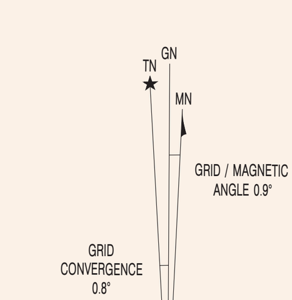

True north, grid north and magnetic north are shown diagrammatically for the centre of the map. Magnetic north is correct for 2000 and moves easterly by about 0.1° in 3 years.

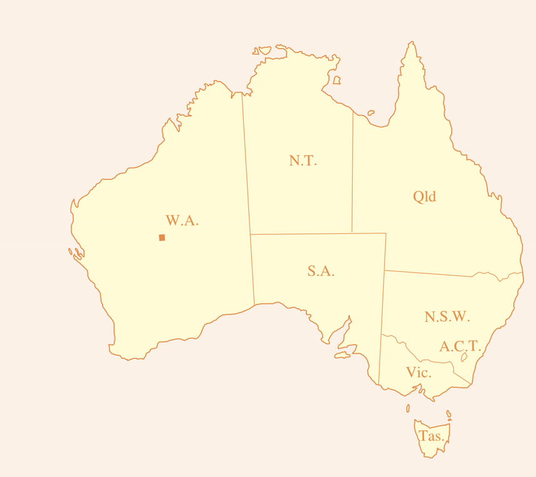

Department of Industry and Resources

CLIVE BROWN, M.L.A.
MINISTER FOR STATE DEVELOPMENT

JIM LIMERICK
DIRECTOR GENERAL

Geological Survey of Western Australia

TIM GRIFFIN
DIRECTOR

SCALE 1:100 000

1000 Metres 0 1 2 3 4 5 6 7 8 9 10 Kilometres

UNIVERSAL TRANSVERSE MERCATOR PROJECTION
HORIZONTAL DATUM: GEOCENTRIC DATUM OF AUSTRALIA 1994
VERTICAL DATUM: AUSTRALIAN HEIGHT DATUM

Grid lines indicate 1000 metre interval of the Map Grid Australia Zone 51

The Map Grid Australia (MGA) is based on the Geocentric Datum of Australia 1994 (GDA94)
GDA94 positions are compatible within one metre of the datum WGS84 positions

Reference points to align maps based on the previous datum, AGD84, have been placed near the map corners

DIAGRAMMATIC SECTIONS

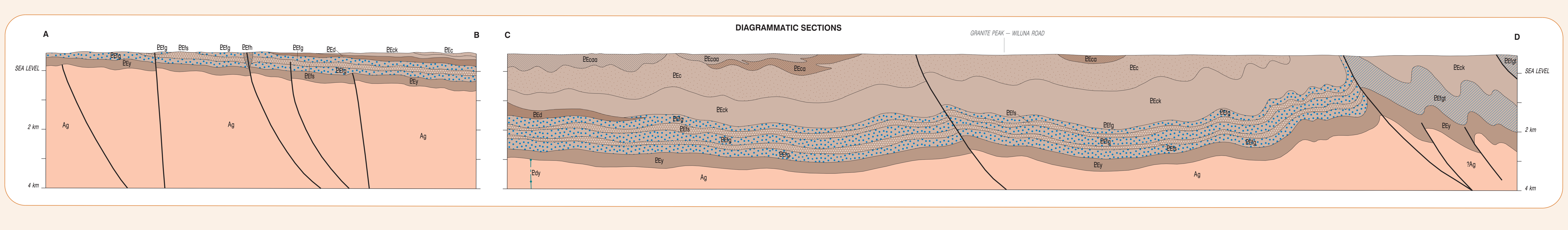

Geology by J. A. Jones and F. Pirajno 1998

Edited by D. Ferdinando and G. Loan

Cartography by D. Ladbrook and B. Williams

Topography from the Department of Land Administration Sheet SG 51-5, 3146, with modifications from geological field survey

Published by the Geological Survey of Western Australia. Digital and hard copies of this map are available from the Information Centre, Department of Industry and Resources, 100 Plain Street, East Perth, WA, 6004. Phone (08) 9222 3459, Fax (08) 9222 3444
Web www.doir.wa.gov.au Email geological_survey@doir.wa.gov.au

The recommended reference for this map is:
JONES, J. A., 2000, Granite Peak, W.A. Sheet 3146: Western Australia Geological Survey, 1:100 000 Geological Series

GRANITE PEAK

SHEET 3146 **FIRST EDITION 2000**

NABBERU

AUSTRALIA 1:100 000 GEOLOGICAL SERIES

GEOLOGICAL SURVEY OF WESTERN AUSTRALIA

SHEET 3046

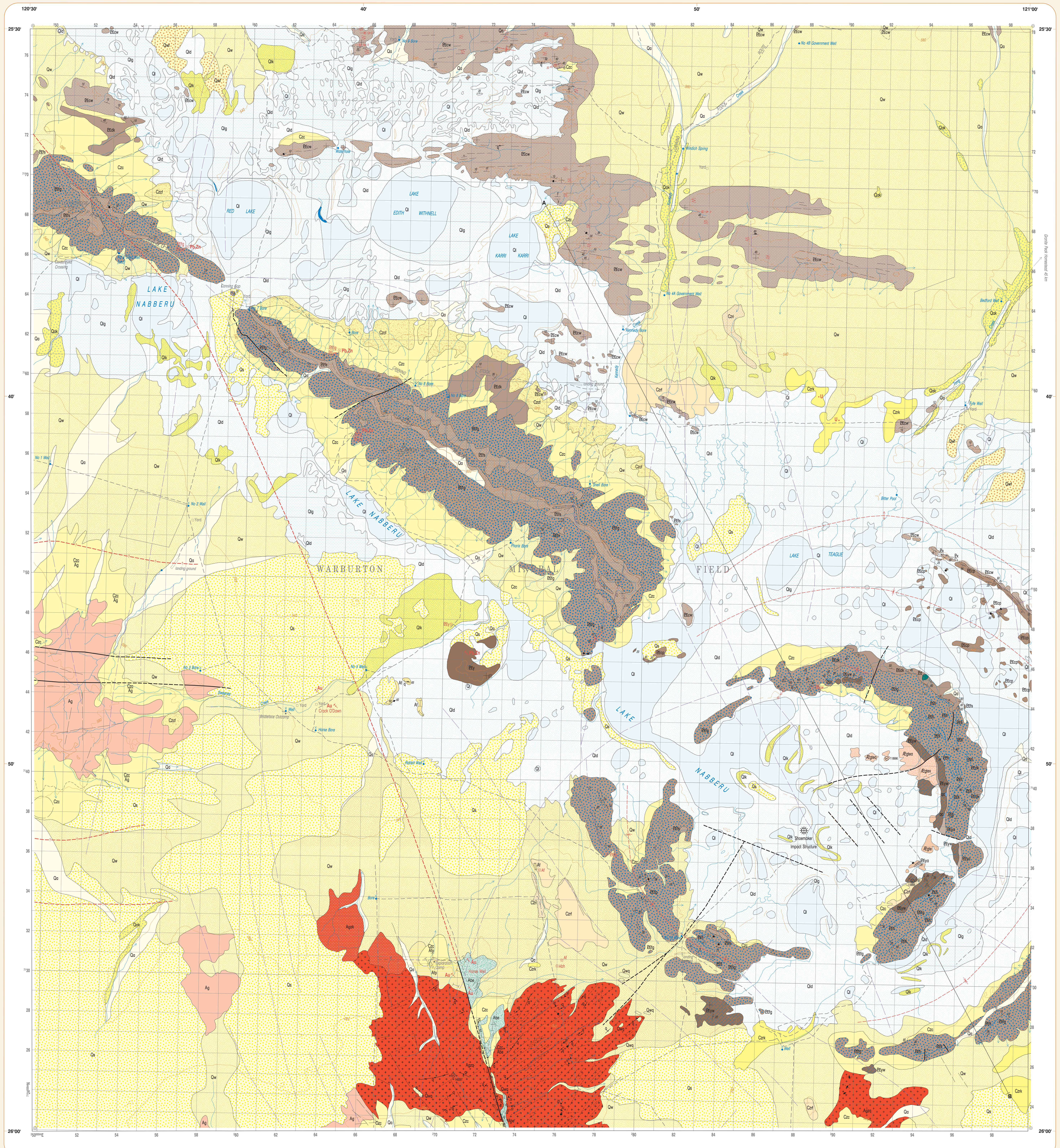

DIAGRAMMATIC SECTION

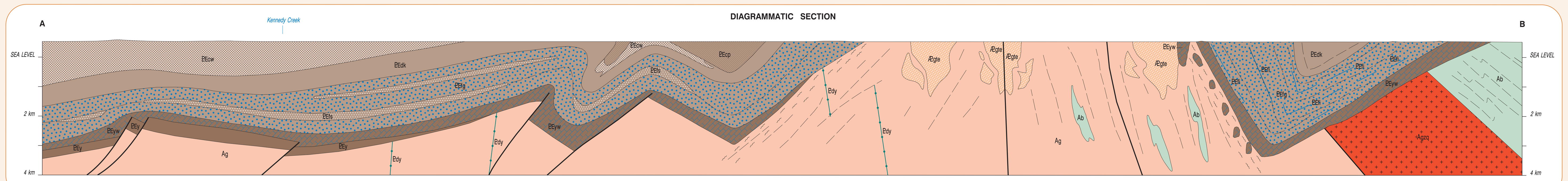

QUATERNARY

CAINOZOIC

PHANEROZOIC

Ql — Qld — Qlg — Qlk; Qa — Qak; Qw — Qwf — Qwq; Qs

- Ql Lacustrine deposits—saline silt, mud, and minor sand in playa lakes; primarily associated with palaeodrainage
- Qld Sand in dunes on or around playa lakes; in places gypsiferous
- Qlg Gypsiferous and saline bedded deposits adjacent to playa lakes
- Qlk Calcrete or gypcrete around playa lakes
- Qa Alluvium—sand, silt, and gravel in channels and channel systems
- Qak Calcrete associated with palaeodrainage and active drainage systems; locally silicified
- Qw Sheetwash—sand, silt, and gravel in areas that lack clearly defined drainage channels
- Qwf Ferruginous gravel in sheetwash areas
- Qwq Quartz rubble adjacent to quartz veins
- Qs Sandplain—unconsolidated sand, and minor silt and clay; with scattered low, vegetated dunes

Czc — Czcf

- Czc Colluvium—loose to consolidated gravel, sand, and silt, in moderate- to high-gradient slope deposits; locally dissected
- Czcf Ferruginous pisoliths and nodules; subordinate ferruginized rock and ironstone rubble

Czrf — Czri — Czrk

- Czrf Ferruginous duricrust; nodular, pisolitic, and massive ferricrete, and associated rubble
- Czri Ironstone; ferruginized rock, massive to rubbly; includes degraded ferruginous crust
- Czrk Pedogenic calcrete; pisolitic, laminar, and nodular authigenic limestone

- q Quartz veins
- qc Hydrothermal chert pod

ꝐEd Dolerite sills

ꝐEx Megabreccia; probably reworked meteorite impact ejecta; predominantly sandstone clasts

PROTEROZOIC

PALAEOPROTEROZOIC

Earaheedy Group

EARAHEEDY BASIN

ꝐEc CHIALL FORMATION: sandstone, siltstone, and shale; generally coarsening upwards

ꝐEcp Princess Ranges Member: quartz arenite; locally glauconitic; minor sandstone

ꝐEcw Wandiwarra Member: fine-grained sandstone; locally glauconitic, commonly hummocky cross-stratified with mud-flake breccia beds; minor interbedded siltstone and shale.

ꝐEdk WINDIDDA FORMATION
Karri Karri Member: siltstone and shale; locally varvoid; minor sandstone and marl

ꝐEf — ꝐEfg — ꝐEfs — ꝐEfi

- ꝐEf FRERE FORMATION: granular iron-formation and granular siliceous iron-formation; minor banded iron-formation, siltstone, and shale
- ꝐEfg Granular iron-formation and granular siliceous iron-formation, in places peloidal; minor siltstone and shale
- ꝐEfs Siltstone and shale; minor sandstone, iron formation, and chert
- ꝐEfi Banded iron-formation; supergene-enriched iron formation

YELMA FORMATION

ꝐEyw Sweetwaters Well Member: stromatolitic dolomite, microbial limestone, chert breccia derived from stromatolitic dolomite *(Asperia digitata, Ephyaltes edingunensis,* and *Pilbaria deverella)* and sandstone

ꝐEy Undivided: sandstone, siltstone, shale, and stromatolitic dolomite with associated chert breccia

ꝐEya Quartz sandstone, coarse grained; locally pebbly

Ꝑdy Mafic dyke interpreted from aeromagnetic data; intruded into Archaean rock (section only)

ARCHAEAN

YILGARN CRATON

ÆRgte — ÆRgtex — ÆRgtea

- ÆRgte TEAGUE GRANITE: leucocratic K-feldspar granite; Archaean granitoid altered by post-impact metasomatism
- ÆRgtex Quartz–microcline(–albite–stilpnomelane) granite; brecciated and silicified
- ÆRgtea Quartz–albite–microcline(–garnet–aegirine–augite) granite

c. 2664 Ma — Agak — Agzq

- Agak Medium-grained leucocratic K-feldspar granite
- Agzq Hornblende quartz–monzonite

Ag Granitoid rock, undivided; generally monzogranite

Af — Afp

- Af Metamorphosed felsic volcanic rock
- Afp Metamorphosed feldspar porphyry

Ab — Abe

- Ab Metamorphosed mafic and ultramafic rock, undivided
- Abe Metabasalt with epidote, garnet–epidote, or clinopyroxene–epidote–chlorite alteration
- Abh Quartz–actinolite hornfels (subsurface only)

Geological boundary
- exposed
- concealed

Fault or shear
- exposed
- concealed
- concealed, interpreted from aeromagnetic data

Strongly foliated rock

Fold, showing axial trace and generalized plunge direction
- anticline; exposed
- syncline; exposed
- syncline; concealed

Small-scale fold-axis, showing trend and plunge
- anticline
- syncline
- M-vergence
- mesoscale folding

Bedding, showing strike and dip
- inclined
- vertical
- horizontal
- strike and dip estimated from aerial photographs
  - 0–15°
  - 15–45°
  - bedding trend

Palaeocurrent, showing trend and sense of direction
- from megaripples, direction unknown

Cleavage, showing strike and dip
- inclined
- vertical

Foliation, showing strike and dip
- inclined
- vertical

Lineation, showing trend and plunge direction
- stretching lineation; inclined

Joint, showing strike and dip
- inclined
- vertical

Joint pattern

Airphoto or Landsat lineament

Aeromagnetic lineament

Meteorite impact structure

Shatter cone locality

Stromatolite fossil locality

Isotopic age determination site with identification number — 118995

Track

Fence, generally with track

Building

Yard — Yard

Breakaway

Sand dune

Contour line, 20 metre interval — 540

Watercourse; with ephemeral pool or waterhole

Waterhole — Waterhole

Bore, well — Bore, Well

Windpump

Prospect (gold, unless otherwise indicated) — Horse Well

Mineral exploration drill hole showing subsurface data — Af

Mineral occurrence
- Lead — Pb
- Uranium — U
- Zinc — Zn

SIMPLIFIED GEOLOGY

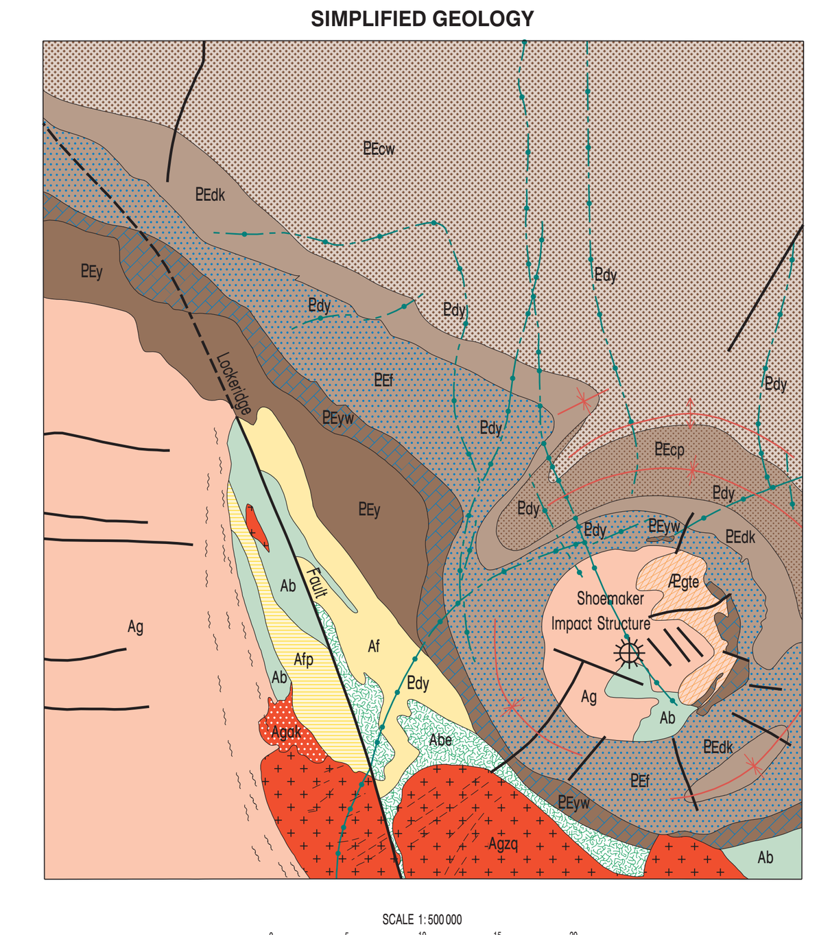

SHEET INDEX

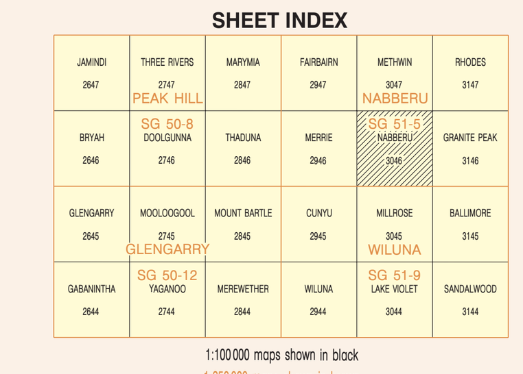

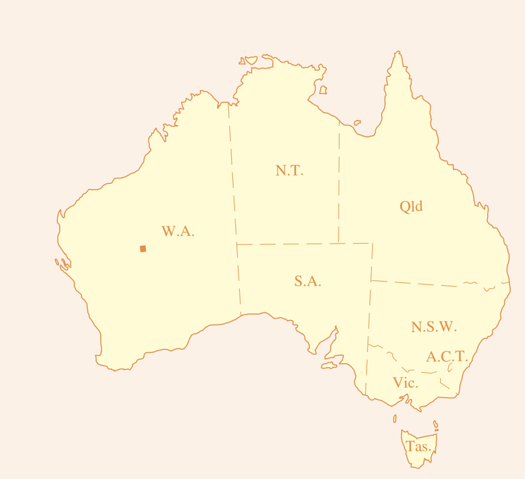

GOVERNMENT OF WESTERN AUSTRALIA

Department of Industry and Resources

Geological Survey of Western Australia

CLIVE BROWN, M.L.A.
MINISTER FOR STATE DEVELOPMENT

JIM LIMERICK
DIRECTOR GENERAL

TIM GRIFFIN
DIRECTOR

Geology by F. Pirajno 1998

Edited by D. Ferdinando and G. Loan

Cartography by S. Hamill and K. Greenberg

Topography from the Department of Land Administration Sheet SG 51-5, 3046, with modifications from geological field survey

Published by the Geological Survey of Western Australia. Copies available from the Information Centre, Department of Minerals and Energy, 100 Plain Street, East Perth, WA, 6004. Phone (08) 9222 3459, Fax (08) 9222 3444

This map is also available in digital form

Printed by the Sands Print Group, Western Australia

The recommended reference for this map is:
PIRAJNO, F., 1999, Nabberu, W.A. Sheet 3046: Western Australia Geological Survey, 1:100 000 Geological Series

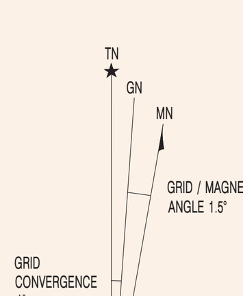

True north, grid north and magnetic north are shown diagrammatically for the centre of the map. Magnetic north is correct for 1998 and moves easterly by about 0.2° in 5 years.

SCALE 1:100 000

1000 Metres 0 1 2 3 4 5 6 7 8 9 10 Kilometres

TRANSVERSE MERCATOR PROJECTION
HORIZONTAL DATUM: AUSTRALIAN GEODETIC DATUM 1984
VERTICAL DATUM: AUSTRALIAN HEIGHT DATUM

Grid lines indicate 1000 metre interval of the Australian Map Grid Zone 51

The Map Grid Australia (MGA) is based on the Geocentric Datum of Australia 1994 (GDA94)
GDA94 positions are compatible within one metre of the datum WGS84 positions

Reference points to align maps based on the previous datum, AGD84, have been placed near the map corners

NABBERU

SHEET 3046 FIRST EDITION 1999

Version 1 — September 2003